

25659

National Library
of Canada

Bibliothèque nationale
du Canada

CANADIAN THESES
ON MICROFICHE

THÈSES CANADIENNES
SUR MICROFICHE

NAME OF AUTHOR/NOM DE L'AUTEUR Dow M. Maharajh

TITLE OF THESIS/TITRE DE LA THÈSE Solubility and Diffusion of Gases in Water

UNIVERSITY/UNIVERSITÉ Simon Fraser University

DEGREE FOR WHICH THESIS WAS PRESENTED/
GRADE POUR LEQUEL CETTE THÈSE FUT PRÉSENTÉE Doctor of Philosophy

YEAR THIS DEGREE CONFERRED/ANNÉE D'OBTENTION DE CE GRADE 1975

NAME OF SUPERVISOR/NOM DU DIRECTEUR DE THÈSE Professor John Walkley

Permission is hereby granted to the NATIONAL LIBRARY OF CANADA to microfilm this thesis and to lend or sell copies of the film.

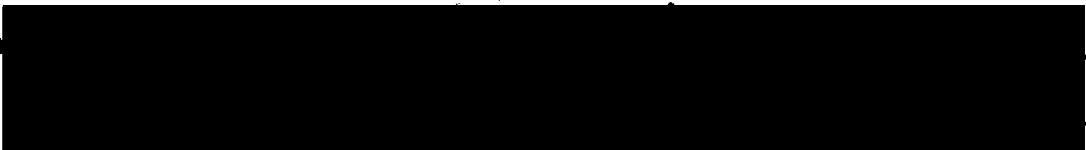
L'autorisation est, par la présente, accordée à la BIBLIOTHÈQUE NATIONALE DU CANADA de microfilmer cette thèse et de prêter ou de vendre des exemplaires du film.

The author reserves other publication rights, and neither the thesis nor extensive extracts from it may be printed or otherwise reproduced without the author's written permission.

L'auteur se réserve les autres droits de publication; ni la thèse ni de longs extraits de celle-ci ne doivent être imprimés ou autrement reproduits sans l'autorisation écrite de l'auteur.

DATED/DATÉ September 2, 1975 SIGNED/SIGNÉ _____

PERMANENT ADDRESS/RÉSIDENCE FIXE



SOLUBILITY AND DIFFUSION OF GASES IN WATER

by

DOW MAHARAJH

B.Sc., Mt. Allison University, 1968

A DISSERTATION SUBMITTED IN PARTIAL FULFILLMENT

OF THE REQUIREMENTS FOR THE DEGREE OF

DOCTOR OF PHILOSOPHY

in the department

of

Chemistry

© DOW MAHARAJH 1973

SIMON FRASER UNIVERSITY

May, 1973

All rights reserved. This thesis may not be reproduced in whole or in part, by photocopy or other means, without permission of the author.

APPROVAL

NAME: Dow M. Maharajh
DEGREE: Doctor of Philosophy
TITLE OF THESIS: Solubility and Diffusion of Gases in Water

EXAMINING COMMITTEE:

Chairman: Derek Sutton

John Walkley
Senior Supervisor

Eberhard Kiehlmann

Ian Gay

Eva M. Voigt

~~Keith Miller~~
External Examiner
Harvard Medical School
Harvard University
Boston, Mass.

March 13, 1975

Date Approved

PARTIAL COPYRIGHT LICENSE

I hereby grant to Simon Fraser University the right to lend my thesis or dissertation (the title of which is shown below) to users of the Simon Fraser University Library, and to make partial or single copies only for such users or in response to a request from the library of any other university, or other educational institution, on its own behalf or for one of its users. I further agree that permission for multiple copying of this thesis for scholarly purposes may be granted by me or the Dean of Graduate Studies. It is understood that copying or publication of this thesis for financial gain shall not be allowed without my written permission.

Title of Thesis/Dissertation:

Solubility and Diffusion of Gases in Water

Author:

(signature)

Dow Mahabir Maharajh

(name)

August 19, 1975

(date)

ABSTRACT

The saturation solubilities of O_2/CH_4 , O_2/N_2 and N_2/CH_4 mixtures in water at $25.00^\circ C$ and 1 atmosphere total pressure are reported at O_2 partial pressures of 0.25, 0.5 and 0.75 atmosphere. The solubilities of oxygen at a partial pressure of 0.5 atmosphere in the presence of 0.5 atmosphere pressure of helium, krypton, methane, nitrogen, oxygen, ethane and carbon tetrafluoride are also reported. The saturation solubility of each gas is lower than expected by Henry's Law. One ternary system, $N_2/O_2/D_2O$, showed that the mutual lowering of solubility found in water also occurred in D_2O solvent. The saturation solubilities of pure Ar, O_2 , N_2 and CF_4 gases in H_2O and D_2O are also reported and where comparison can be made to reported literature values it is seen to be good.

The design of a medium pressure gas solubility apparatus is also reported. Oxygen and nitrogen solubilities have been measured in water from 0 to 3 atmospheres in increments of 0.25 atmospheres. A ternary system, $N_2/O_2/H_2O$, has been studied and, for a constant O_2 partial pressure, the lowering of the N_2 solubility from the expected Henry's law value decreases with increase of N_2 partial pressure.

Current theories for the prediction of the solubility of gases in water are discussed.

Data for the dissolution of a gas into a pure solvent, water, measured both with the gas held above the solvent and with the gas held below the solvent are presented. It is shown that diffusion coefficients measured by the latter method are in good agreement with those determined by other workers. The former data shows the gas uptake to be far greater than may be anticipated assuming the dissolution process to be simply a diffusion mechanism. It would appear that for the gas above the solvent the dissolution of the gas results in a density increase at the interface which gives rise to an added convection mechanism. A comparison of rates of dissolution for carbon dioxide and argon in water is made, and it is shown that the uptake with the gas above the solvent may follow either a pseudo non-steady state or pseudo steady state rate law.

Diffusion coefficient values are reported over a 0 to 35°C temperature range for Ar, CO₂, CH₄, CH₃Br, CH₃Cl, and CHCl₂F in water. Various empirical theories relating these diffusion coefficient values to the viscosity of water and the size of the diffusing solute molecule are examined. None are found valid. McLaughlin's hard sphere theory is examined and found in surprisingly good agreement with experiment.

TABLE OF CONTENTS

<u>LIST OF TABLES</u>	vi
<u>LIST OF FIGURES</u>	vii
<u>INTRODUCTION</u>	1
<u>CHAPTER I</u> Solubility of gases in water	11
Introduction	12
Thermodynamic relations for solubility of gases in water	15
Experimental	23
Results	40
Discussion	56
<u>CHAPTER II</u> Diffusion of gases in liquids	67
Introduction	68
Theories of diffusion in liquids	70
Methods for measuring diffusion coefficients of dilute solutes	93
Theory for our methods	109
Results and discussion	112
Conclusion	136
<u>CHAPTER III</u>	139
Conclusions	140
<u>REFERENCES</u>	145
<u>APPENDIX</u>	
Theory incorporating the interfacial tension 'h' and the convection 'u'	150
<u>DISCUSSION</u>	165

LIST OF TABLES

Table I	:	Saturation solubility data comparison	45
Table II	:	Saturation solubility of gas mixtures	47
Table III(a)	:	Solubility of O ₂ /N ₂ mixtures from (0-3) atmos. at constant P _{O₂} = 0.5 atmos.	48
Table III(b)	:	Solubility of gases in D ₂ O and H ₂ O at 25°C.	48
Table IV	:	Comparison of solubilities of gas mixtures using different experimental methods.	49
Table V	:	Diffusion coefficient values for gases in water at 25.00°C.	121
Table VI	:	System Ar/H ₂ O	122
Table VII	:	System CO ₂ /H ₂ O	123
Table VIII	:	System CH ₄ /H ₂ O	124
Table IX	:	System CH ₃ Cl/H ₂ O	125
Table X	:	System CH ₃ Br/H ₂ O	126
Table XI	:	System CHCl ₂ F/H ₂ O	127

LIST OF FIGURES

Fig. 1	General solubility apparatus.	25
Fig. 2	Schematic diagram of apparatus of analysis of dissolved gas.	29
Fig. 3	High pressure apparatus.	34
Fig. 4	Pressure dependence of solubility of O ₂ and N ₂ in water.	39 50
Fig. 5	Saturation solubility of O ₂ /CH ₄ and O ₂ /N ₂ gas mixtures at various partial pressures of oxygen.	51
Fig. 6	Pressure dependence of solubility of mixture of O ₂ and N ₂ (0-3) Atmos. at constant P _{O₂} = 0.50.	52
Fig. 7	Solubility of oxygen plotted against "other gas" solubility as pure gas in water.	53
Fig. 8	Typical peaks from binary gas mixture in H ₂ O.	54
Fig. 9	Solubility of gases in water using the oxygen electrode.	55
Fig. 10	Dependence of X ₂ on number density (ρ).	60
Fig. 11	Open tube diffusion apparatus.	101
Fig. 12	The diffusion cell and the dessicator vessel.	108
Fig. 13	Diffusion of nitrogen in benzene solution.	128
Fig. 14	Rate of dissolution of Argon in benzene.	129
Fig. 15	Temperature dependence of diffusion of carbon dioxide in water.	130
Fig. 16	Temperature dependence of diffusion of Argon in water.	131
Fig. 17	Dependence of log D ₂ on the reciprocal absolute temperature $\left(\frac{1}{T}\right) ^\circ\text{K}^{-1}$.	132
Fig. 18	Dependence of gas diffusion coefficient (log D ₂) on the viscosity of water (log η ₁).	133

Fig. 19	Temperature dependence of diffusion coefficient of Argon with Wilke-Chang and McLaughlin approx.	134
Fig. 20	Diffusion coefficient of gas (D_2) plotted against the self-diffusion coefficient of water (D_1) at the same temperature.	135
Fig. 21	Diffusion of nitrogen gas in benzene at 25°C.	169
Fig. 22	Pseudo non-steady state diffusion in the presence of natural convection.	170
Fig. 23	Pseudo steady state diffusion in the presence of natural convection.	171
Fig. 24	Dissolution of Ar into benzene solvent.	172
Fig. 25	Absorption of CO_2 in water at 25°C.	173
Fig. 26	Area dependence of the velocity 'u'.	174

9
Dedication

To Ms. Frances Elizabeth Wentzell

ACKNOWLEDGEMENTS

The work presented in this thesis owes much to the inspiration and guidance of Dr. John Walkley, who as supervisor has influenced the author throughout his graduate school career. For his scientific ideas, many of which appear here, his interest and most of all his approachability go the author's sincere thanks.

Thanks for reading the first manuscript are due to Ms. Frances Wentzell who has been a colleague for three years, then an associate for the last four years. This period has been marked by discussions and arguments, but more importantly by a true and lasting friendship.

I also thank Dr. W. Ng for his computational assistance and Mr. Eddie Maharajh for reading the final manuscript.

Thanks to Dr. A. Sherwood for his help in the design of my solubility apparatus.

Thanks to Mr. Peter Hatch and his associates in the glass-blowing shop for their assistance in the past four years. This period has been marked by discussions, arguments and debates which have sometimes touched on scientific topics - but more importantly by a true friendship.

In fact the last four years at Simon Fraser University have produced a multitude of persons and personalities who academically and socially have done much to make the author's somewhat chequered career a happy one. They are too numerous to list here - so

these thanks alone might be inadequate but, in the present context, must suffice.

Thanks to Mr. Rod McMillan and Mr. Claude Lassigne, and Dr. Avijit Purkayastha for their many ideas and help during this work.

I thank the National Research Council of Canada and Water Resources of Canada for financial support.

I would like to thank Ms. Merrily Dominelli and Mrs. Mary Toots for typing this thesis.

Simon Fraser University
Burnaby 2, B.C. Canada
April, 1973

Dow Maharajh

Symbols used in this thesis

μ_1	chemical potential
f_1	fugacity of 1
G	Gibbs Free energy
n_1	no. of moles of component 1
P_1	partial pressure
K_1	Henry's Law constant
X_1	mole fraction of 1
T	temperature ($^{\circ}$ K)
R	gas constant
S	entropy
H	enthalpy
a_1	activity of component 1
k	Boltzmann constant
E	Internal energy
A	Helmholtz free energy
G_c	free energy due to cavity formation
G_1	free energy of interaction
V_1	molar volume of 1
D	diffusion coefficient
ξ	frictional coefficient
L	phenomenological coefficient
M	molecular weight
h	Plank's constant
η	viscosity
q	partition function
t	probability
ρ	number density

Introduction

"And like a man to double business
bound, I stand in pause when shall
I first begin."

(Hamlet III, 2, 40)

Introduction

No exact theory of liquid water, accounting for all of its properties, has appeared so far. This is not unexpected in view of the unsettled state of the theory of liquids in general and of the complications arising from the special interactions existing in water.

Modern theory of the structure of liquid water was inaugurated by Bernal and Fowler (1). They proposed that water has a definite structure, the structure of tridymite, quartz and close-packed spheres. The Bernal and Fowler method was criticized on the grounds that the various crystallographic forms are too rigid (2).

The theory of water structure with the greatest number of adherents at the present time appears to be the "flickering cluster" model proposed by Frank and Wen (3) and more recently developed by Nemethy and Scheraga (4). Frank and Wen postulated that the formation of H-bonds in water is predominantly a co-operative phenomenon that gives rise to constantly forming and dissolving "flickering clusters" of very brief half-lives, yet long enough "to constitute a meaningful existence of the cluster". These clusters are mixed with non-hydrogen bonded molecules, which constitute the rest of the system, the whole held together by very strong van der Waals forces.

An important class of water models represents liquid water as having a distorted or loosened ice structure. In the structure proposed by Samoilov (5) the ice structure is distorted, but in liquid water, the interstitial sites are occupied by water molecules. A similar model was advanced by Forslund(6). Pople (7) suggested that there is extensive distortion, but not breaking, of H bonds.

In many ways similar to the loosened ice models are the various clathrate or cage models. These models go a step beyond the water - filled interstitial spaces of the loosened ice models and suppose the presence in the liquid water of large cavities. These cavities are filled with water molecules that Frank and Quist (8) claim are monomeric and free to rotate. The model is based on analogy with the structure of the clathrate-compounds in which molecules are engaged in the lattice of other molecules.

The water model of Davis and Litovitz (9), like the model of Bernal and Fowler (1) and the later simplified model of Wada (10), postulates that liquid water is a mixture of two different structural forms. Both forms are puckered hexagonal rings, in one the rings are open-packed with extensive H-bonding between them and in the other they are close-packed so that the resulting structure is nearly a body centered cubic configuration. The

Frank and Wen model is the most suitable model to account for many of the observed properties of liquid water. This model is based on a physically reasonable picture, which takes into account the properties required of hydrogen bonded structures and includes features which can account for both the liquid state and solid-like features of water. The model is in agreement with spectral data and provides a qualitative explanation for relaxational properties. Its most significant result is the ability to account for the thermodynamic functions and volume properties of liquid water over a range of 70°C above the melting point of water.

The thermodynamic properties of gases dissolved in water have for a long time been of considerable interest. Dissolved in typical nonpolar solvents, gases have saturation solubilities (1 atmosphere; 25°C) $X_2 \approx 5 \times 10^{-4}$; entropies of solution $(\bar{S} - S^G) \approx 5$ cal./deg.-mole and enthalpies of solution $\Delta H_2^{\circ} \approx 400$ cal./mole. In water, gases exhibit comparatively low solubilities, $X_2 \approx 10^{-5}$, a negative entropy of solution $(\bar{S} - S^G) = -15$ cal./deg.-mole, and enthalpies of solution, $\Delta H \approx 4000$ cal./mole. Again the partial molal volumes of gases dissolved in non-polar solvents are typically 10 c.c./mole larger than those in water. The difference in properties is obviously a matter of the difference in the structure of water and that of a non-polar solvent. It

suffices then that a study of the properties of gases dissolved in water might help in the elucidation of the 'structure' of water itself.

Uhlig (11) proposed a cavity model in which he considered the solubility process to take place in two steps: first, doing work on the solvent against the solvent surface tension to create a cavity, and second placing the gas molecule in this cavity. The energy of interaction between the gas and solvent molecules can then be calculated. Eley (12) considered a two-step process similar to that of Uhlig's but was able to more carefully evaluate the separate contributions of each step in the energy and entropy changes involved. His approach gave a reasonable interpretation of the thermodynamic behaviour of gases in both water and organic solvents, although he showed that the case for water was more complicated, due to the possibility of structural modifications.

If a nonpolar solute (e.g. oxygen) is dissolved in a polar liquid solvent 2 (e.g. water), the chemical potential of the solute is

$$\mu_1 = \mu_1^\circ + RT \ln \frac{f_1}{f_1^\circ}$$

If a salt is now added to the solution the fugacity f_1 will be changed. This change may be an increase (salting-

out) or a decrease (salting-in), and is often quite large.

Certain salts (e.g. those containing tetraalkyl ammonium ions) increase the solubility by more than an order of magnitude (salting-in), and also change the solvent selectivity for various solutes; others decrease the solubility (salting-out). Partial molal properties of the dissolved gas are also profoundly affected by the addition of salt.

Many theories have been put forward to explain these changes (13). Most of these theories can explain cases where increased solubility is observed but can not explain a solubility decrease. Recent papers by Gubbins (14), and Masterton (15) have been able to successfully explain both situations. Gubbins based his method on the perturbation theory for mixtures and applied it to the prediction of the thermodynamic properties of gases dissolved in electrolyte solutions. His theory is found to be superior over previous theories for salt effects. The calculations are best for salting-out systems. The qualitative feature of salting-in is predicted by the theory, but quantitative predictions are not satisfactory for such systems. He attributes this to approximations made in evaluating the perturbation terms.

Pierotti (16) developed a theory of gas solubility

using equations for calculating the reversible work required to introduce a hard-sphere into a fluid. His theory allowed the calculation of the saturation solubility, the heat of solution, and the partial molar volume of the dissolved gas. For both polar and nonpolar solvents good agreement was found between the experimental and calculated properties. Pierotti's theory works very well considering that no assumptions concerning the structure of the solvent were taken into account.

"Two structure models" of water have been successfully used (17, 18) to explain some of the properties of water and aqueous solutions. By using different variants of this model (19) it was shown that the equilibrium between the two forms of water is shifted towards the associated form when gas is dissolved in water. This is in accord with the theory of Frank and Evans (20) concerning the iceberg formation around a dissolved gas molecule, but no reason for such a formation was given.

Ben-Naim and Baer (21) have determined the solubility of argon in water-ethanol mixtures at six temperatures and nine concentrations between 0.015 and 0.25 mole fraction ethanol. At low temperatures there is a maximum in the solubility at low ethanol concentrations. This is explainable in terms of the influence of ethanol on the structure of water. Small amounts of ethanol increase the concentration

of the ice-like form of water at low temperature, at about 30° the ice-like structure of water is breaking down and the argon solubility tends to increase monotonically from its value in pure water to its value in pure ethanol. Dissolved argon itself influences the amount of ice-like water present. The entropies of solution in argon in pure water are negative as compared to pure alcohol. This suggested to Ben-Naim and Baer that the abnormally low entropy of solution of argon in pure water cannot be attributed to an active formation of ice-like water but that the argon shifts the already existing equilibrium toward the ice-like forms. A similar study of argon solubility in water-p-dioxane system is reported by Ben-Naim and Morgan (22). The maximum in the argon solubility at low concentrations and low temperatures seen in the water-ethanol system was not found in the water-dioxane system. This is interpreted to mean p-dioxane has a destabilizing influence on the large compact clusters of water molecules at all p-dioxane concentrations and temperatures studied.

An alternative way of looking at the solubility of gases in water is that recently proposed by Hildebrand (26). Basing his theory on the Pople model (7), he found a linear relation between loss of entropy and molar surface area. He claims that the differences in entropy of gases in

water is a matter of surface area of the molecule rather than of the molecule volume. Molecules and drops of varying sizes could hardly lose entropy in any consistent fashion by surrounding themselves with any reasonable sort of "icebergs".

Yu V. Gurikov (23) has applied a uniform and non-uniform model to a ternary solution of two nonpolar gases in water. On using the uniform model, he found a salting-out effect i.e. the solubility of each component decreases. He found a salting-in effect on using the two-structure uniform model.

Since 1940 a great deal of gas solubility work at high pressure has appeared and the understanding of gas solubility at both low and high pressures has improved (24). Krichevsky and Kasarnovsky (25) have developed a thermodynamic equation for calculating the solubility of slightly soluble gases at high pressure in solvents of low vapor pressure. Their equation is only empirical. The partial molal volumes calculated from their equation seldom agree with the experimentally determined partial molal volumes. They claimed that the departure of \bar{V}_2 from the experimental \bar{V}_2 is taken as a sensitive test for discovery of deviations from Henry's Law. This will be discussed later.

In the light of the above discussion of work previously done on gases dissolved in water it was decided

that two phenomena deserved investigation.

The effect of a second dilute solute upon the saturation solubility of a gas appears to offer a useful way of studying the general water-structure problem. A study has been made of the saturation solubilities of gas mixtures in water. For these systems any effect (salting-in, salting-out) should allow an interpretation that is self-consistent with that explanation of solubility thermodynamic properties of each of the pure gases in water. The systems studied generally included oxygen as one of the components of the gas mixture.

Hildebrand has recently suggested that the comparison of diffusion coefficient data for gases in water and in non-polar solvents may help to elucidate the role of the water cage structure (26). Apart from the practical use of such data, the diffusion coefficient values should be sensitive to possible "structural" features. The gases studied have been chosen because they cover a hydrate decomposition pressure (at 0°C) from 311 atmospheres (CH₃Cl) to 12.3 atmospheres (CO₂) and a decomposition temperature (at 1 atmosphere pressure) from +11.1°C (CH₃Br) to -42.8°C (Ar). Also, studies of the temperature dependence of the diffusion coefficient of a wide range of gases measured using the same experimental technique have been made.

Chapter 1

"If you have had your attention directed to the novelties in thought in your own lifetime, you will have observed that almost all really new ideas have a certain aspect of foolishness when they are first produced."

A.N. Whitehead (1861-1947)

Introduction

The variety of approaches which have been used to determine the solubility of gases in liquids is an adequate testimonial to man's ingenuity. The equipment used ranges in complexity and cost from mass spectrometers to simple van Slyke apparatus, in time from minutes to many hours, and in precision from purely qualitative to the highly precise.

This study is to complement research on the diffusion of gases and mixtures of gases in water. An examination of the literature shows that there is a vast body of data for the solubility of gases in liquids. Unfortunately there exist few measurements of solubility of gas mixtures in liquids. Scarcity of solubility data for mixtures is due, in part to experimental difficulties in analysing for the mixtures.

Volumetric and chemical methods were rejected as being impractical. Electrometric techniques are sensitive to chemical interferences and are restricted to oxygen and hydrogen. As a result, gas chromatography was selected as the most appropriate technique.

Battino (27) in his review of solubility of gases compared the errors in the measurement of solubilities of gases in liquids for a large variety of techniques. Most manometric methods gave a precision of $\pm 2\%$, and the Winkler method for measuring oxygen solubilities gave a

precision of $\pm 3\%$. The gas chromatographic method gave a precision of $\pm 2\%$.

The application of gas chromatography to the determination of small amounts of dissolved gases in solution offers several advantages not found in either manometry or mass spectrometry. The method is less time consuming, sample size can be kept small, the instrumentation is relatively simple, and no loss is experienced in precision. For the case of mixtures of gases in liquids, the g.p.c. has the advantage of resolving for each compound in the mixture.

Gas chromatography has already been applied to analysis of dissolved gases in water. However, the difficulty in obtaining a good sample for analysis has not always received proper considerations. The system selected in this study ensures the removal of the sample without perturbing its equilibrium at a given temperature and pressure.

Equilibrium between the gas and liquid phases has been obtained by shaking a mixture of the two and by bubbling the gas through the liquid. Data obtained by both techniques compare very well.

Data are presented for the solubility of nitrogen, oxygen, argon, methane and carbon tetrafluoride in D_2O and H_2O and for mixtures of methane-oxygen, methane-

nitrogen and nitrogen-oxygen in H_2O and nitrogen-oxygen in D_2O at partial pressures of each component of 0, 0.25, 0.50, 0.75 and 1 atmosphere. Data are also presented for the solubility of nitrogen and oxygen at (0-3) atmospheres, and for the saturation solubility of oxygen at a partial pressure of 0.5 atmosphere in the presence of half atmosphere partial pressure of helium, nitrogen, methane, ethane, and krypton. The results are discussed analytically in terms of the water structure problem.

Thermodynamic relations for solubility of gases in water

1) The Gibbs-Duhem Equation

The Gibbs-Duhem equation provides a basis for calculating the activity of the solvent in a binary solution. It can be shown that for a constant temperature and pressure the total free energy of a homogeneous phase may be expressed as

$$G_{T,P} = \sum_1 n_1 \mu_1 \quad [1]$$

In particular, for a binary mixture, we have

$$G_{T,P} = n_1 \mu_1 + n_2 \mu_2 \quad [2]$$

Differentiation of this relationship leads to

$$dG_{T,P} = \mu_1 dn_1 + \mu_2 dn_2 + n_1 d\mu_1 + n_2 d\mu_2 \quad [3]$$

If eq'n [3] is compared to

$$dG = -SdT + VdP + \mu_1 dn_1 + \mu_2 dn_2 + \dots + \mu_1 dn_1$$

at constant T and P

$$dG_{T,P} = \mu_1 dn_1 + \mu_2 dn_2 \quad [4]$$

Thus,

$$n_1 d\mu_1 + n_2 d\mu_2 = 0 \text{ at constant T and P.}$$

This is known as the Gibbs-Duhem relation. In general form

$$\sum_1 (n_1 d\mu_1)_{T,P} = 0 \quad [5]$$

Since $d\mu_1 = RT d \ln a_1$, we may write eq'n [4] in the following forms for binary mixtures at constant T and P: where a = activity, μ_1 = chemical potential of component 1 and n_1 = mole fraction of 1.

$$n_1 dn_1 + n_2 dn_2 = 0 \quad [6]$$

or, dividing by the total number of moles,

$$X_1 dn_1 + X_2 dn_2 = 0 \quad [7]$$

Hence

$$dn_2 = \frac{-X_1}{X_2} dn_1 \quad [8]$$

One solution for the Gibbs-Duhem arises when all of the components obey the relation (28)

$$P_1 = K_1 X_1 \quad [9]$$

Here K_1 is a function of temperature and pressure only and may or may not be equal to P_1^* - the vapour pressure of the pure component 1.

For simplicity it will be supposed that the total pressure, as well as the temperature, is held constant by the presence in the gaseous phase of a component which is insoluble in the solution. Under these conditions K_1 is constant and thus

$$\begin{aligned} d \ln P_1 &= d \ln K_1 + d \ln X_1 \\ &= d \ln X_1 \\ &= \frac{1}{X_1} dX_1 \end{aligned} \quad [10]$$

Thus, provided that eq'n [9] is satisfied for all components of the solution, we can multiply eq'n [10] through by X_1 and sum over all these components to obtain

$$\sum X_1 d \ln P_1 = \sum dX_1$$

This is clearly zero since $\sum X_1 = 1$. Thus eq'n [9]

satisfies the condition

$$\sum X_1 d \ln P_1 = 0$$

and therefore satisfies the Gibbs-Duhem equation. In brief eq'n [9] is a permissible relation between P_1 and X_1 if it applies to all the components of a particular solution.

Thermodynamical Calculations of Solubilities at High Pressures

A method of calculation of solubilities of gases in one special case where the solubilities of the gases and the vapour pressure of the solvent are small is discussed.

When the concentration of a solute is small the fugacity of the solvent can be calculated by means of Raoult's law, the fugacities of the components being connected according to the equation of Gibbs-Duhem

$$X_1 d \ln f_1 + X_2 d \ln f_2 = 0 \quad [10]$$

(X_1 , X_2 and f_1 , f_2 are mole fractions and fugacities of either solvent and solute respectively).

It can be shown that there exists a direct proportionality between f_2 and X_2 , known as Henry's law

$$f_2 = K X_2 \quad [11]$$

where K is Henry's coefficient.

Wiebe et al (29) have shown that their experimental data on the solubility of gases in water is poorly expressed by equation [11]. It would seem to follow as a thermodynamical consequence that Henry's law would be obligatory for the dissolved gas. But Wiebe et al found that the experimental data are evidently in contradiction to this theoretical deduction.

It is easy to show how the usual equation of Henry has to be corrected in order to predict the solubility of gases

in water.

The integration of the Gibbs-Duhem equation, and supposing that the fugacity of the solvent obeys Raoult's law, gives Henry's law

$$f_2 = KN_2' \quad [12]$$

N_2' is certainly not the experimentally measured concentration of the solute gas. N_2' is the concentration which could be obtained through compensation of the gas pressure by means of the corresponding tension of the solution.

The transition from N_2' to N_2 can be made by means of the well known equation

$$\left(\frac{\partial \bar{G}_2}{\partial P} \right)_T = \bar{V}_2 \quad [13]$$

where \bar{G}_2 is the partial molal free energy of the dissolved gas and \bar{V}_2 is its partial molal volume.

Since the concentration of the gas is small

$$d\bar{G}_2 = RT \, d \ln N_2 \quad [14]$$

Substituting equation [13] into equation [14] gives us

$$\left(\frac{\partial \ln N_2}{\partial P} \right)_T = \bar{V}_2 / RT \quad [15]$$

Integration of equation [15] with the supposition of independence of \bar{V}_2

$$\ln N_2 = \ln N_2' - \frac{\bar{V}_2 P}{RT} \quad [16]$$

From equation (12) and (16) we find

$$\log \frac{f_2}{N_2} = \log K + \frac{V_2 P}{2.303 RT} \quad [17]$$

The second term in equation [17] is very small (10^{-4}) for low pressures. Thus it is safe to say that Henry's law holds for low pressures (<10 atmospheres).

Temperature dependence of solubility

(1) Entropy of solution

The entropy of solution of a solute, ΔS may be related to the temperature coefficient of its solubility by means of the thermodynamic equation

$$\Delta S = - \left[\frac{\partial \Delta G}{\partial T} \right]_{P, X} = \left[\frac{\partial \Delta G}{\partial \ln X_2} \right]_{P, T} \left(\frac{\partial \ln X_2}{\partial T} \right)_{\Delta G, P} \quad [18]$$

The second term on the right is the change of solubility with temperature at constant pressure if $\Delta G = 0$.

In the first term, $\Delta G = RT \ln f_2/f_2^\circ$, where f_2 is the fugacity of the solute in the solution and f_2° is that of the pure solute, that is, f_2° is not a function of X .

Thus we can write

$$\left[\frac{\partial \Delta G}{\partial \ln X_2} \right]_{T, P} = RT \left(\frac{\partial \ln f_2}{\partial \ln X_2} \right)_{P, T} = RT \left(\frac{\partial \ln a_2}{\partial \ln X_2} \right)_{P, T} \quad [19]$$

Thus, equation (18) becomes

$$\Delta S = R \left(\frac{\partial \ln X_2}{\partial \ln T} \right)_{P, \text{sat.}} \left(\frac{\partial \ln a_2}{\partial \ln X_2} \right)_{P, T} \quad [20]$$

In the dilute region, where Henry's law holds (i.e. $a_2 = KX_2$), $\frac{\partial \ln a_2}{\partial \ln X_2} = 1$. Thus equation [20] becomes

$$\Delta S = R \left(\frac{\partial \ln X_2}{\partial \ln T} \right)_{P, \text{ sat.}} \quad [21]$$

Thus, a plot of $\ln X_2$ versus $\ln T$ gives a straight line with slope $\frac{\Delta S}{R}$.

(ii) Enthalpy of solution

Since at saturation solubility $\Delta G = 0$, we may write for the enthalpy of solution,

$$\Delta H = T\Delta S = RT \left(\frac{\partial \ln X_2}{\partial \ln T} \right)_{P, \text{ sat.}} \left(\frac{\partial \ln a_2}{\partial \ln X_2} \right)_{P, T} \quad [22]$$

$$= -R \left[\frac{\partial \ln X_2}{\partial \left(\frac{1}{T} \right)} \right]_{P, \text{ sat.}} \left(\frac{\partial \ln a_2}{\partial \ln X_2} \right)_{P, T} \quad [23]$$

Again, in the dilute region, where Henry's law holds (i.e. $a_2 = kX_2$)

$$\frac{\partial \ln a_2}{\partial \ln X_2} = 1$$

Thus equation [23] becomes

$$\Delta H = -R \left[\frac{\partial \ln X_2}{\partial \left(\frac{1}{T} \right)} \right]_{\text{sat.}, P} \quad [24]$$

(iii) Thermodynamic properties for statistical thermodynamics and the partition function

We will consider, for simplicity, that the only parameter determining the energy levels ϵ_1 is the volume. For corrected boltzons,

$$S = k \ln t = k \Sigma (N_1 \ln \frac{G_1}{N_1} + N_1) \quad [25]$$

Substituting $N_1/G_1 = (N/q) e^{-\beta \epsilon_1}$ into the logarithm term, but keeping the other N_1 's

$$\frac{S}{k} = (\Sigma N_1) \ln q/N + \beta \Sigma N_1 \epsilon_1 + \Sigma N_1 \quad [26]$$

From the Helmholtz free energy A,

$$A = E - TS = -kNT \ln \frac{q}{N} - kNT \quad [27]$$

The chemical potential is given by $\mu = \left(\frac{\partial A}{\partial N} \right)_{T,V}$.

Remembering, q is not a function of T and V but of N

$$\begin{aligned} \mu &= \left(\frac{\partial A}{\partial N} \right)_{T,V} = -kT \ln \frac{q}{N} - kNT \frac{\partial [\ln q/N]}{\partial N} - kT \\ &= -kT \ln \frac{q}{N} \end{aligned} \quad [28]$$

For the Gibbs free energy $G = N\mu$; so

$$G = -k NT \ln \frac{q}{N} \quad [29]$$

Experimental Procedures

Gas chromatography provides a convenient and rapid means for the determination of the solubility of gases in water. Dissolved gases are readily removed from solution by dispersing a stream of helium carrier gas through the liquid sample and passing the gases to a suitable detector. Techniques based on this principle involving the syringe injection of a liquid sample into a suitable gas stripping cell have been described by Gubbins (30) and Swinnerton (31). However, the transfer of the sample may readily lead to errors particularly when the liquid temperature differs appreciably from the ambient. The technique described below overcomes these difficulties and simplifies the operation involved.

The Varian Aerograph gas chromatograph Model 90-3 was used in this work. This instrument employs a compact single column and uses a thermal conductivity type detector. The output signal from the detector was recorded on a 1mv -Varian Aerograph Model 20 recorder, with a chart speed of $\frac{1}{2}$ inch per minute.

The apparatus is set up as shown in Fig. 1. All connections through which the gas and water pass were made with swagelock fittings (Columbia Valve Fittings) to avoid absorption and contamination with grease.

The vacuum line was constructed entirely of Pyrex glass with the analysis line of copper tubing ($\frac{1}{8}$ "). This apparatus has facilities for degassing the solvent, measuring and transferring the gas mixture, saturating the solvent, obtaining samples of the saturated mixture and then its gas chromatographic analysis. These specialized facilities were interconnected to allow quantitative and efficient handling of the materials.

(1) Degassing Technique

The solvent (distilled water) was degassed by a sublimation technique. The degassing unit is shown in, Fig. 1 . About 20 mls of distilled water is poured into A through the Whitey valve ($\frac{1}{4}$ "). This valve is then closed and a liquid nitrogen 'trap' is slowly placed under the bulb (A) until all the water is frozen. The stop-cock B is then opened to the vacuum line to evacuate the complete unit. During the complete degassing process the Hg diffusion pump is isolated. The liquid nitrogen trap is then removed. Liquid nitrogen is then poured into the cold finger C. The bulb is then heated with a heat-gun to vaporize the frozen water onto the cold finger. This process takes about two hours - i.e., evacuating and vapourizing all the water. The vacuum is then closed off at B. The frozen water on the cold finger

Fig. 1

Solubility apparatus

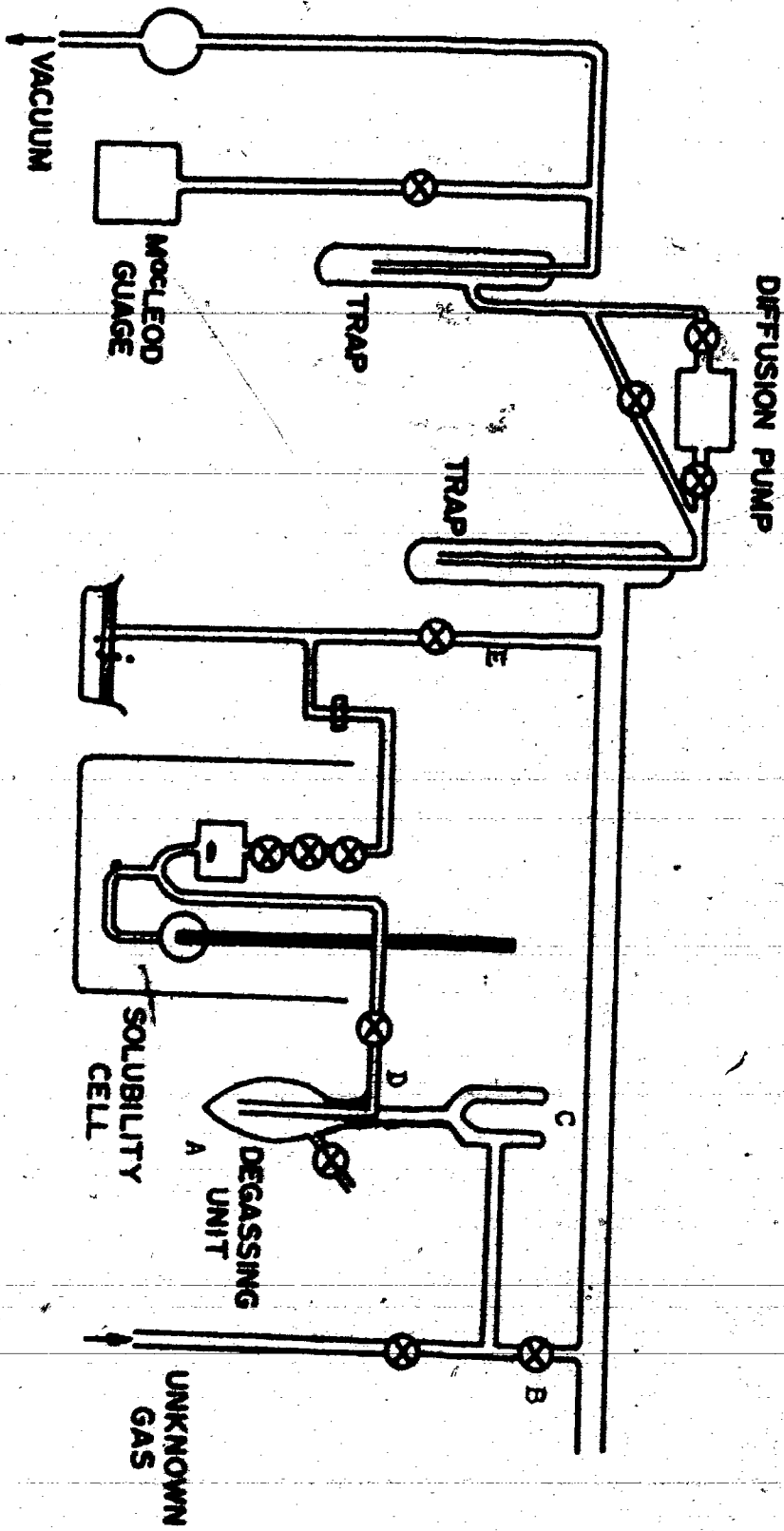


Fig. 1

melts and runs back into bulb A.

Preliminary runs were done to test the efficiency of this degassing process. Samples of the degassed distilled water were analysed on the gas chromatograph to test for any gases remaining. There was no detectable trace when run at maximum sensitivity on the gas chromatograph.

(2) The Vacuum Line

Evacuation of the apparatus to a pressure of 10^{-6} torr was achieved by a large single-stage mercury diffusion pump backed by a mechanical oil pump (Precision Scientific Co., Model No. 75). Situated between the diffusion pump and the mechanical pump was a removable trap immersed in liquid nitrogen to protect the pump from evacuated contaminants. In addition another mechanical pump (Precision Scientific Model No. S35) was connected to selected parts of the apparatus, including a portable hose attachment so that various operations requiring only partial evacuation could be performed. A McLeod gauge was used to measure the pressure in the system.

(3) Saturation Technique

The saturation solubility cell is shown in Fig. 1

The solubility cell is connected to the degassing unit at D, a side arm from the bulb A. The solubility cell is also connected to the vacuum line at point E. The saturation solubility cell was thoroughly evacuated (10^{-6} mm Hg) and thermostated to $25.00 \pm 0.01^{\circ}\text{C}$ by a water tank controlled by a Haake thermostat unit. The temperature was read on a Quartz thermometer which had been standardized at ice-water and dry-ice acetone temperatures. As the solubilities of the gases in water are very small ($X_2 \sim 10^{-5}$), a fluctuation of $\pm 0.10^{\circ}\text{C}$ affects the solubility only $\pm 0.05\%$ (27), thus the temperature control used in these experiments affects the mole-fraction solubility (X_2) in the second decimal place. About 20 ml of the degassed water was pushed into the solubility cell by means of the gas or the gas mixture under study. The gas was then bubbled through the base of the solubility cell. The water was stirred by a magnetic operated stirring bar ($\frac{1}{2}$ ") from the outside of the thermostated tank. This method of achieving equilibrium avoided the possibility of supersaturation. Equilibrium saturation solubility was found to be reached after bubbling and stirring for about 12 hours.

(4) Sample Collection

After saturation, the solution was allowed to

settle so as to allow the bubbles of gas in the solution to rise. The saturated solvent was slowly displaced upwards by mercury into three sample tubes of known volume. These are connected to the saturation cell and also thermostated in the same tank. The volume of each sample tube is $1.00 \pm .001$ mls. The valves of each sample tube were then closed and the tubes removed from the thermostated tank. The tubes were then disconnected from the solubility cell.

(5) Analysis Technique

The sample tube was placed in the gas stripping line for analysis, diagrammatically represented in Fig. 2. During the equilibration period for the gas chromatograph to warm up and attain best working conditions, stopcock 4 was closed and stopcock D was adjusted to position 2 so that the helium carrier gas by-passed the solubility sample cell and passed directly to the column and the detector.

The lines connecting the sample tube were then evacuated through stopcock 3, with stopcock 4 closed, 5 and 6 were opened and the Hg level from bulb C at the mark A. Stopcock 3 was then closed and the Hg level from bulb C was brought to the mark B. Stopcock 4 was then opened and stopcock 5 closed. The three-way ball valve D (Columbia Valve) was then adjusted to position

Fig 2

Schematic diagram of apparatus for analysis of dissolved gas.

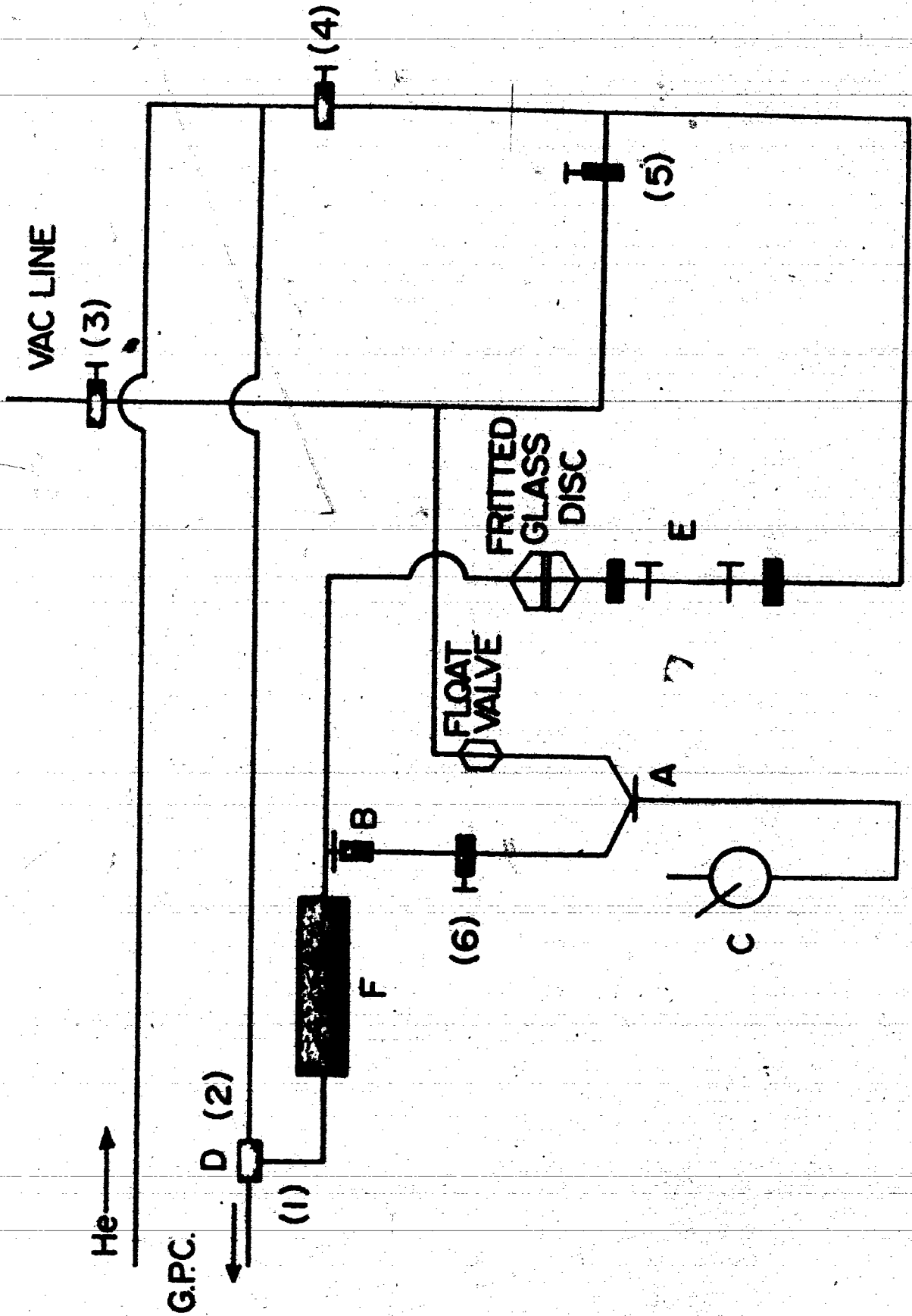


FIG 2

1. The sample valve is opened and the helium pushes the sample via the medium fritted glass disc. Dissolved gas was rapidly stripped from the sample by the helium gas stream and passed to the detector via the drying tube (F) which served to remove the solvent vapour. The drying tube contained a 50:50 mixture of anhydrous calcium chloride and calcium sulphate. The column used to separate the gases was a 6 feet by $\frac{1}{4}$ inch 30-60 mesh molecular sieve 5A. A slight modification to the Varian Aerograph gas chromatograph was undertaken so as to allow analysis to be done at 0°C. A dummy column was placed in the oven and the separating column was connected outside the injection port and the by-pass. All analyses were done with the column immersed in an ice-bath. This proved to be very effective for achieving separation of all the gases used.

Upon elution from the column the products were analysed on a Varian Aerograph Model 90-P3. The detector was maintained at 50°C and the filament current at 150 mamps. Signals from the gas chromatograph were fed into an Aerograph Model 20 recorder.

Helium used as the carrier gas was dried by passing it through a molecular sieve column. The divided flow was maintained at 70 ml per minute through the reference side of the detector.

The accuracy of the method of analysis depends on the accuracy of calibration. The gas chromatograph was calibrated by determining the peak areas of measured samples of the pure gas over a range roughly corresponding to the range of solubilities obtained in these experiments. Areas were measured with a Gelman 39321 planimeter.

A plot of the measured peak area vs the number of moles of gas, calculated from PVT relationships, gives a straight line calibration curve with intercept zero, showing the required linearity between the concentration of a gas and instrument response. From the calibration curve the concentration of dissolved gas can be estimated to $\pm 0.05\%$. Random errors may be expected to occur from ambient temperature changes, fluctuations in carrier gas flow rate and time variations in the stripping of the solution by the carrier gas. To estimate the combined effect of these variables on the precision of the method, a known sample of the gas was done prior to doing runs on that day.

(b) Gas Mixture

The required gas mixture was made by using a flow rate technique. Nupro Double Pattern very fine metering valves are used for extremely accurate flow control (as low as 100 cc per hour for gases). The two flow rates are set by the valves in the ratio desired. The

gases are mixed in a bulb (1000 cc) and then passed through a glass coil (6 ft) which is in the thermostated tank before being bubbled through the solubility cell. A sample of the gas mixture is analysed, before passing through the solubility cell, on the gas chromatograph to check the proportion of the gases. This was done at three hour intervals to ensure that the flow rate did not change.

(7) Pressure Apparatus

Owing to the experimental difficulties, gas solubilities measured at high pressure are seldom very accurate and are often unsuitable for calculation of the derived thermodynamic quantities. The determinations consist essentially in bringing the solvent into equilibrium with the gas at a known total pressure, taking a sample of the liquid phase and determining its composition. Individual methods differ in the manner in which the attainment of equilibrium is accelerated (stirring, shaking, circulating the liquid or bubbling the gas) and as to whether sampling is continuous or intermittent. Sampling is the most critical operation and no method has yet been devised which is entirely free from objections. The difficulties arise from lack of visual control and the large concentration gradients which may occur during the withdrawal of samples. The present method has the advantage of being accurate and relatively simple.

The apparatus consists of three parts:

- (i) gas line, for compressing the gases.
- (ii) an equilibrium apparatus in which the solvent is saturated with gas and from which a sample of the liquid phase is taken at constant temperature and pressure.
- (iii) an apparatus for analyzing the sample.

The equilibrium apparatus (fig 3) comprises the equilibrium bomb A, of capacity 1000 ml, containing the two-phase system, connected to a Bourdon tube gauge and mounted on a cradle, so that it may be rocked to accelerate the attainment of equilibrium, and the sampling cylinder B (capacity 1 ml), which is fitted with a needle valve at each end and filled with gas at the same pressure as the equilibrium vessel.

In carrying out a determination, the evacuated vessel A is filled with 100 mls of distilled water, and pumped out to remove dissolved air. The gas is then introduced from the lecture bottles via the gas lines and the vessel is rocked in a thermostat using a Bodine stirrer (37 lbs Torque, 4.5 r.p.m. 60 cycles 115 V).

After attainment of equilibrium (indicated by a 12 hour constancy of gas pressure), the valve at the bottom of the equilibrium vessel is opened and the sample is withdrawn by letting the column of solution slowly displace the gas in the sampling vessel through a needle valve. At the same time, the pressure in the equilibrium

Fig. 3

High Pressure Apparatus

HIGH PRESSURE APPARATUS

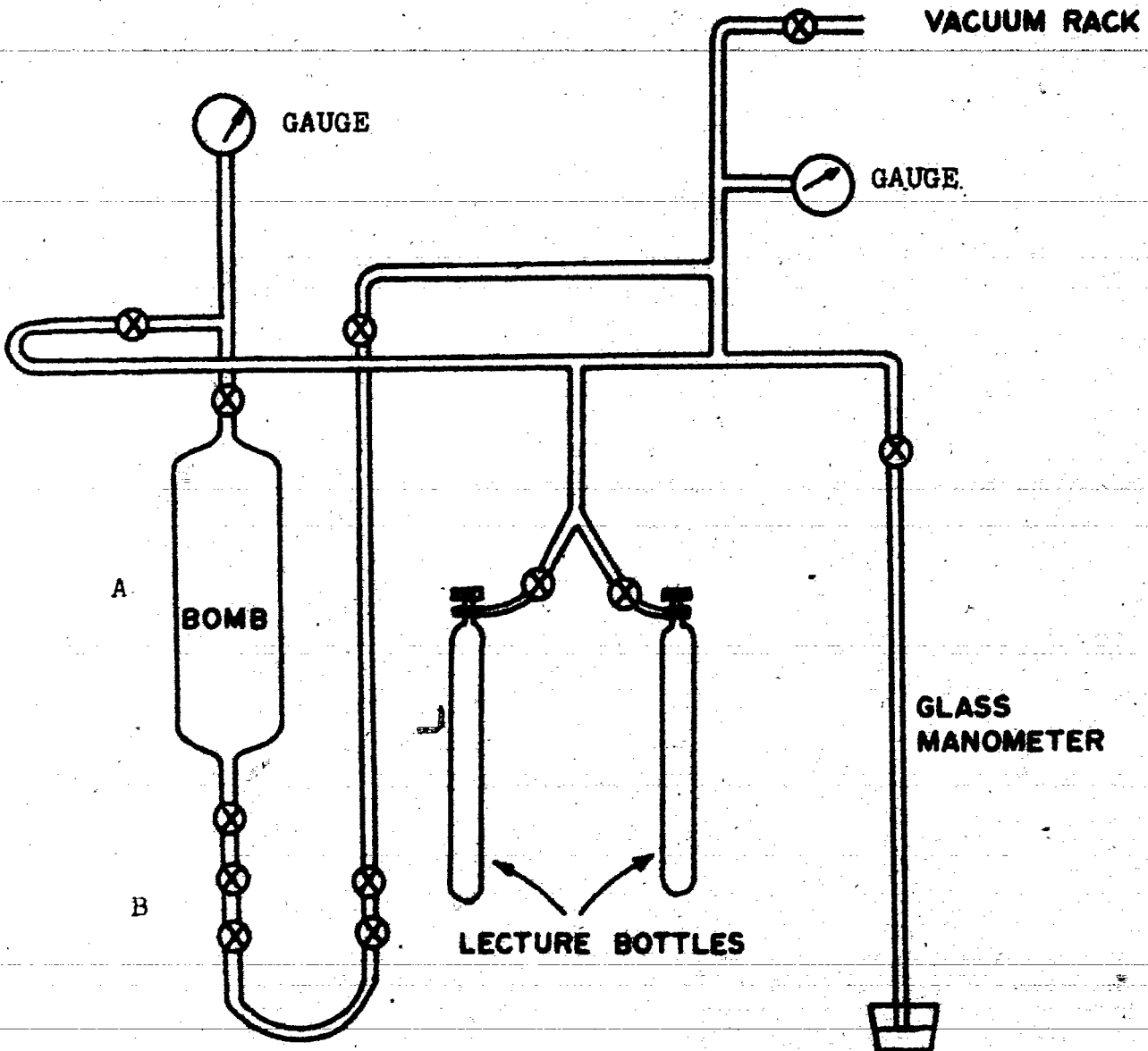


Fig. 3

vessel is maintained constant to ± 0.03 atmos by admitting gas from the gas line. In effect, the equilibrium and the sampling vessels form two arms of a U-tube and the solution is allowed to rise slowly in the arm represented by the sampling vessel and is isolated there at the end of the process.

Constancy of temperature to within $\pm 0.02^\circ\text{C}$ is ensured by housing the equilibrium and sampling vessels in a large water thermostat. The temperature was read off a Quartz thermometer. The sample tube is taken off and replaced by another one. The sample is analyzed on the gas chromatograph - the technique which has been discussed before.

The Oxygen Analyzer

The Beckman Model 777 Laboratory Oxygen Analyzer is a direct-readout instrument for the analysis of gaseous and dissolved oxygen. Based on the polarographic principle, it combines the simplicity required in many applications with a high degree of precision and repeatability.

Two basic units - a sensor and an amplifier - form the analyzer. The sensor detects the oxygen content, and the amplifier amplifies and attenuates the sensor signal, which may be read directly on the meter.

(a) The Sensor

The sensor consists of a gold cathode separated by an

epoxy casting from a tubular silver anode. The anode is electrically connected to the cathode by a layer of potassium chloride gel. The entire anode-cathode assembly is separated from the sample by a gas-permeable Teflon membrane which fits firmly against the cathode surface. The inner sensor body is contained in a plastic housing and comes in contact with the sample only through the Teflon membrane. When oxygen diffuses through the membrane, it is electrically reduced at the cathode by an applied voltage. ($\approx .8V$) This reaction causes a current to flow between the anode and cathode which is proportional to the partial pressure of oxygen in the sample.

(b) The Amplifier

Amplification is achieved in two stages. A preamplifier first picks up the sensor direct current signal and converts it to an alternating current signal which is then amplified. The amplified signal is demodulated to direct current again, to move the meter needle.

As a check on our solubility of mixtures of gases in water results, use was made of the Beckman Model 777 Laboratory Analyzer described above. This procedure of analyzing for oxygen eliminates the transferring and handling of the samples.

The oxygen electrode is placed vacuum tight in a small cell which is attached to the modified high pressure apparatus.

(i) Error Analysis of Results

A typical experimental result:

Saturation solubility of oxygen in water at $25.00 \pm 0.01^\circ\text{C}$ and 1.00 atmos pressure.

<u>Number of run</u>	<u>Saturation solubility of O_2 in water as Bunsen coefficient $\times 10^3$</u>
1	28.65
2	28.67
3	28.69
4	28.65
5	28.68
6	28.69

Average = 28.67

Standard deviation of the mean = ± 0.02

Typical measurement of the area of a peak by the Planimeter

<u>Number of run</u>	<u>Units on Planimeter</u>
1	132
2	130
3	131
4	133
5	132
6	131

Average = 132

Standard deviation of mean = ± 1.08

Since 1 unit corresponds to 0.0645 cm^2

Standard deviation of mean on area (cm^2) = ± 0.07

From the calibration curve an error of $\pm 0.05 \text{ cm}^2$ makes a negligible error in the solubility, thus the error in the measurement of the area is so small, one can neglect it.

One can say then that no loss in error is incurred from the measurement of areas of the peaks, the only error is between run to run, giving a standard deviation of ± 0.02 .

Temperature control

Battino (27) calculated an error of 0.05% in the solubilities of gases in water for a change of $\pm 0.1^\circ\text{C}$. This error is not large enough to effect the result, as we can maintain the temperature to $\pm 0.01^\circ\text{C}$.

Calibration curve

One can read off solubilities to $\pm 0.05\%$. This error is not large enough to effect our results. Fig. 4(a).

Cell size

The cells are calibrated to $\pm 0.001 \text{ mls}$. This error in volume corresponds to an error less than 0.01% which is negligible.

Fig. 4(a)

Calibration Curve - dissolved oxygen
(at 25.00°C)

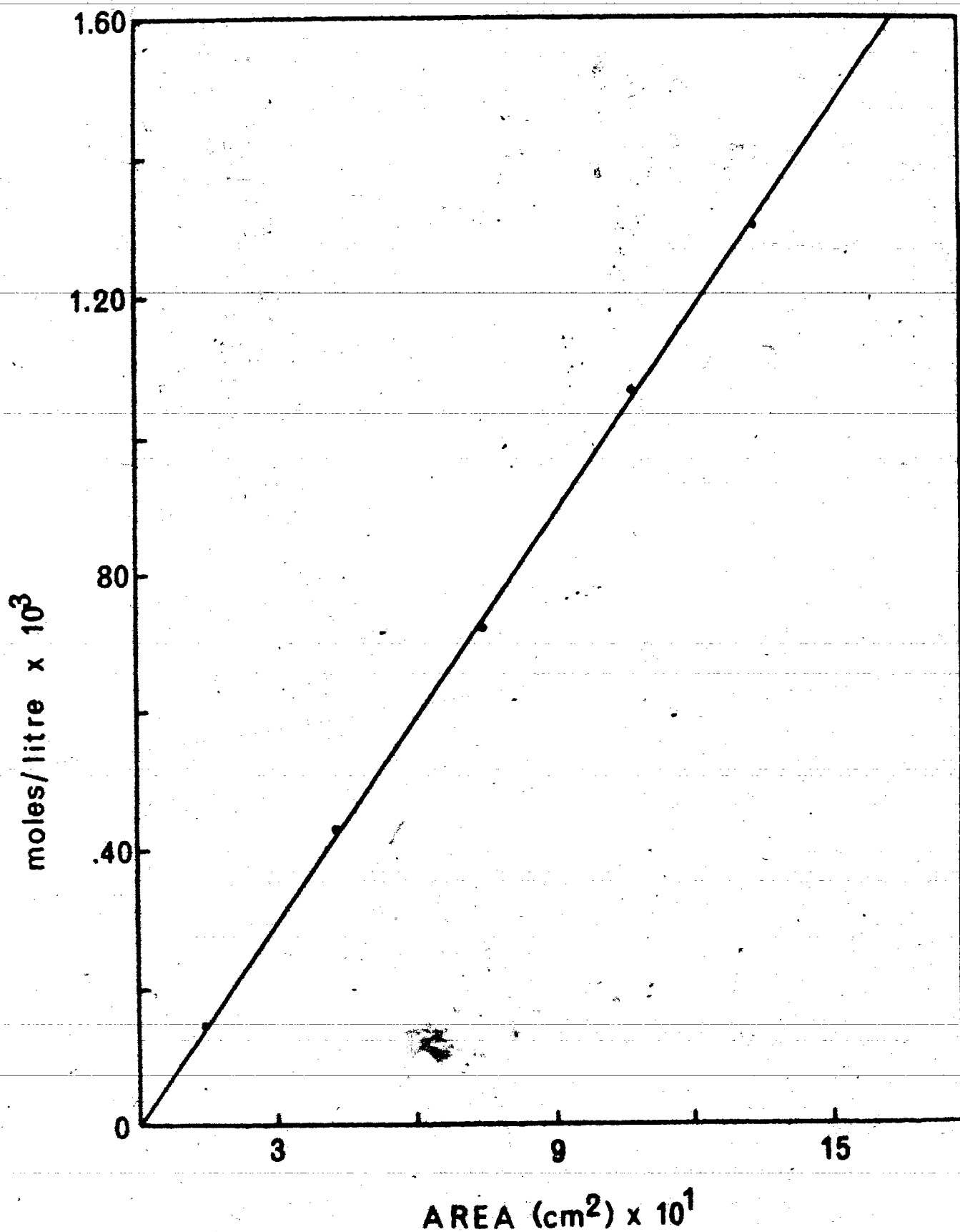


FIG. 4A

RESULTS

The solubilities of oxygen, nitrogen, methane, carbon tetrafluoride and argon were measured in D_2O and H_2O at $25^\circ C$. The results are recorded in Table IIIb. These results allow a comparison of the solubilities to be made with data obtained using the same experimental technique. The values are also compared with the already published literature values. Only our value for the saturation solubility of nitrogen in water (H_2O) is significantly unlike the values obtained by other workers for the solubilities of pure gases in water. We have checked our value several times and we are unable to account for the disagreement with other workers (Table I). As far as is known by the author, the only previous data for the solubility of gases in D_2O is that for argon (32) and for methane, ethane, n-butane and benzene (33). As is seen in Table IIIb, our values for argon and methane in D_2O compare very well with those of Ben-Naim. As the results agree with the already published values (except for nitrogen) the gas chromatographic technique is a reliable one for measuring solubilities of gases in water.

The solubilities of pure oxygen and nitrogen in distilled water were measured using the solubility apparatus modified for measuring solubility at high pressures. These values compare very well with the already published

literature values (27). The saturation solubility value obtained at one atmosphere pressure compares very well with the value using the "gas-bubbling" saturation technique.

The solubility of oxygen and of nitrogen in water at 25°C was measured at partial gas pressures of 0.25, 0.50, 1.00, 2.00 and 3.00 atmospheres.

Henry's Law type plots were done - i.e. a plot of Patmos vs concentration (Fig. 4). Straight lines were obtained - the slope of which is the Henry's Law constant (K). The solubility values compare within 1% of the already published literature value (25) and the K value consistent with the measured pressure value (16).

In Table II we give saturation solubility values for each component of the three mixtures studied (oxygen-methane, methane-nitrogen, nitrogen-oxygen), at partial pressures of each component of 0, 0.25, 0.50, 0.75 and 1 atmosphere. All data have been measured at a total pressure of one atmosphere and at a temperature of 25.00 ± 0.01°C.

In figure 5, typical plots of the saturation solubility as a function of partial pressure are shown. The plots demonstrate the depression in solubility from the expected Henry's Law line. The curves for the sum of the

mole/litre solubilities of the two dissolved gases are also drawn.

A pressure dependence of the solubility of oxygen-nitrogen mixtures in distilled water was measured over the range 0.5 to 3.0 atmospheres, keeping the pressure of oxygen constant at 0.50 atmosphere. A plot is given in Fig. 6. The plot demonstrates the depression of the solubility from the expected Henry's Law line. Data are given in Table 6.

In Table IV we present data for the saturation solubility of oxygen at a partial pressure of 0.5 atmosphere in the presence of a half atmosphere partial pressure of helium, nitrogen, ethane, methane and krypton.

In Figure 7, the solubility of oxygen at $P_{O_2} = 0.5$ atmosphere against that of the other component gas as a pure gas at a pressure of 1 atmosphere is shown.

It is seen that a considerable depression in solubility (as compared to the saturation solubility of pure oxygen in water at a half atmosphere pressure) occurs with gases both more soluble and less soluble than oxygen. For the He, C_2H_6 , and Kr runs, analysis of the water samples was made only for the dissolved oxygen content.

As our results are somewhat unexpected, experiments were made to ensure the observed behaviour was free from some sort of systematic error.

(1) In the above experiments, a gas mixture of the required composition was bubbled through the water until saturation was achieved. Some runs were made in which the water was first saturated by bubbling through one of the gases at one atmosphere pressure and then bubbling into this solution the gas mixture with each component at a partial pressure of 0.5 atmosphere. Good agreement between the two variations on technique was obtained.

(2) Some runs were also done without the drying tube in the gas analysis line and using a Poropak Q column. The Poropak Q resolves the water peak downfield from the gas mixture. Good agreement between the two methods was obtained.

(3) Some runs were done using mixed gases obtained from Matheson and Co. Ltd., to ensure the mixing of our gases is an accurate technique. Two mixtures were done - 52% O_2 + 48% N_2 and 20.9% O_2 + 79.1% N_2 . The data obtained fell on the curve obtained using our mixing technique.

In figure 8 recorder output peaks are given for an O_2/N_2 mixture in water at 25°C.

Some runs were also done using the oxygen electrode to measure the oxygen saturation solubility in a 1:1 mixture of oxygen and nitrogen at a total pressure of 1 atmosphere. The instrument was calibrated by obtaining

percentage saturation for known pure oxygen saturation solubilities at 0.50 and 1 atmosphere (Fig. 9). Our value for the oxygen saturation solubility in the 1:1 mixture of nitrogen and oxygen compared very well with our previous value obtained from the techniques described previously.

As these experiments agree within 1% of the results using the previous method, it can be said that there is no obvious systematic error involved in the method used for obtaining saturation solubilities.

TABLE I

Saturation solubility comparison

of gases in water at $25.00 \pm 0.01^\circ\text{C}$ and 1.00 atmos.

α = Bunsen coefficient[†]

Gases	This Work $\alpha \times 10^3$	Winkler (a) Method $\alpha \times 10^3$	Volumetric Method $\alpha \times 10^3$	Gas Chromato- Method
Oxygen	$28.67 \pm .01$	$28.54 \pm .03$	28.48 ± 0.02 (b)	$28.62 \pm .01$ (i)
Nitrogen	$16.13 \pm .02$	-	28.50 ± 0.02 (c)	$14.80 \pm .02$ (l)
Methane	$29.12 \pm .02$ (-	14.66 ± 0.02 (b)	
			14.63 ± 0.02 (d)	
			30.86 ± 0.01 (e)	$29.05 \pm .01$ (j)
Argon	$31.14 \pm .01$	-	31.73 ± 0.02 (f)	
			31.21 ± 0.02 (g)	
Carbon- tetrafluoride	4.93 ± 0.02	-	31.18 ± 0.02 (h)	
			4.88 ± 0.03 (h)	

[†] $\alpha = \frac{CR 273}{p}$ where C = concentration in moles/litre

- (a) C.N. Murray and J.P. Riley, Deep-Sea Research, 16, 311 (1969).
- (b) C.E. Klots and B.B. Benson, J. Marine Res., 21, 48 (1963).
- (c) T.J. Morrison and F. Billett, J. Chem. Soc., 3819 (1952).
- (d) J.C. Morris, W. Stumm and H.A. Galal, Proc. Amer. Civil Engrs. 85, 81 (1961).
- (e) K.W. Miller and J.H. Hildebrand, J. Amer. Chem. Soc., 90, 3001 (1968).
- (f) R.A. Pierotti, J. Phys. Chem., 69, 281 (1965).
- (g) A. Ben-Naim and S. Baer, Trans. Farad. Soc., 59, 2735 (1963).
- (h) J.T. Ashton, R.A. Dawe, K.W. Miller, E.B. Smith and B.J. Stickins, J. Chem. Soc. (C) 1793 (1969).
- (i) J.W. Swinnerton, V.J. Linneboom^{es} and C.H. Cheek, Anal. Chem., 34 483 (1962)
- (j) C. McAuliffe, Nature, 200, 1092 (1963).

TABLE II
SATURATION SOLUBILITY OF GAS MIXTURES IN H₂O
AT 25.00°C ± .01

1. <u>N₂-O₂ System</u>					
P _{O₂} (atmos)	0	0.25	0.50	0.75	1.0
10 ⁵ X _{O₂}	0	0.43 ± .01	0.85 ± .02	1.50 ± .03	2.30 ± .04
10 ⁵ X _{N₂}	1.30 ± .03	0.86 ± .02	0.52 ± .01	0.19 ± .01	0
2. <u>CH₄-O₂ System</u>					
P _{O₂} (atmos)	0	0.25	0.50	0.75	1.0
10 ⁵ X _{O₂}	0	0.52 ± .01	1.05 ± .02	1.72 ± .03	2.30 ± .04
10 ⁵ X _{CH₄}	2.34 ± .04	1.64 ± .03	0.95 ± .02	0.46 ± .01	0
3. <u>CH₄-N₂ System</u>					
P _{N₂} (atmos)	0	0.25	0.50	0.75	1.0
10 ⁵ X _{N₂}	0	0.23 ± .01	0.54 ± .01	0.86 ± .02	1.30 ± .03
10 ⁵ X _{CH₄}	2.34 ± .04	1.64 ± .03	1.10 ± .02	0.41 ± .01	0

All data measured at 25.00°C (± 0.01) and at 1 atmosphere total pressure.

TABLE III

SOLUBILITY OF O₂/N₂ MIXTURE FROM
0-3.00 ATMOS AT CONSTANT P_{O₂} = 0.50 ATMOS.

a)

P _{O₂}	P _{N₂}	O ₂ m/l x 10 ³	N ₂ m/l x 10 ³
0.50	0.50	0.47 ± .01	0.30 ± .01
0.50	1.50	0.40 ± .01	1.05 ± .02
0.50	2.50	0.35 ± .01	1.77 ± .03

SOLUBILITY OF GASES IN D₂O AND H₂O @ 25°C

α = BUNSEN COEFFICIENT

b)

[data at 1 atmos: pressure]

Gases	H ₂ O	D ₂ O	H ₂ O	D ₂ O
	α x 10 ³	α x 10 ³	α x 10 ³ Ben-Naim(53)	α x 10 ³ Ben-Naim(53)
Ar	31.14 ± 0.01	33.26 ± 0.01	31.21 ± 0.02	33.76
O ₂	28.67 ± 0.01	23.52 ± 0.01	28.48 ± 0.02	-
N ₂	16.13 ± 0.02	16.64 ± 0.02	14.66 ± 0.02	-
CH ₄	29.12 ± 0.02	32.47 ± 0.02	30.33 ± 0.02	32.97
CF ₄	4.93 ± 0.02	6.27 ± 0.02	4.88 ± 0.03 ^(a)	-

(a) J.T. Ashton, R.A. Dawe, K.W. Miller, E.B. Smith and B.J. Stickins, J. Chem. Soc.(C), 1793 (1969).

TABLE IV

Comparison Table for Methods Discussed Above.

SOLUBILITIES ($X_2 \times 10^5$) IN H₂O

AT 25.00 ± 0.01°C

System	This Method		Previous Method	
(1) CH ₄ /O ₂ 1:1	CH ₄ : 0.94 x 10 ⁺⁵	O ₂ : 1.02 x 10 ⁺⁵	CH ₄ : 0.95 x 10 ⁺⁵	O ₂ : 1.05 x 10 ⁺⁵
(2) CH ₄ /O ₂ 1:1	CH ₄ : 0.94 x 10 ⁺⁵	O ₂ : 1.03 x 10 ⁺⁵	CH ₄ : 0.95 x 10 ⁺⁵	O ₂ : 1.05 x 10 ⁺⁵
(3) N ₂ /O ₂ 48%:52%	N ₂ : 0.46 x 10 ⁺⁵	O ₂ : 0.95 x 10 ⁺⁵	N ₂ : 0.45 x 10 ⁺⁵	O ₂ : 0.95 x 10 ⁺⁵
79.1%:20.9%	N ₂ : 0.23 x 10 ⁺⁵	O ₂ : 0.39 x 10 ⁺⁵	N ₂ : 0.23 x 10 ⁺⁵	O ₂ : 0.38 x 10 ⁺⁵

107

Fig.4

Pressure Dependence of solubilities O_2 and N_2 in water.

Legend

O Oxygen

X Nitrogen

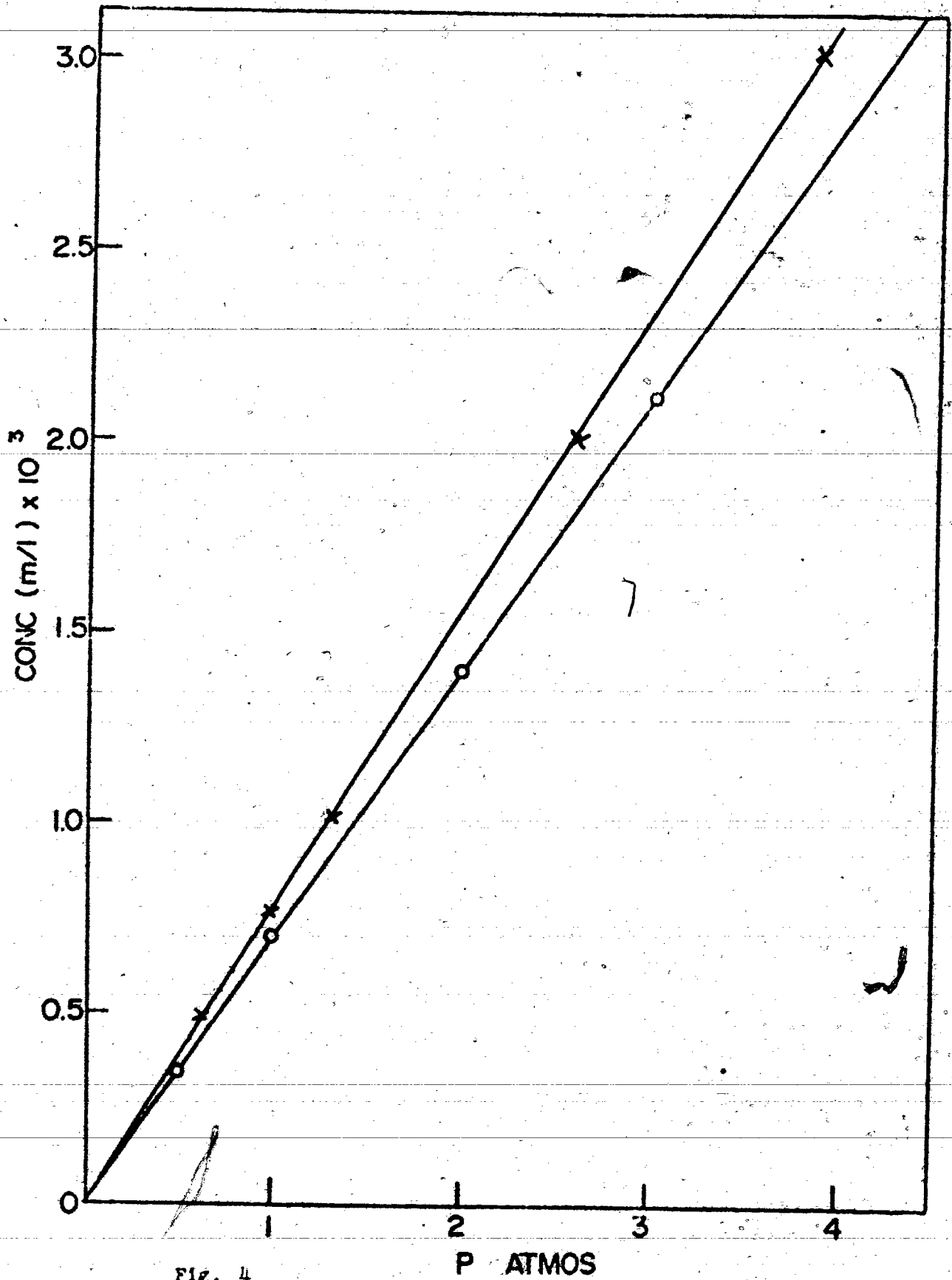


Fig. 4

Fig 5

Saturation solubility of O_2-CH_4 and O_2-N_2 gas mixtures at various partial pressures of oxygen. Solvent, water. Temperature $25.00^\circ C$. 1 atmosphere total pressure.

Legend:

Open data points - Nitrogen/Oxygen;

Δ nitrogen, \circ oxygen.

Solid data points - Methane/Oxygen;

\blacktriangle methane, \bullet oxygen.

Total mole/litre of $CH_4 + O_2$, \blacklozenge

Total mole/litre of $N_2 + O_2$, \diamond

MOLES / LITRE

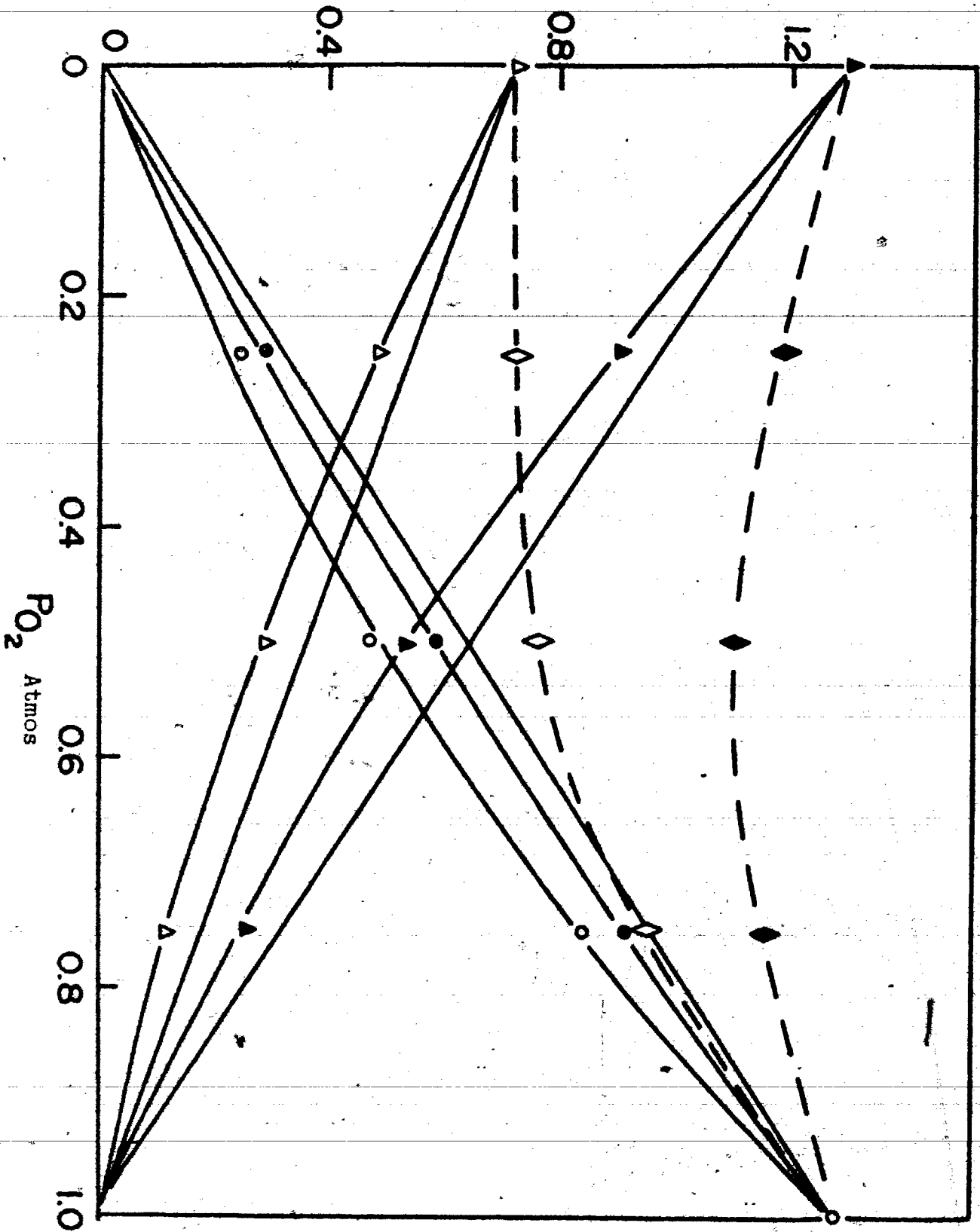


Fig 5

Fig. 6

Pressure dependence of the solubility of N_2 gas in the presence of oxygen at a constant partial pressure of 0.5 atmos.

NITROGEN
CONC. $\times 10^3$ m/l

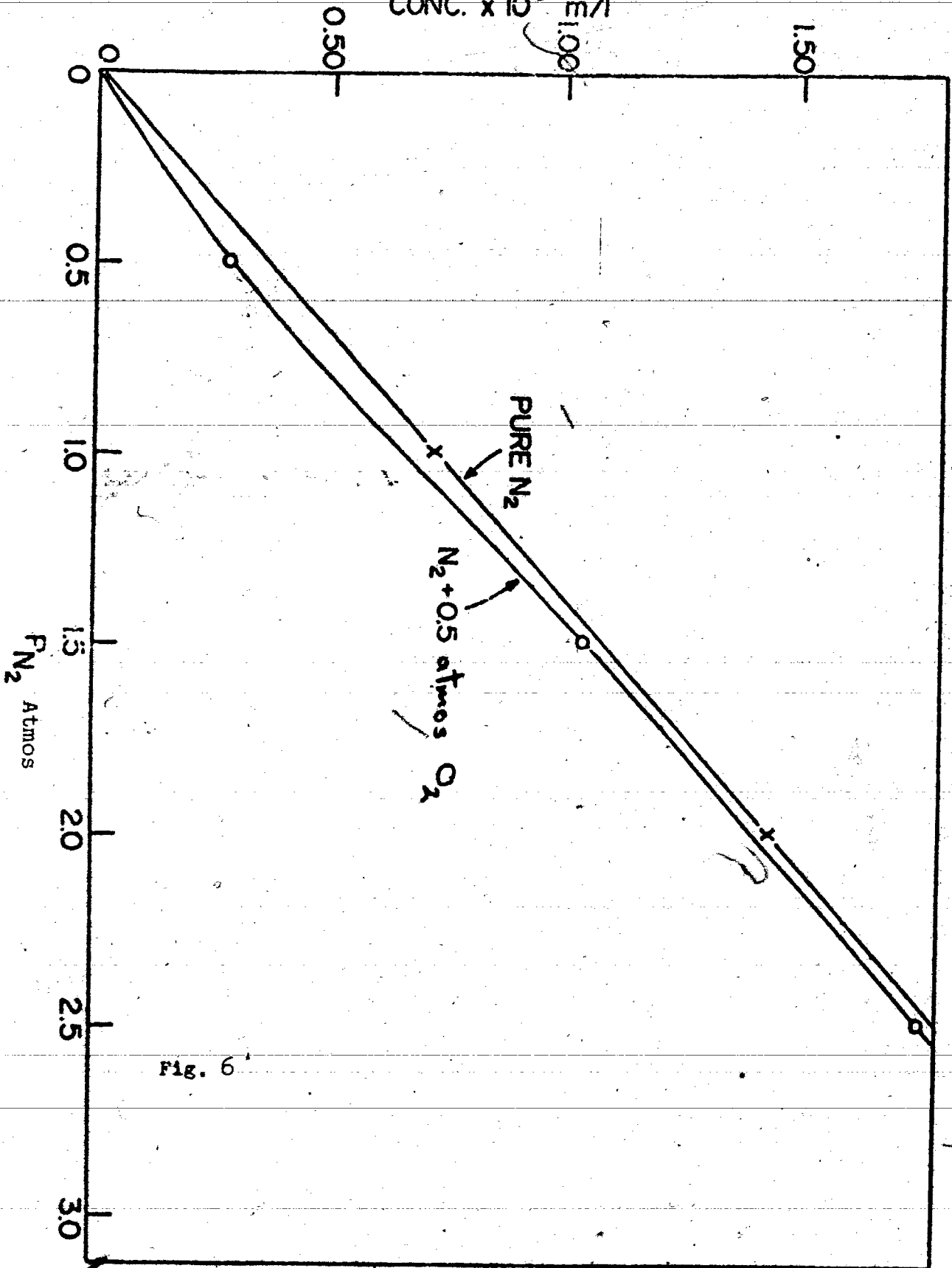


Fig. 6

Fig 7

Solubility of oxygen (at 0.5 atmosphere partial pressure in presence of another gas at 0.5 atmosphere partial pressure) plotted against "other gas" solubility as pure gas in water at 25.00°C and 1 atmosphere.

$10^3 x_2$ AT $P_{O_2} = 0.5$ ATMOS. IN PRESENCE
OF 0.5 ATMOS. "OTHER GAS"

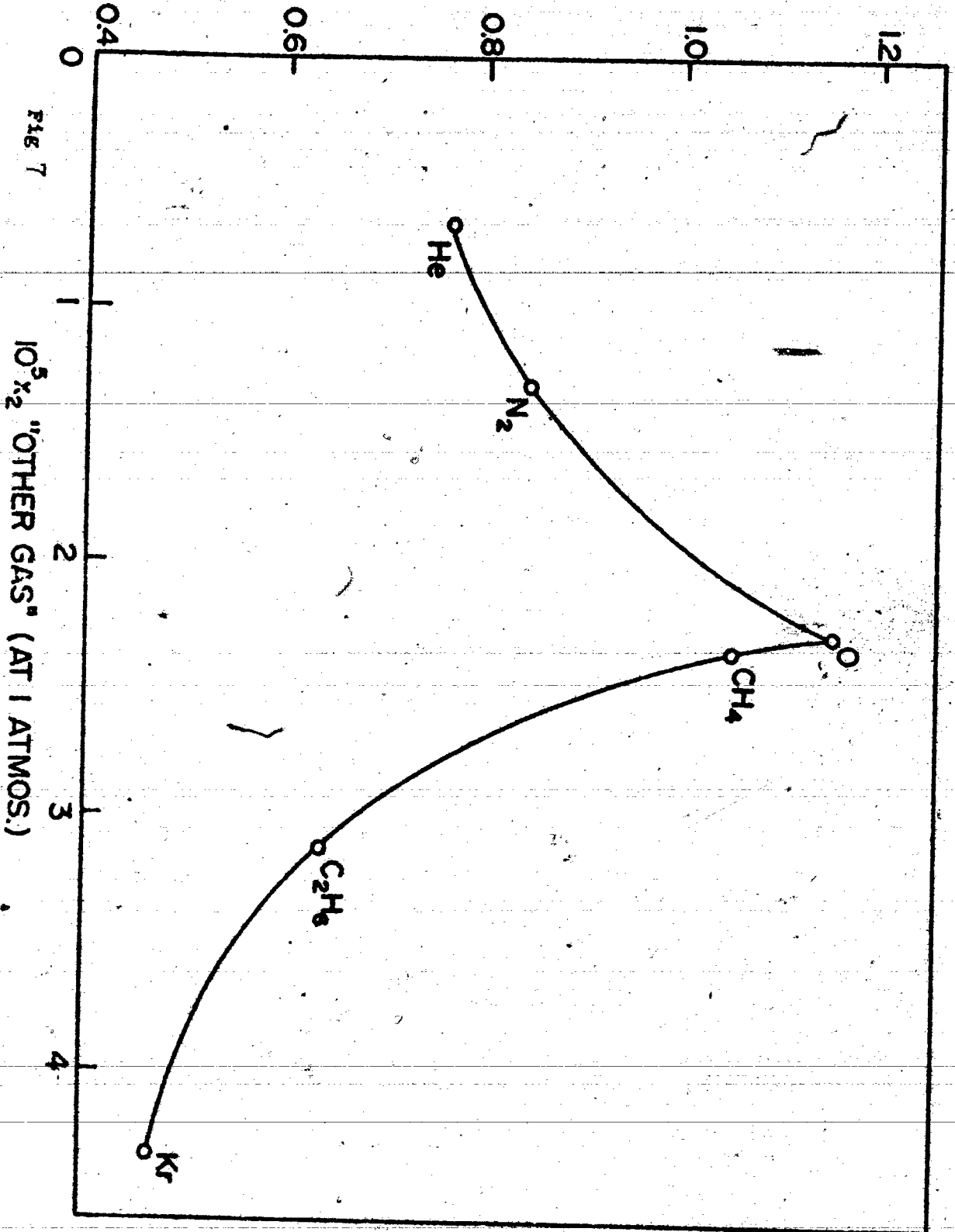


FIG 7

$10^5 x_2$ "OTHER GAS" (AT 1 ATMOS.)

Fig. 8

Typical peaks from binary gas mixture.

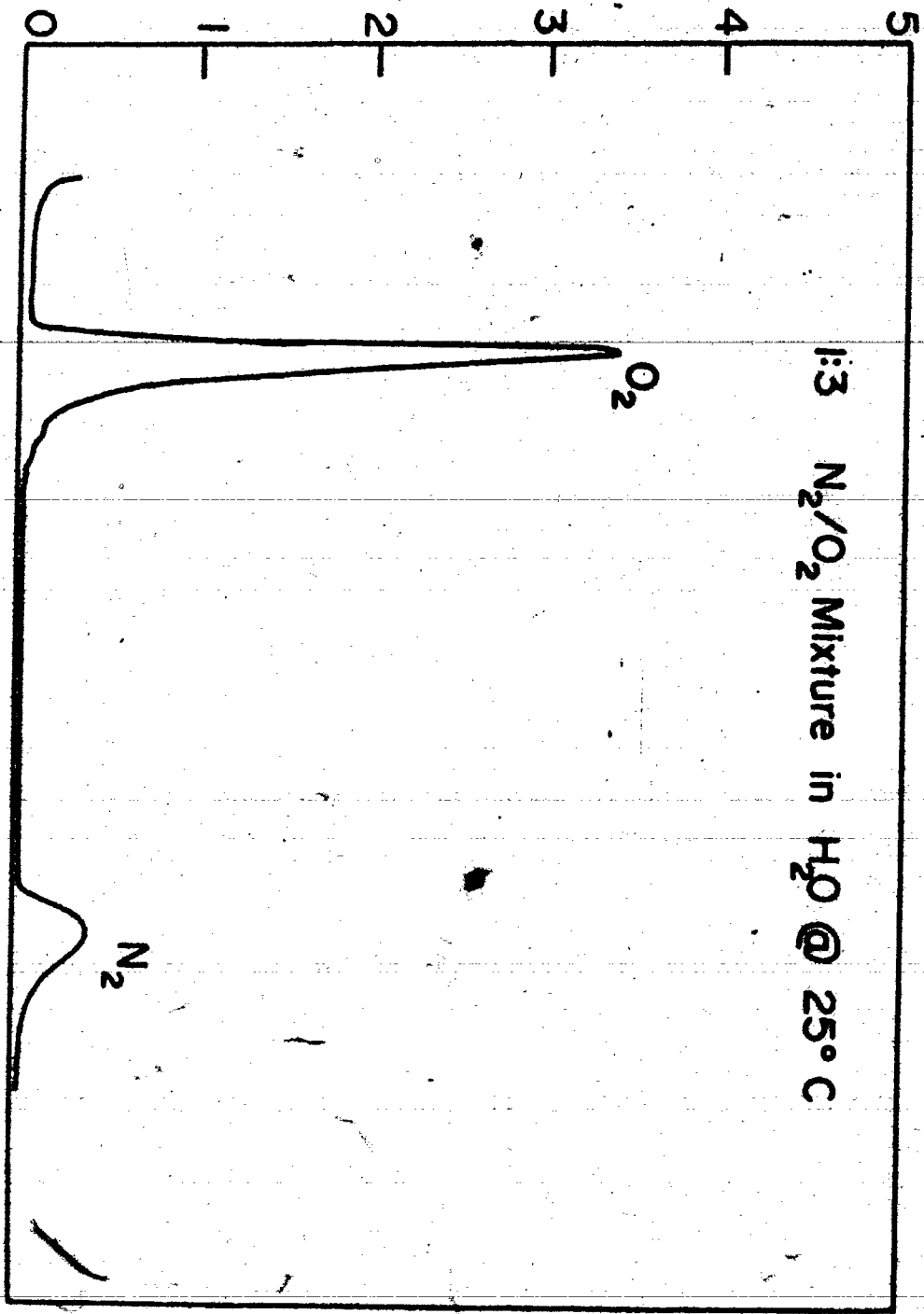


Fig. 8

Fig. 9

Solubility of gases in water using the Oxygen
electrode.

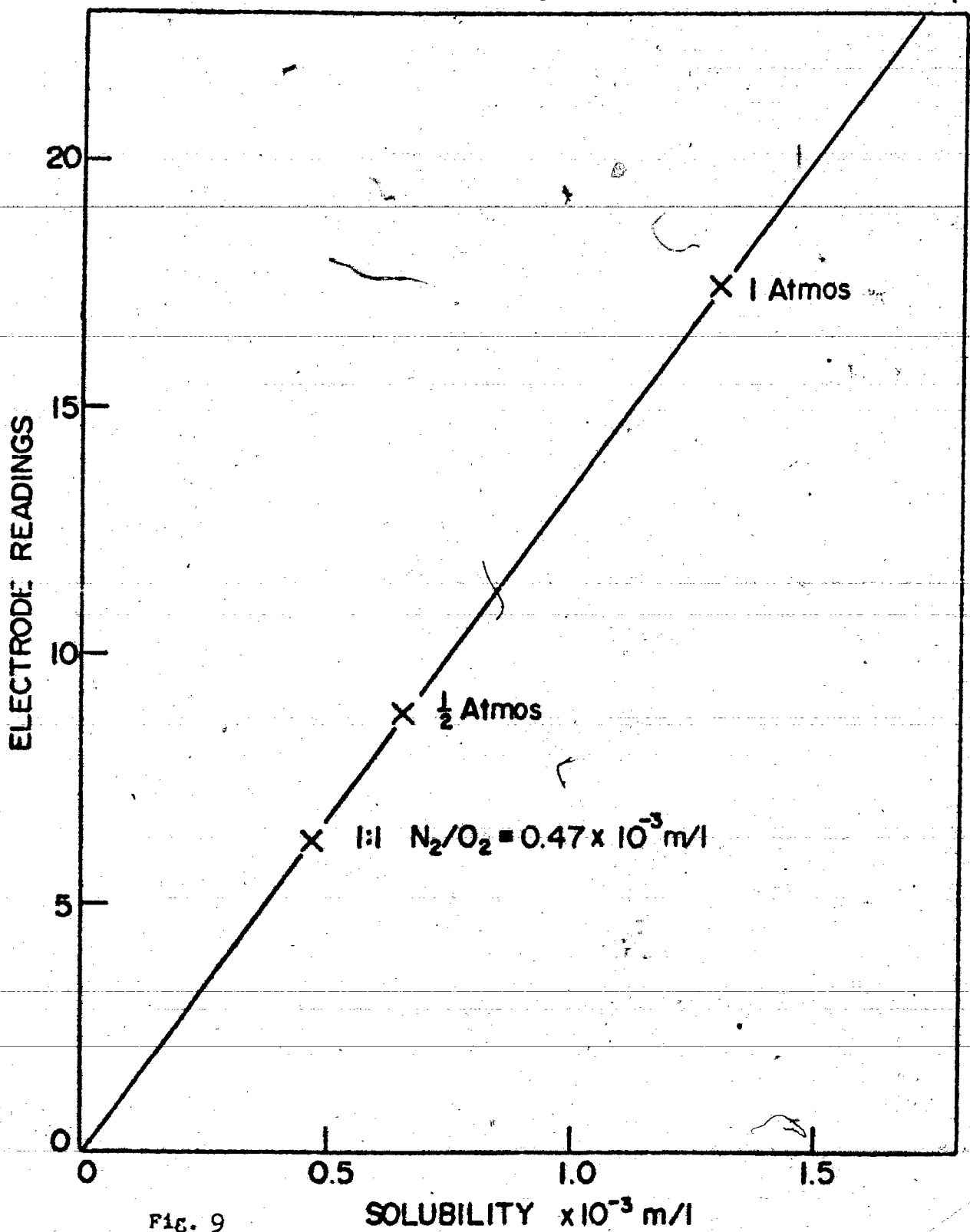


FIG. 9

DISCUSSION

The experimental data obtained require the explanation of two phenomena - the difference in solubility of gases in D₂O and H₂O, and the mutual decrease in solubility of gas mixtures in D₂O and H₂O. We must assume that both phenomena have the same basic explanation.. If we first ignore the water structure arguments we are led to seek an explanation in terms of the Pierotti theory. (16)

The only physical parameters varying in the Pierotti equation for $\ln K_H$,

$$\ln K_H = \bar{G}_c/RT + \bar{G}_1/RT + \ln(RT/V_1)$$

are the number density, ρ , of the solvent and the molecular polarizability α of the solute.

$$\begin{aligned} \bar{G}_c = & RT \left(\frac{6y}{1-y} \right) \left(\frac{a_{12}}{a_1} \right)^2 - \left(\frac{a_{12}}{a_1} \right) + 18 \left(\frac{y}{1-y} \right)^2 \left(\frac{a_{12}}{a_1} \right)^2 \\ & - \left(\frac{a_{12}}{a_1} \right) + 0.25 - \ln(1-y) \\ & + N\pi Pa_1^3 \left\{ 4 \left(\frac{a_{12}}{a_1} \right)^3 - 2 \left(\frac{a_{12}}{a_1} \right)^2 + \left(\frac{a_{12}}{a_1} \right) - \frac{1}{8} \right\} \end{aligned}$$

where

$$y = \frac{\pi a_1^3 \rho}{6}, \text{ and } a_{12} = \frac{a_1 + a_2}{2}$$

where a_1 is the hard sphere diameter of molecule 1 (solvent) and 2 (solute), and where

$$\bar{G}_1 = -3.555 R \pi \rho a_{12}^3 E_{12} / V - 1.33 N_A \pi \rho \mu_1^2 \alpha_2 / \sigma_{12}^3$$

The above equation for $\ln K_H$ is insensitive to ρ , the number density, thus the values of $\rho_{H_2O} = 3.337 \times 10^{22}$ and $\rho_{D_2O} = 3.321 \times 10^{22}$ give a small change in solubilities eg. $K_H(CH_4/H_2O) = 3.94$, $K_H(CH_4/D_2O) = 3.90$. One notes that this is smaller than the experimentally observed value. The theory also predicts the solubility of gases in D_2O to be lower than in H_2O . This is contrary to the experimental data except for the case of oxygen which has a lower D_2O solubility.

We will now examine the solubility of gas mixtures by the Pierotti theory.

1) Since the solubility of each solute is small, there are no $i-j$ interactions, and we cannot use the Pierotti theory to explain the observed results in the way used by Masterton and Lee (15) in their calculation of salting coefficients in the Setschenow equation.

ii) Consideration of the non-ideality of the gas phase.

(a) the use of Dalton's Law for the gas phase the assumption that the total pressure is the sum of the partial pressures of the gases

is independent of the assumption of the ideality of the gas phase,

(b) the linearity of our Henry's Law plot and the value of our Henry's Law constant show that deviation from ideality is negligibly small.

(c) calculation of the fugacity for the gas mixture shows very little deviation from $p=1$ atmos, eg, in a 1:1 mixture of O_2 and N_2 the fugacities are 0.5044 and 0.5045. Thus, we can assume each component of the gas mixture behaves as an ideal gas.

Since the fugacity of the gas phase is approximately the same as the pressure, the assumption by Pierotti that the gas phase is ideal in writing the chemical potential of the solute in the gas phase is a good one.

As the results obtained using O_2 /electrode method agree with the results from the gas chromatograph within 1%, this suggests that the observed lowering of the solubilities is not an artefact of the experiment.

We may calculate the Henry's Law constant (K_H) and thus the solubilities (X_2) using Pierotti's equation, making the number density a variable. If this is done for each component of a gas mixture then the number density dependence of the mole fraction (X_2) can be found. Such

plots are given for O_2 and N_2 in Fig. 10. It is seen that the presence of one gas changes the number density ρ - this can be interpreted as arising from a change in the structure of water. It is also noticed that there is a big change in X_2 for a small change in ρ at the lower mole fraction, suggesting that there reaches a point where our solvent is so highly structured that no solute molecule can be dissolved in the solvent. Lucas (35) in a recent paper emphasises the same point as is made above. He claims that as the number density increases there is a decrease in the number of the bonds between the water molecules - this may be interpreted as follows: since there is more room in the open "more-hydrogen-bonded" structure of water than in the broken down structure, the solute is more easily soluble in the former than in the latter. If, then, there is a decrease in the number of bonds between the water molecules, there will be a decrease in solubility.

We will now look at the water structure arguments to explain the two phenomena observed in the experimental measurements.

First, we will look at the difference in gas solubilities in D_2O and H_2O . We consider the "two structural model" of Wada (10). Liquid water is assumed to consist of two kinds of molecules in chemical equilibrium: the

Fig. 10

Dependence of X_2 on number density (ρ_{H_2O})

Legend;

O_2 o ; N_2 x.

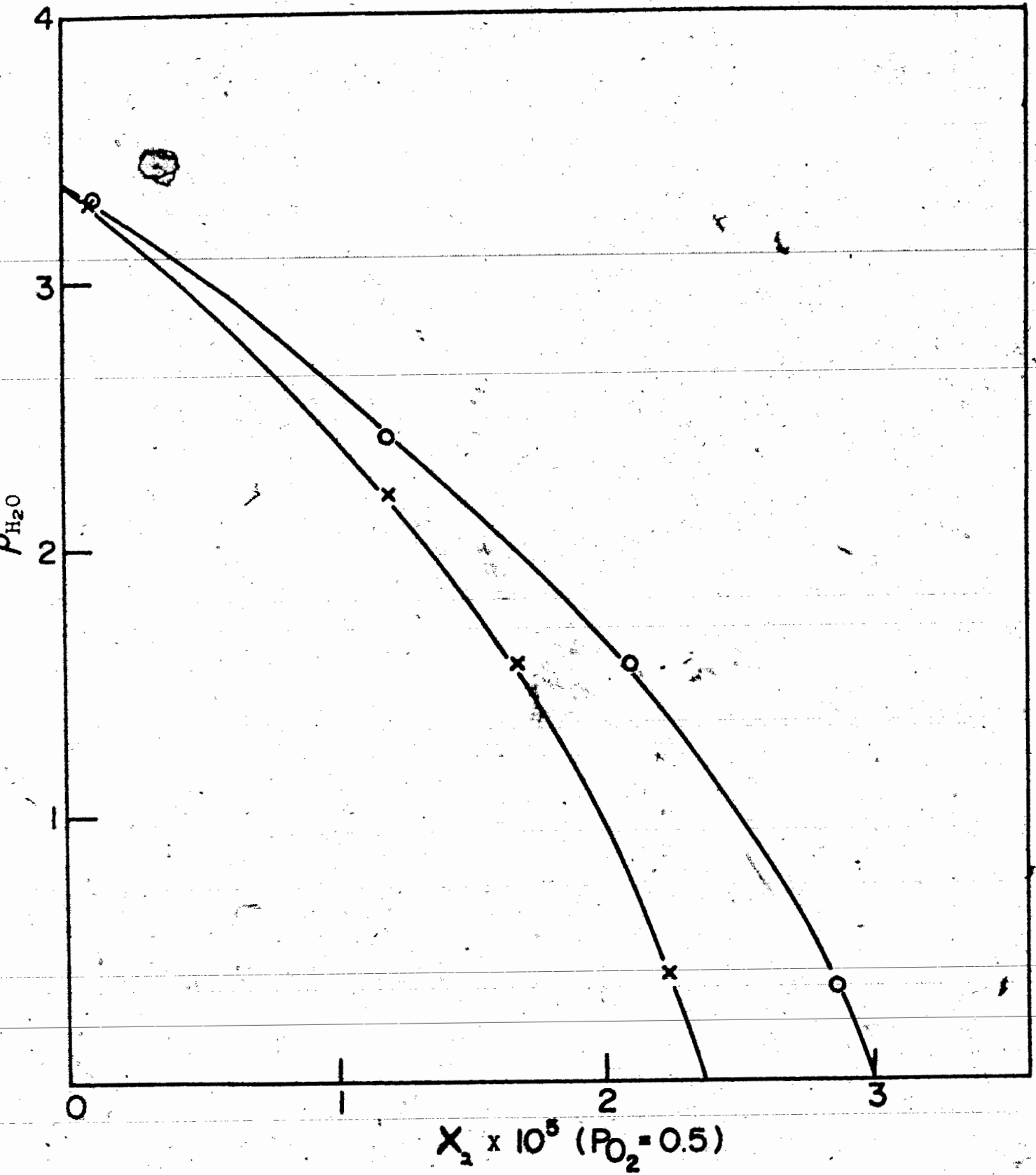


Fig. 10

monomeric water molecules (ρ molecules), that is, molecules not linked by hydrogen bonds to other molecules, and molecules of water which are fully hydrogen bonded (1 molecules). It is suggested (32) that there is an increase in the concentration of 1 form in D_2O which leads to a higher degree of ordering in that solvent. Thus, following Eley's arguments, it can be concluded that the greater the number of cavities, (which is proportional to the concentration of 1 form), the greater the degree of ordering i.e. there is a greater "degree of crystallinity" of the solvent D_2O . Since there is a greater number of cavities in D_2O than in H_2O one would expect there is a higher probability of the solute entering the D_2O structure than the H_2O structure. Thus we would predict a higher gas solubility in D_2O than H_2O . We found this is true for CF_4 , CH_4 , N_2 and Ar but not for O_2 .

Ben-Naim (36) recently explained the difference in the solubility of gases in D_2O and H_2O on the strength of the hydrophobic interaction of a pair of gas solutes in H_2O and D_2O . Hydrophobic interaction (37) refers to the indirect part of the Gibb's free energy change for bringing two solute particles from fixed positions at infinite separations to some close distance, the whole process being carried out within the liquid at constant pressure and temperature.

Ben-Naim argues that there is a stronger hydrophobic interaction between the solutes in H_2O compared to D_2O , thus the solubility is less in H_2O than D_2O . This is probably true for Ar, CH_4 , N_2 and CF_4 . The oxygen solubility doesn't fall into the above category i.e. O_2 is less soluble in D_2O than H_2O . A possible explanation is that since D_2O is more hydrogen-bonded than H_2O there is probably a greater degree of interaction between the oxygen molecules and D_2O than H_2O causing less penetration into the water structure by the oxygen molecules.

For all the binary gas systems examined the same trend is observed, the solubility of each gas is lowered from the expected Henry's Law value. For oxygen at any partial pressure the relative lowering of its saturation solubility increases with the difference between its solubility as a pure gas in water and the solubility of the other component as a pure gas in water. This is illustrated in Fig 7.

Many studies have been made of the change in saturation solubility of a gas from the addition of an added solute. Ben-Naim (32) has discussed the solubility of argon in dilute aqueous solutions of nonelectrolytes in terms of the two-structure model of water. Wen and Hung (38) have similarly used this theory to explain the thermodynamic properties of hydrocarbon gases in aqueous tetra-

alkyl ammonium salt solutions.

In the present study, the mutual lowering of solubility occurs at extremely low mole fraction of each component ($\sim 10^{-5}$). We can thus discount any theory for which the observed effect depends upon a $(\text{solute})_i - (\text{solute})_j$ interaction term. In this sense, we can discount the early theories of Eley (12) and of Frank and Evans (20). Similarly, the theory developed by Masterton and Lee (15), based on the approach of Shoor and Gubbins (40), can only be used when the $(\text{solute})_i - (\text{solute})_j$ interaction affects the free energy of both forming a cavity in solution and in placing the (gas) solute molecule into the cavity. This will not happen at the low mole fraction solubilities of each dissolved gas and will not explain the observed results.

The two-structure model of Ben-Naim (32) and of Namiot (39) has been most successful both in explaining the seemingly anomalous properties of the inert gases in water and of the effect of the presence of electrolyte and nonelectrolyte solutes upon their solubility. In this model water is assumed to consist of monomeric water and of bound clusters of molecules. The presence of the solute affects the equilibrium between these species. In discussing the effect of added non-electrolytes it appears that solute molecules containing 'inert' groups stabilize the

structure whilst other solutes have the opposite effect. The stabilization is enhanced by the greater the interaction of the solute with monomer water. Stabilization of the water structure by methyl alcohol enhances the number of cavities in the water and increases the solubility of gas (41).

The experimental data show the solubility of each component to be lowered, and in fact, the total number of solute species in solution to be less than the algebraic expectation (i.e. the sum of the expected Henry's Law solubilities). This requires the destabilization of the water by each of the two gases, i.e. a lowering in the number of available voids. Thus, on this two-structure model the explanation required to account for the properties of the pure gases in water is contradictory to their properties in water as a gas mixture.

Gurikov (23) has discussed the solubility of gas mixtures in terms of both the two-structure model (42) and the uniform model (8). For both models there exists an equilibrium between 'free' water molecules and water molecules which are part of some structure formation. The two models are quite different in their description of the nature of the 'structured' water and in the expected increase or decrease in the number of free 'voids' upon the addition of a non-electrolyte.

In Gurikov's theory, he obtains an equation for the change in the thermodynamic potentials of component 1, dissolved in pure water and in a dilute aqueous solution of component 2. Using values for $\nu = 2$ and $f^\circ = 0.80$ (notations given in the theory) Δ_μ values were calculated. They are positive ($\approx 1-2$ kcal) and suggest a salting out effect, which is similar to his arguments based on the fraction of free voids. This is contrary to the prediction of the uniform model. For the latter model Δ_μ is found to be negative (≈ -2.30 kcal) and thus predicting a salting in effect (i.e. a mutual increase in the solubility of each gas).

Gurikov's theory can only explain the trend in solubility i.e. there is an increase (or decrease) in solubility depending on whether Δ_μ is negative (or positive). It does not predict the magnitude of the solubility.

From the above discussion, one can say that no adequate theory exists to account for the observed behaviour. However one notes as the solubilities of the gases in the mixture are lowered, this conflicts with Henry's Law. Meyers and Quinn (34) recently calculated Henry's constant (K) using our data and found K is reduced by a factor of 10^{20} from its value at infinite dilution. Henry's Law is obeyed for the pure gases up to at least 0.5 mole % dissolved gas. At one atmosphere the mole % dissolved

gas is about 0.001, or sometimes less. Therefore one would expect Henry's Law to work to a very high accuracy under the conditions studied.

Ben-Naim and Baer (21) in their studies of the solubility of argon in ethanol-water mixtures found an increase in the solubility of argon at 0.015 mole fraction ethanol. In the present studies, the mole fraction we are looking at is $\sim 10^{-5}$, much lower than Ben-Naim. Probably, the mixture of gases in water is behaving like the ethanol-water system, except in this case, there is a lowering of solubilities.

Chapter II

"For up and down and round says he,
Go all appointed things and losses on the
round-about means profits on the swings."

P.R. Chalmers (1872-1940)

Introduction

The investigation of the diffusion of gases in water was undertaken in order to test out various empirical equations relating the diffusion coefficient D to various molecular properties of the gases. In as much as the Pierotti theory for gas solubility appears to give a reasonable successful prediction of the solubility of gases in water, the diffusion data is also used to examine the recently proposed theory of McLaughlin. This theory has the rigorous Enskog theory as its basis and, like the Pierotti theory, is essentially a theory based upon the hard sphere equation of state.

An examination of the literature shows some data to exist for the diffusion coefficients of simple gases in water but most of this is for room temperature conditions. Much of the published data is now regarded as unreliable but in the discussion of the results a comparison is made of the data obtained in this study to those data of other workers.

Apart from purely experimental or analytical difficulties the two main problems besetting the measurement of diffusion in liquids are first a well defined set of conditions under which the diffusion takes place and second the occurrence of a convectational mixing mechanism on top of the chemical potential induced diffusion. Two techniques

are described for measuring the diffusion of a gas in water. The inverted tube method, places the diffusing gas below the water column. It is seen that the open-tube method is subject to large density convection effects. The inverted tube method gives diffusion coefficient data in good agreement with the values of other workers. A comparison of the two techniques shows how large the effect of the added density convection mechanism is upon the overall rate of dissolution of the gas.

Theories of Diffusion in Liquids

Historically, developments of suitable expressions for a diffusion coefficient have generally followed either a hydrodynamic, a thermodynamic, a kinetic, or a quantum-statistical approach to the problem.

The classical hydrodynamic development of the diffusion coefficient was originally made by Nernst (43), and Einstein (44). According to the Nernst-Einstein equation, the diffusion of a single molecule, designated as i , through a medium, designated j , may be described by the relation

$$D_{ij} = \frac{kT}{\xi_{ij}} \quad [1]$$

where k is Boltzmann constant, and ξ_{ij} is the frictional coefficient or the mobility of the molecule (i.e. the steady state velocity, U_i , attained by a particle under a unit force, F , $\xi_{ij} = U_i/F$). According to Einstein,

$$F_i = 6\pi r_i \mu_j U_i \quad [2]$$

where r_i is the radius of the diffusing molecule and μ_j is the viscosity of the solvent. Eq'n[2] can only be true under the premise that the solvent is a continuum, with no tendency for the fluid to "slip" at the surface of the diffusing spherical molecule, and with the diffusing particles considerably larger than the solvent molecules. Eq [1] then becomes

$$\frac{D_{ij}u_j}{kT} = \frac{1}{6\pi r_1} \quad [3]$$

which is called the Stokes-Einstein equation. The hydrodynamic theory suggests that the shapes of the diffusing molecules may be important since the drag coefficient varies with particle shapes.

A formalized approach to evaluating diffusion coefficients was made by DeGroot (45) applying Onsager's phenomenological coefficient to the thermodynamics of irreversible processes. From a combination of the phenomenological equations and the usual diffusion equation, the diffusion coefficient is defined as

$$D_{ij} = - \frac{L_{ij}}{c_i} \frac{\partial \mu_i}{\partial c_i} \quad [4]$$

where L_{ij} is a phenomenological coefficient and μ_i is the chemical potential. The theory gives no indication of the form of L_{ij} as a function of concentration and involves difficulties in determining μ_i experimentally. For these reasons, this theory is little used.

Initial kinetic approaches utilized the fact that in gaseous systems the average kinetic energy of a molecule is a function of temperature only. Based upon Graham's law (which states that the diffusion coefficient varies inversely as the square root of the molecular weight), the first truly successful attempt to formulate a diffusion

theory was made by Arnold (46), after making certain corrections. Arnold proposed the following equation, which is similar to the equation developed by Gilliland (47) for gases,

$$D_{ij} = \frac{BT^{\frac{3}{2}} \sqrt{\frac{1}{M_1} + \frac{1}{M_2}}}{\delta \mu^{\frac{2}{3}} F^2} \quad [5]$$

where M_1 and M_2 are the molecular weights of the solute and solvent, B is a proportionality constant, μ is the sum of the molecular diameters, and δ is a correction factor. Unless the abnormality factors are known in advance (from empirical data) eq'n [5] is not useful in predicting diffusivities of dissolved gases.

Recently, Eyring and Ree (48) have applied absolute rate theory to diffusion process by assuming that the energy of activation for the diffusion process is that energy required to form an extra space in the liquid to allow the molecules to move. Applying the basic form of the expression for the rate of reaction, K may be expressed as

$$K = \frac{kT}{h} \frac{f^*}{f} \exp(-E_0/kT) \quad [6]$$

For the fundamental diffusion process the diffusion coefficient is given by:

$$D = \lambda^2 K \quad [7]$$

where λ is the distance between equilibrium positions, Eq'n [7] may then be combined with eq'n [6] to give

$$D = \lambda^2 \left(\frac{kT}{h}\right) \left(\frac{f^*}{P}\right) \exp(-E_0/kT) \quad [8]$$

and if the diffusion process is carried out without any volume changes, eq'n [8] may be rewritten:

$$D = \lambda^2 e^{\left(\frac{kT}{h}\right)} \exp\left(\frac{\Delta S^*}{R} - E_0^*/RT\right) \quad [9]$$

$$D = B^* \exp\{-E_0^*/RT\}$$

where

$$B^* = \lambda^2 e^{\left(\frac{kT}{h}\right)} \exp\left\{\frac{\Delta S^*}{R}\right\} \quad [10]$$

Sufficient data have now been correlated with the Eyring equation to show that with present knowledge of molecular parameters the method yields values of the proper order of magnitude (49). However, calculated values of diffusion coefficients compared to experimental values show that the Eyring equation frequently predicts low values. The equation fails to predict correctly diffusivities in nonideal systems of aqueous solutions.

Another interesting equation for diffusion processes is established by combining eq'n [9] with the equation developed by Eyring (48) for viscosity. By assuming that λ and K^0 are the same for the processes of diffusion and viscous flow, the following equation can be derived for D:

$$D = \frac{\lambda_1}{\lambda_2 \lambda_3} \left(\frac{kT}{\mu} \right) \quad [11]$$

where λ_1 , λ_2 and λ_3 are distance characterizing the spacing layers of molecules in the quasi-crystalline liquid lattice. This is a particularly useful relation and has been used by many investigators to develop semi-empirical relations for estimating diffusion coefficients. As equation [11] requires specification of λ_1 's, it falls in the same category as the Arnold equation in predicting diffusivities of dissolved gases. Since variation of diffusion coefficients with solute species have been noted, Chang and Wilke (50) empirically modified the Eyring theory of absolute reaction rates and the Stokes-Einstein equation [3]. The correlation was made through the group $F = T (D_{12}\eta)$. Within the limits of the available experimental data, F was essentially independent of temperature for a given system, but was a function of the molal volume of the solute.

In 1955 Wilke and Chang (50) performed several experiments and obtained data to supplement that used by Wilke in 1949. Experimental data from 178 experiments were reproduced with an average deviation of 10%. Their data indicated that F was a smooth function of the solute molal volume having a slope of 0.7 at low molal volumes and apparently merged with the Stokes-Einstein equation at high molal volumes. Over the middle range of molal

volumes, the curve may be represented by a line of slope 0.6; therefore they assumed that $D_{12}\eta/T$ was proportional to V_0 .

To determine the effect of solvent properties on diffusivity, a wide variety of variables such as solvent molal volume, heat of vaporization, molecular weight, etc., were examined. Of these the molecular weight appeared to correlate the data most successfully. Although there is a considerable scatter of the data, a line with slope value one half correlates each system fairly well on a plot of $\log D_{12}\eta/T$ vs M_2 .

From the above results Wilke concluded that an equation for unassociated liquids of the form

$$D_{12} = (\text{const.}) \frac{TM_2^{1/2}}{\eta V_0^{0.6}} \quad [12]$$

would successfully include the interaction of solvent and solute; the constant was determined empirically to be 7.4×10^{-8} . The solutes considered were oxygen, nitrogen and carbon dioxide.

For H_2O the plot of $\log D_{12}/T$ vs $\frac{\log \eta V_0^{0.6}}{M_2^{1/2}}$ fell above the line for unassociated liquids. By assigning a molecular weight to H_2O of 2.6 times the nominal weight, the curve was brought into agreement with the curve for unassociated liquids.

Scheibel (51) made a correction to the original

Wilke correlation. It is possible to express Wilke's correlation without the solvent factor as

$$D_{12} = 8.2 \times 10^{-8} \frac{[1 + (3V_{O1}/V_{O2})^{2/3}T]}{\eta V_{O1}^{1/3}}$$

Othmer and Thakar (52) followed the principle used effectively to correlate many other properties of matter: plotting logarithmically the property of one material against the same property of another on a scale based on the vapour pressure of a reference substance. If diffusivity is expressed as a rate process which varies exponentially with the temperature, by introduction of the Clausius-Clapeyron equation it can be shown that $\log D_{12} = \frac{E_D}{L} \log P^* + \text{const.}$ This suggested that a log plot of D_{12} vs the vapour pressure of a reference substance at equal temperatures would give a straight line of slope E_D/L .

The equation which best represented the data for water as the solvent was

$$D_{12} = \frac{14.0 \times 10^{-5}}{\eta_0^{1.1} V_0^{0.8}}$$

No completely satisfactory method has yet been proposed for estimating diffusion coefficients from either basic molecular data or other physical properties

of the system. This is largely due to lack of understanding the liquid state.

We have made use of McLaughlin's (53) application of hard sphere theory to the diffusion of gases in water, benzene and carbon tetrachloride. The calculated values compare very well with the experimental data. The theory is discussed in detail below.

Application of hard-sphere theory to diffusion of gases in liquids.

Recently, McLaughlin (53) made use of Thorne's extension of the Enskog theory for diffusion in a dense mixed hard-sphere fluid. We have made use of his theory to calculate diffusion coefficients of gases in liquids.

For the complete discussion the reference states will be b_{11} and b_{22} for pure dense fluids, where b_{11} refers to the solvent (1), and b_{22} to the solute (2); for the mixed dense fluid we define new values: b_{11}^* for the solvent in the mixture and b_{22}^* for the solute in the mixture.

Besides the equations for the pure fluid there are a set of equations for the transport properties of mixed hard-sphere fluids which have been developed by Thorne (54). In this section, these equations are applied to diffusion in systems which are of practical importance and for which, at present, discussion and prediction are largely based on the Stokes-Einstein equation in one form or another.

Diffusion Theory

For the case of the mutual diffusion coefficient D of a binary hard-sphere dense fluid, Thorne's equation can be written

$$nD = \pi_0 \mathfrak{D} g_{12}(\sigma_{12}) \quad [13]$$

where

$n = \frac{N}{V}$ is the number density of the dense fluid.

$$n = n_1 + n_2 \text{ and } 2\sigma_{12} = \sigma_{11} + \sigma_{22}$$

$g_{12}(\sigma_{12})$ = contact radial distribution function for the mixture.

π_0 = number density of the dilute fluid

\mathfrak{D} = mutual diffusion coefficient of the corresponding infinitely dilute gas at the same temperature.

$g_{12}(\sigma_{12})$ is related to the pressure by the equation

$$\frac{P}{kT} = \sum_i n_i + \frac{2}{3} \pi \sum_{ij} n_i n_j \sigma_{ij}^3 g_{ij}(\sigma_{ij}) \quad [14]$$

For the case of the pure fluid of species 1 eq'n [14] reduces to

$$\frac{P}{nkT} = 1 + 4b_{11}g(\sigma) \quad [15]$$

where $b_{11} = \frac{\pi n \sigma_{11}^3}{6}$

b_{11} is the ratio of the volume of the molecules to the volume V of the system. \mathfrak{D} is given by (54).

$$\mathfrak{D} = \frac{3}{8\pi_0 \sigma_{12}^2} \left[\frac{kT(m_1 + m_2)}{2\pi m_1 m_2} \right]^{1/2} \quad [16]$$

which reduces for the case of self-diffusion (i.e.

$m_1 = m_2$ and $\sigma_{11} = \sigma_{22}$) to

$$D_1^0 = \frac{3}{8\pi\sigma_{11}^2} \left(\frac{KT}{\pi m_1} \right)^{\frac{1}{2}} \quad [17]$$

As eq'n [13] has the term $g_{12}(\sigma_{12})$ - the pair distribution function - it is necessary to obtain an expression for it from the equilibrium theory. McLaughlin made use of the Percus-Yevick equation in deriving $g_{12}(\sigma_{12})$ and $g(\sigma)$. Percus and Yevick equation (55) enabled Wertheim (56) and Thiele (57) to obtain analytic expressions for $g(\sigma)$ and Lebowitz (58) one for $g_{12}(\sigma_{12})$.

There is a familiar method of calculating the equation of state when the radial distribution function is known. It is the relation

$$P = nkT - \frac{n^2}{6} \int r^4 v'(r)g(r)d^3r \quad [18]$$

which was originally derived from the virial theorem (54). The Percus Yevick equation may then be solved analytically for the hard-sphere potential (59). The resulting pressure equation of state is

$$\frac{P}{nkT} = [(1 + 2x + 3x^2)/(1 - x)^2] \quad [19]$$

where $x = \frac{1}{4} \rho$

$$\rho = \frac{2}{3} (\pi\sigma_{11}^3 n)$$

thus

$$x = \frac{\pi\sigma_{11}^3 n}{6} = b_{11}$$

Substituting into eq'n [19]

$$\frac{P}{nKT} = \frac{(1 + 2b_{11} + 3b_{11} + 3b_{11}^2)}{(1 - b_{11})^2} \quad [20]$$

But $\frac{P}{nKT} = 1 + 4b_{11}g(\sigma)$

Thus, $g(\sigma) = \frac{1 + 2b_{11} + 3b_{11}^2}{(1 - b_{11})^2} - \frac{1}{4b_{11}}$

$$= \frac{1 + 2b_{11} + 3b_{11}^2 + 2b_{11} - b_{11}^2 - 1}{4b_{11}(1 - b_{11})^2}$$

$$= \frac{4b_{11} + 2b_{11}^2}{4b_{11}(1 - b_{11})^2}$$

$$\therefore g(\sigma) = \frac{2 + b_{11}}{2(1 - b_{11})^2} \quad [21]$$

The virial pressure is obtained explicitly from the solution of the Percus-Yevick equation since for the case of a mixture of hard-spheres

$$\frac{P}{KT} = \sum n_i + \frac{2}{3\pi} \sum_{ij} n_i n_j \sigma_{ij}^3 g_{ij}(\sigma_{ij})$$

where $g_{ij}(\sigma_{ij})$ is the contact value of the radial distribution function, for which the Percus-Yevick equation gives as derived in ref. (58),

$$g_{ij}(\sigma_{ij}) = [\sigma_j g_{11}(\sigma_1) + \sigma_1 g_{jj}(\sigma_j)] / 2\sigma_{ij} \quad [22]$$

where

$$g_{1j}(\sigma_{11}) = \left\{ (1 + \frac{1}{2}\xi) + \frac{3}{2} \left(\frac{\pi}{6} \right) n_j \sigma_{jj}^2 (\sigma_{11} - \sigma_{jj}) \right\} (1 - \xi)^{-2} \quad [23]$$

where $\xi = b_{11}^* + b_{22}^*$

ξ is for the mixture of solute plus solvent. Later on b_{11}^* and b_{22}^* will be defined for the mixture.

Using eq'n [13] we can find an expression for the mutual diffusion coefficient of a dense hard-sphere mixed fluid of molecules of different diameters.

From eq'n [13]

$$\frac{nD}{\pi c D} = \frac{1}{g_{12}(\sigma_{12})} = \frac{1}{[\sigma_{22}g_{11}(\sigma_{11}) + \sigma_{11}g_{22}(\sigma_{22})] / 2\sigma_{12}} \quad [24]$$

To simplify the algebra, let

$$A = \sigma_{22}g_{11}(\sigma_{11})$$

and $B = \sigma_{11}g_{22}(\sigma_{22})$

$$A = \sigma_{22} \left\{ (1 + \frac{1}{2}\xi) + \frac{3}{2} \left(\frac{\pi}{6} \right) n_2 \sigma_{22}^2 (\sigma_{11} - \sigma_{22}) \right\} (1 - \xi)^{-2}$$

and

$$B = \sigma_{11} \left\{ (1 + \frac{1}{2}\xi) + \frac{3}{2} \left(\frac{\pi}{6} \right) n_1 \sigma_{11}^2 (\sigma_{22} - \sigma_{11}) \right\} (1 - \xi)^{-2}$$

Thus,

$$A+B = \frac{1}{(1 - b_{11}^* - b_{22}^*)^2} [2\sigma_{12} + \sigma_{11}(2b_{22}^* - b_{11}^*) + \sigma_{22}(2b_{11}^* - b_{22}^*)] \quad [25]$$

and

$$\frac{1}{g_{12}(\sigma_{12})} = \frac{2\sigma_{12}(1-b_{f1}^*-b_{g2}^*)^2}{2\sigma_{12}+\sigma_{11}(2b_{g2}^*-b_{f1}^*)+\sigma_{22}(2b_{f1}^*-b_{g2}^*)} \quad [26]$$

Dividing top and bottom of L.H.S. of eq'n [26] by σ_{11}

$$\frac{1}{g_{12}(\sigma_{12})} = \frac{(1-b_{f1}^*-b_{g2}^*)^2 \frac{2\sigma_{12}}{\sigma_{11}}}{\frac{1}{\sigma_{11}} [2\sigma_{12}-\sigma_{11}b_{f1}^*-\sigma_{22}b_{g2}^*+2\sigma_{11}b_{g2}^*+2b_{f1}^*\sigma_{22}]} \quad [27]$$

$$\frac{1}{g_{12}(\sigma_{12})} = \frac{(1-b_{f1}^*-b_{g2}^*)^2 \frac{2\sigma_{12}}{\sigma_{11}}}{\frac{1}{\sigma_{11}} [(2\sigma_{12}-\sigma_{11}b_{f1}^*-\sigma_{11}b_{g2}^*-\sigma_{22}b_{f1}^*-\sigma_{22}b_{g2}^*)+3\sigma_{11}b_{g2}^*+3\sigma_{22}b_{f1}^*]} \quad [28]$$

which simplifies to

$$\frac{1}{g_{12}(\sigma_{12})} = \frac{(1-b_{f1}^*-b_{g2}^*)^2 \frac{2\sigma_{12}}{\sigma_{11}}}{(1-b_{f1}^*-b_{g2}^*) \frac{2\sigma_{12}}{\sigma_{11}} + (\frac{b_{g2}^*}{\sigma_{22}} + \frac{b_{f1}^*}{\sigma_{11}}) 3\sigma_{22}} \quad [29]$$

But
$$\frac{1}{g_{12}(\sigma_{12})} = \frac{nD}{\pi_0 D}$$

Thus,

$$\frac{nD}{\pi_0 D} = \frac{(1-b_{f1}^*-b_{g2}^*) \frac{2\sigma_{12}}{\sigma_{11}}}{(1-b_{f1}^*-b_{g2}^*) \frac{2\sigma_{12}}{\sigma_{11}} + (\frac{b_{g2}^*}{\sigma_{22}} + \frac{b_{f1}^*}{\sigma_{11}}) 3\sigma_{22}} \quad [30]$$

For the case of mutual diffusion in a dense mixed hard-sphere fluid where the molecules have the same size $\sigma_{11} = \sigma_{22}$ Longuet-Higgins, Pople and Valleau (59) give the result

$$D = \frac{\sigma_{12}}{4} \left\{ \frac{\pi kT(m_1+m_2)}{2m_1m_2} \right\}^{\frac{1}{2}} \left(\frac{P}{nkT} - 1 \right)^{-1} \quad [31]$$

Substituting for

$$\left(\frac{P}{nkT} - 1 \right)^{-1} = \frac{1}{4b_{11}g(\sigma)} = \frac{(1-b_{11})^2}{2b_{11}(b_{11}+2)}$$

$$D = \frac{\sigma_{12}}{4} \left\{ \frac{\pi kT(m_1+m_2)}{2m_1m_2} \right\}^{\frac{1}{2}} \frac{(1-b_{11})^2}{2b_{11}(b_{11}+2)} \quad [32]$$

Eq'n [32] can be rewritten as

$$D = \frac{\sigma_{12}\pi}{4} \left\{ \frac{kT(m_1+m_2)}{2\pi m_1m_2} \right\}^{\frac{1}{2}} \frac{(1-b_{11})^2}{2b_{11}(b_{11}+2)} \quad [33]$$

From eq'n [16].

$$\frac{8\pi\sigma_{12}^2}{3} = \left\{ \frac{kT(m_1+m_2)}{2\pi m_1m_2} \right\}^{\frac{1}{2}}$$

Substituting in eq'n [33],

$$D = \frac{\sigma_{12}}{4} \pi \frac{8\pi\sigma_{12}^2}{3} \frac{(1-b_{11})^2}{2b_{11}(b_{11}+2)} \quad [34]$$

$$= \frac{\sigma_{12}^3}{3} \frac{8\pi\pi}{b_{11}(b_{11}+2)} \frac{(1-b_{11})^2}{2}$$

$$b_{11} = \frac{\pi n \sigma_{12}^3}{6}$$

$$= \frac{\sigma_{12}^3}{3\pi n \sigma_{12}^3} \frac{8\pi\pi b}{(b_{11}+2)} \frac{(1-b_{11})^2}{2}$$

$$= \pi_0 \frac{8(1-b_{11})^2}{(b_{11}+2)}$$

[35]

With an additional condition, $m_1 = m_2$ (and $\sigma_{11} = \sigma_{22}$), Longuet-Higgins and Pople (60) further found a result for the pure fluid by considering the exponential decay of the auto correlation function.

Their result is

$$D_1^0 = \frac{\sigma}{4} \left(\frac{\pi kT}{m} \right)^{\frac{1}{2}} \left(\frac{P}{nkT} - 1 \right)^{-1} \quad [36]$$

Substituting for

$$\left(\frac{P}{nkT} - 1 \right)^{-1} = \frac{(1 - b_{11})^2}{2b_{11}(1 - b_{11})}$$

we get after rearranging

$$D_1^0 = \frac{3}{4n\sigma^2} \frac{(1 - b_{11})^2}{(b_{11} + 2)} \left(\frac{kT}{\pi m} \right)^{\frac{1}{2}} \quad [37]$$

Substituting,

$$\left(\frac{kT}{\pi m} \right)^{\frac{1}{2}} = \frac{D_1^0 \cdot 8\pi\sigma^2}{3} \quad \text{from eq'n [17]}$$

$$nD_1^0 = \pi\sigma D_1^0 \frac{2(1 - b_{11})^2}{(b_{11} + 2)} \quad [38]$$

Application to the Diffusion of Gases in Liquids

At present there is a great deal of data for the diffusion of gases in liquids but little has been done to determine these factors which control the temperature dependence of the diffusion coefficients of such systems or to calculate the diffusion coefficients from statistical-mechanical theories.

Rather than calculate D (mutual diffusion) ~~ab~~ initio we look at the ratio D/D_1^0 .

Thus eq'n [30], divided by eq'n [38] gives

$$\frac{D}{D_1^0} = \frac{(1-b_{11}^*-b_{22}^*)^2 \frac{2\sigma_{12}}{\sigma_{11}} D (2+b_{11})}{2D_1^0 (1-b_{11})^2 [(1-b_{11}^*-b_{22}^*)^2 \frac{\sigma_{12}}{\sigma_{11}} + (\frac{b_{22}^*}{\sigma_{22}} + \frac{b_{11}^*}{\sigma_{11}}) 3\sigma_{22}]}$$

[39]

Substituting for D and D_1^0 and simplifying we get

$$\frac{D}{D_1^0} = \left(\frac{m_1+m_2}{2m_2}\right)^{\frac{1}{2}} \left(\frac{\sigma_{11}}{\sigma_{12}}\right)^2 \frac{(1-b_{11}^*-b_{22}^*)^2 (2+b_{11})}{(1-b_{11})^2 [(1-b_{11}^*-b_{22}^*)^2 + \frac{3b_{22}^* \sigma_{11} + 3b_{11}^* \sigma_{22}}{\sigma_{12}}]}$$

[40]

We will now look at the general values of b_{11}^* and b_{22}^* in the mixed-hard spheres. Mole fraction is defined as

$$X_1 = \frac{N_{11}}{N_{11} + N_{22}}$$

Lebowitz and Rowlinson (61) defined mole fraction in a binary mixture of hard-spheres as

$$X_1 = \frac{\rho_1}{\rho_1 + \rho_2} \quad [41]$$

where

$$\rho_1 = \frac{N_{11}}{V_{11}} N \quad \text{in a mixture}$$

N = Avogadro's number,

N_{11} = No. of moles of 1 in the mixture

V_{11} = molar volume of 1

ρ_1 = number density of 1 in the mixture.

$$\text{Thus } X_1 = \frac{\frac{N_{11}}{V_{11}}}{\frac{N_{11}}{V_{11}} + \frac{N_{22}}{V_{22}}}$$

Comparing eq'n [40] and eq'n [41] we find that they are equal only if the V's are the same.

Thus

$$\rho_1 = \frac{N_{11}}{V_m} N$$

where $V_m = N_{11}V_{11} + N_{22}V_{22}$

(i) for b_{11}^* in the mixture

$$b_{11}^* = \frac{N_{11}N\pi\sigma_{11}^3}{V_m^6} \quad [42]$$

$$= \frac{N_{11}N\pi\sigma_{11}^3}{(N_{11}V_{11} + N_{22}V_{22})^6} \quad [43]$$

Dividing top and bottom by $\frac{N_{11}}{N_{11} + N_{22}}$

$$b_{11}^* = \frac{X_1N\pi\sigma_{11}^3}{(X_1V_{11} + X_2V_{22})^6} \quad [44]$$

(ii) for b_{22}^* in the mixture

$$b_{22}^* = \frac{N_{22}N\pi\sigma_{22}^3}{V_m^6} \quad [45]$$

$$= \frac{X_2N\pi\sigma_{22}^3}{(X_1V_{11} + X_2V_{22})^6}$$

Dividing top and bottom by V_{22}

$$b_{22}^* = \frac{X_2V_{22}}{X_1V_{11} + X_2V_{22}} \cdot \frac{N\pi\sigma_{22}^3}{V_{22}}$$

$$= \frac{X_2V_{22}}{X_1V_{11} + X_2V_{22}} b_{22}$$

(iii) when $X_1 \rightarrow 1, X_2 \rightarrow 0$

(a) Eq'n [43] then becomes

$$b_{11}^* = \frac{X_1N\pi\sigma_{11}^3}{V_{11}^6}$$

$$= b_{11}$$

(b) Eq'n [45] then becomes

$$b_{22}^* = X_2 \frac{V_{22}}{V_{11}} b_{22}$$

$$= 0$$

Since we are studying systems in which the solubilities of the dissolved gases are small, we are dealing with the case $b_{11}^* = b_{11}$ and $b_{22}^* = 0$.

Thus eq'n [40] for the special case becomes

$$\frac{D}{D_1^0} = \left(\frac{m_1 + m_2}{2m_2} \right)^{\frac{1}{2}} \left(\frac{\sigma_{11}}{\sigma_{12}} \right)^2 \frac{(1-b_{11})^2 (2+b_{11})}{(1-b_{11})^2 [2(1-b_{11}) + \frac{3b_{11}\sigma_{22}}{\sigma_{12}}]}$$

$$= \left(\frac{m_1 + m_2}{2m_2} \right)^{\frac{1}{2}} \left(\frac{\sigma_{11}}{\sigma_{12}} \right)^2 \frac{2 + b_{11}}{2(1-b_{11}) + \frac{3b_{11}\sigma_{22}}{\sigma_{12}}} \quad [46]$$

Diffusion coefficients are calculated using the above equation for various systems and compared with the experimental values.

The validity of this theory will be discussed later.

Diffusion equation and its solution for the open-tube and inverted tube.

The development of an analytical theory of diffusional flow began in 1855, when Fick (62) applied Fourier's equation for the flow of heat to the flow of matter by diffusion.

The mathematical theory of diffusion in isotropic media is based on the rate of transfer of diffusing substance through a unit area of a section which is proportional to the concentration gradient measured normal to the section i.e.,

$$F_x = -D \frac{\partial c}{\partial x} \quad [47]$$

where F_x is the rate of transfer per unit area of section, c is the concentration of diffusing substance, x is the space coordinate measured normal to the section, and D is called the diffusion coefficient.

By considering the mass balance of an element of volume it is easy to show that the fundamental differential equation of diffusion takes the form

$$\frac{\partial c}{\partial t} = D \left(\frac{\partial^2 c}{\partial x^2} + \frac{\partial^2 c}{\partial y^2} + \frac{\partial^2 c}{\partial z^2} \right) \quad [48]$$

provided D is a constant. When D depends markedly on the concentration c and also when the medium is not homogenous so that D varies from point to point, eq'n

(2) becomes

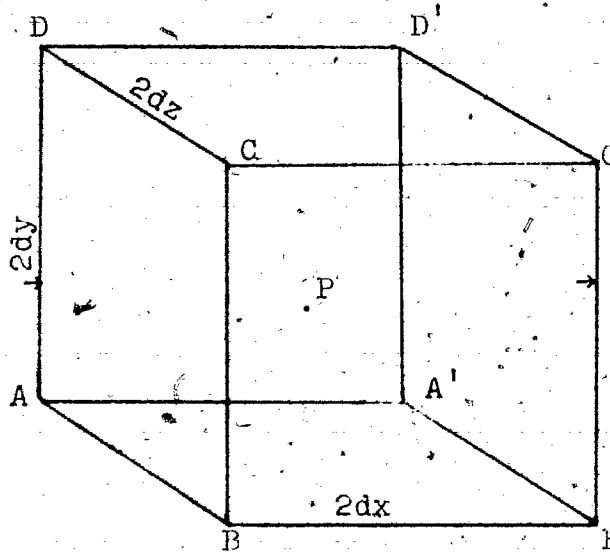
$$\frac{\partial c}{\partial t} = \frac{\partial}{\partial x} \left(D \frac{\partial c}{\partial x} \right) + \frac{\partial}{\partial y} \left(D \frac{\partial c}{\partial y} \right) + \frac{\partial}{\partial z} \left(D \frac{\partial c}{\partial z} \right) \quad [49]$$

where D may be a function of x, y, z and c. Frequently, diffusion occurs effectively in one direction only, i.e. there is a gradient of concentration only along the x-axis; in such cases eq'n [48] and [49] reduce to

$$\frac{\partial c}{\partial t} = D \frac{\partial^2 c}{\partial x^2} \quad [50]$$

and $\frac{\partial c}{\partial t} = \frac{\partial}{\partial x} \left(D \frac{\partial c}{\partial x} \right)$ respectively.

The fundamental differential equation of diffusion in an isotropic medium is derived from eq'n [47] as follows:



The element of volume is in the form of a rectangular parallelepiped whose sides are parallel to the axis of coordinates and are of lengths 2dx, 2dy, 2dz. The

centre of the element is at $P(x,y,z)$, where the concentration of diffusing substance is c . ABCD and A'B'C'D' are the faces perpendicular to the axis of x . Then the rate at which diffusing substances enter the element through the face ABCD in the plane $y-z$ is given by $4dydz(F_x - \frac{\partial F_x}{\partial x} dx)$, where F_x is the rate of transfer through unit area of the corresponding plane through P.

Similarly, the rate of loss of diffusing substance through the face A'B'C'D' is given by

$$4dydz (F_x + \frac{\partial F_x}{\partial x} dx)$$

The contribution to the rate of increase of diffusing substance in the element from these two faces is thus equal to $-8dx dy dz \frac{\partial F_x}{\partial x}$.

Similarly, from the other faces we obtain $-8dx dy dz \frac{\partial F_y}{\partial y}$ and $-8dx dy dz \frac{\partial F_z}{\partial z}$. But the rate at which the amount of diffusing substance in the element increases is also given by $8dx dy dz \frac{\partial c}{\partial t}$ and hence we have immediately

$$\frac{\partial c}{\partial t} = \frac{\partial F_x}{\partial x} + \frac{\partial F_y}{\partial y} + \frac{\partial F_z}{\partial z}$$

where

$$\frac{\partial F_x}{\partial x} = -D \frac{\partial^2 c}{\partial x^2}$$

Using Fick's second law and boundary conditions for various geometric shapes, one can find a solution to it, which can enable one to calculate the diffusion coefficient D .

Methods for measuring diffusion coefficients of dilute solutes.

Considerable efforts have been spent in devising equipment in which the variables of concentration, distance, and time can be observed in such a manner during a diffusion process that the diffusion coefficient, D , can be calculated from one of the various mathematical forms of the basic diffusion equations:

For a number of earlier methods, excellent reviews of both the mathematical and experimental aspects of the diffusion process have been given by Barrer (63), Carslaw and Jaeger (64), Crank (65), and Jost (66). Since detailed developments of these methods are available in the literature, this presentation will be confined to a brief summary of the most useful contributions to classical diffusion measurements.

There have been a number of ways of classifying diffusion measurements, but in general the experiments can be divided into two broad classes (67). They are

1. techniques where diffusion occurs in a pseudo stationary state and where the diffusion rate and concentration gradient can be measured.

2. (a) techniques where a given initial concentration distribution at a starting time is known and the concentration distribution at the end of the experiment can be determined, an unsteady state method (67), or

(b) techniques which are similar to part (a), except that the concentration distribution is determined continuously or at intervals throughout the experiment.

(A) Previous Methods

1) Pseudo-Stationary State Diffusion Measurements. (67)

Although restricted to rather few types of experimental methods, calculations by use of Fick's first law are simple. If it is possible to measure the diffusion flux, F , in a given system with a known concentration gradient, then the value for D is immediately calculable, for

$$D = \frac{F}{\left(\frac{\partial c}{\partial z}\right)}$$

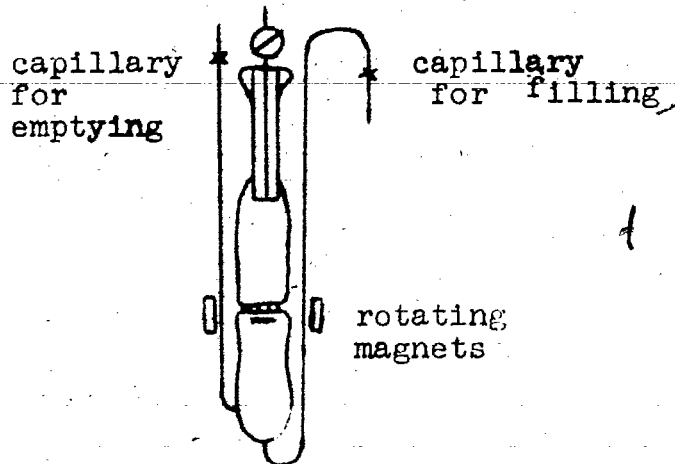
It is possible to integrate the above equation if D is assumed constant and the concentration is a linear function of distance. The most useful application of this type is with diaphragm cells, where diffusion takes place across a porous diaphragm connecting two cells in which the concentrations are maintained uniform.

Another application of the constant flux method is the diffusion process involving a vertical tube open at both ends, placed with each end in a reservoir of uniform concentration. Although the diaphragm cells have been widely used for diffusion measurements, serious discrepancies exist among data obtained by different investiga-

tors (67) using this technique.

(a) Diaphragm Method

This is a pseudo steady-state method (67). The diaphragm is a metal disc, with many holes, sealed across a cylinder.



The dissolved gas diffuses through the holes from a solution of higher concentration to one of lower concentration. Saturation is maintained by having the gas above a small layer of liquid on the disc. If the cross-sectional area is not known, each cell must be individually calibrated using a solution of known diffusivity, and a technical difficulty is involved in measuring very small concentra-

tion changes. A more important disadvantage are surface effects within the holes of the disc. These non-constant effects could affect the rate of mass transfer across the disc, thus influencing the value of D . These effects might change with concentration and solvent.

(b) Absorption of the gas into a liquid jet.

This is a steady-state (67) laminar flow system, and the experiment involves three steps: diffusion in the gas phase, diffusion in the liquid phase and interfacial resistance. The advantages include the simple design of the equipment, the freedom from convection currents, and the speed with which the experiment can be done. The two main difficulties are obtaining an initial uniform velocity at the jet tip, and the needed very accurate solubility data. It has been calculated (68) that an error of 1% in solubility data would lead to a 2% error in the diffusion coefficient.

(c) Ringbom Method

The equipment for this method consists of a gas-saturated and a gas free column separated by a pure gas phase. The gas-saturated water is connected to a reservoir. The volume of gas moving into the pure water is measured by observing the rate of the gas saturated water moving into the displaced gas space. The two problems with this method are the influence of convection currents, and very accurate temperature control is needed.

2) Unsteady-State Diffusion Measurements

The second classification of diffusion measurements includes those methods in which the initial concentration distribution is known as well as the concentration distribution in parts of the diffusion system at some later time. The mathematical solutions are theoretically possible for a number of geometrically shaped cells useful in diffusion studies so long as the concentration distribution is a continuous function of distance and time.

For this case, the differential equation to be solved is

$$\frac{\partial c}{\partial t} = D \frac{\partial^2 c}{\partial x^2}$$

Depending upon the length of the diffusion cell, the mathematical solutions can be divided into three major types:

(a) For a semi-infinite boundary (67):

Concentration distribution and gradient at time

't' are

$$c = A \operatorname{erf} \frac{x}{2\sqrt{Dt}}$$

and

$$\frac{\partial c}{\partial x} = \frac{A}{\sqrt{\pi Dt}} \operatorname{erf} \frac{-x}{2\sqrt{Dt}}$$

or

$$\frac{\partial c}{\partial x}_{x=0} = \frac{A}{\sqrt{\pi Dt}}$$

(b) For a finite boundary of length, l, in contact

with a semi-infinite boundary (67), the concentration distribution at time 't' is given by

$$c = A \operatorname{erf} \frac{l-x}{2\sqrt{Dt}} + \operatorname{erf} \frac{l+x}{2\sqrt{Dt}}$$

(c) For a finite boundary (67):

Concentration distribution at time 't' is

$$c = \sum_{n=0}^{\infty} A_n \cos\left(\frac{n\pi x}{l}\right) \exp\left[-\left(\frac{n\pi}{l}\right)^2 Dt\right] \quad (n=1,2,3,\dots)$$

These are probably the most used of all solutions to diffusion studies as the boundary conditions are fulfilled practically by allowing diffusion to proceed for such a time that the concentration at the remote end of the diffusion cell remains unchanged.

Some methods for steady-state measurements (67) are:

(a) Dissolution of a stationary bubble into an essentially infinite liquid

The rate of solution of a stationary gas bubble in a liquid is governed both by the solubility and the diffusion coefficient of the gas. The liquid at the bubble surface maintains a gas concentration equal to C_g , the saturated solution concentration, and diffusion is considered to occur radially outward into an infinite solution, and to be independent of concentration. The bubble radius as a function of time can then be measured to give D . The two main disadvantages of using gas bubbles to find

the diffusion coefficient are effects due to surface tension, and effects caused by the collapse of the bubble and the consequent 'stirring' of the solution.

(B) Methods used in this investigation

I Open-Tube Method

The method used was that of following the rate of gas absorption into the liquid as a function of time.

The apparatus used was similar to that of Houghton et. al. (69). The diffusion cell was a uniform tube of 24 cm² cross-sectional area and 25 cm. length. The average diffusion length for 200 minutes (the duration of a typical 'run') is less than 2 cm. After filling the diffusion cell with the degassed solvent, thermal equilibrium was established by keeping the cell thermostated ($25 \pm 0.01^\circ\text{C}$) for at least 24 hours prior to allowing the gas into the cell above the solvent. The volume of gas diffusing into the solvent was measured with a calibrated manometer. The gas was kept at constant temperature.

Special care was taken to ensure that the liquid was at equilibrium prior to a run and also that the system was free of any surface-active contaminants.

Experimental Procedure

The apparatus for measuring the diffusion coefficients is shown in Fig. 11.

With stopcocks 1, 2, 7, 11, 13, and 16 open the

Fig 11

Open-Tube Diffusion Apparatus.

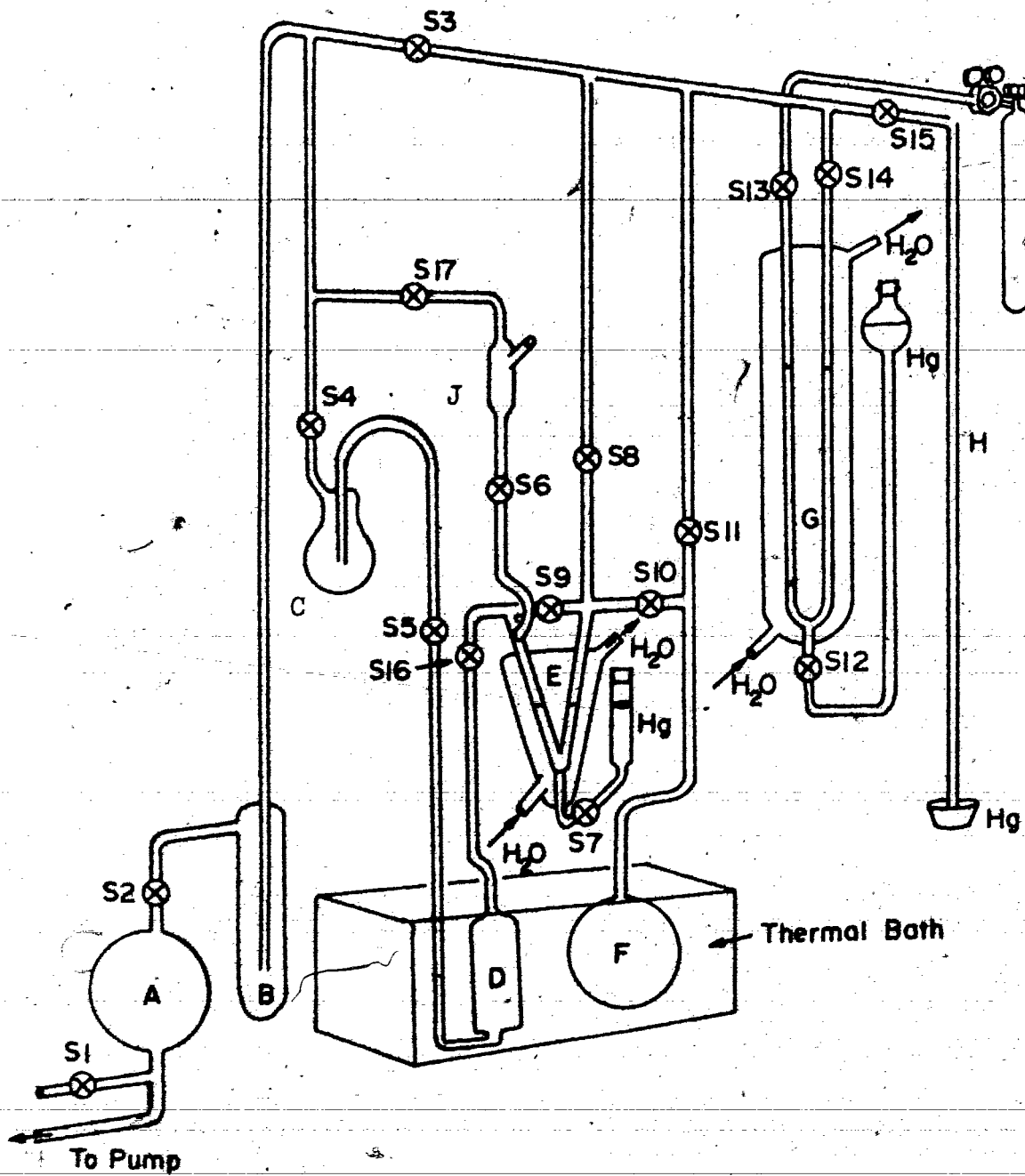


Fig 11

mercury level in manometer E was lowered by opening stopcock 9 and lowering the accompanying B mercury reservoir. Fisher spectroquality solvent was introduced into flask C, or if solvent from a previous run was used, the flask was evacuated, and then stopcock S₅ (Hg sealed) was opened to allow the solvent to flow back into flask C. S₅ was then closed. The mercury level in manometer G was lowered by opening stopcock S₁₂ and lowering the accompanying Hg reservoir. S₁₂ and S₁₃ were then closed.

The system was then evacuated: S₁₁ had been opened and S₂ closed, liquid nitrogen was put in trap E. After shutting S₁, the pump was turned on and both S₂ and S₃ were opened. The solvent was then degassed by warming and evacuating. The degassing procedure was repeated about three times, then S₄ and S₃ were closed.

To transfer the solvent to the diffusion tube D, either a beaker of very hot water was placed under flask C and the solvent vapour pressure was permitted to transfer the solvent when stopcock S₅ was opened, or pressure of added Helium gas was used to transfer the liquid.

(The Helium gas has a very low solubility in water, and therefore would not affect the diffusion coefficients.)

When D was almost filled, stopcocks S₅ and S₁₆ were shut.

The gas storage bulb was then filled with the required gas: with stopcock S₁₃ open, the needle valve was opened,

and then closed. Stopcocks S_{13} and S_3 were then closed. The gas cylinder, S_{13} , and the needle valve were then opened. When the Hg level in H had reached an internal pressure of 1 atmosphere, the gas cylinder, the needle valve and S_{13} were closed. After allowing the Hg level in manometer G to rise, by opening S_{12} , S_{13} was opened to the atmosphere. The pump was turned off and S_1 was opened. Finally, a little solvent from J was allowed into manometer E by opening S_6 , then the Hg level in the manometer was allowed to rise, with solvent levels equal in the two arms.

To start a run, stopcocks 11 and 7 were closed, after stopcock 16 had been opened, at which point the timer was started. Changes in the volume of gas were measured as a function of time. The levels of mercury in the two arms of the manometer E determined the volume. The Hg level (cm) was observed with a cathetometer at $t=0$. At any time $t > 0$, the two levels of Hg were adjusted by opening S_7 until the level in the right arm had risen to the level in the left arm. The new height of the Hg levels was recorded with the time.

The manometer arm was calibrated previously. The area of the diffusion-tube D was measured previously.

Calibration of Diffusion Cell for Open-Tube

The cell was cleaned with distilled water and dried thoroughly in an oven at 100°C . The cell was then clamped

onto a stable retort stand, free from vibration. Distilled water was then poured into the cell by means of a constricted funnel, to about 5 cm. from the bottom. This level was marked with black ink in such a manner that the meniscus coincides with the ink mark.

The height of this water level was read off by means of a Gaertner cathetometer. The cell was then weighed on a sagittorial balance. Precautions were taken to ensure that there was no loss of water through the capillary while weighing. The period of handling was short to ensure minimum loss of water, by evaporation.

More distilled water was poured into the cell to about 15 cm. from the bottom. Special care was taken to ensure that the sides of the cell were not wetted while pouring in the water. This was avoided by filling the cell from the bottom. The height of this level was again read by means of the Gaertner cathetometer. The cell was weighed again, taking the precautions mentioned above.

Calculation of the Area of the Cell

Density of water (71) at 24°C	= 0.997296 gm/cc
2nd Height of water level	= 93.880 cm
1st Height of water level	= <u>83.070</u> cm
Height of water	= <u>10.810</u> cm
2nd Weight of water + cell	= 436.900 gm
1st Weight of water + cell	= <u>252.890</u> gm
Weight of water	= <u>184.010</u> gm

34

$$\text{Density (f)} = \frac{\text{Mass}}{\text{Volume}} = \frac{\text{Mass (m)}}{\text{Length}(l) \times \text{Area (A)}}$$

$$\therefore \text{Area (A)} = \frac{m}{lf}$$

$$A = \frac{184.010}{10.810 \times 0.997296} = 17.0683 \text{ cm}^2$$

This is a typical result. Several measurements were made. The accuracy is $\pm 0.001\%$.

II. The Inverted-Tube Method

A method for the dissolution of a gas into a semi-infinite cylinder of pure solvent was considered in (I). We called the experimental technique the 'open-tube method'. It appears from studies to be discussed later that for certain systems this method has definite limitations. Where the dissolved gas brings about a density increase in the surface layer, as compared to the density of the pure solvent, the simple diffusion dissolution process is complicated by the onset of a convection mechanism(70).

To avoid this natural convection term we have investigated the inverted tube method wherein the solvent is held in a capillary above a small slug of the dissolving gas. The denser solution formed by the dissolution of the gas remains below the less dense pure solvent and thus in the accepted sense convection through the formation of a

density gradient is avoided.

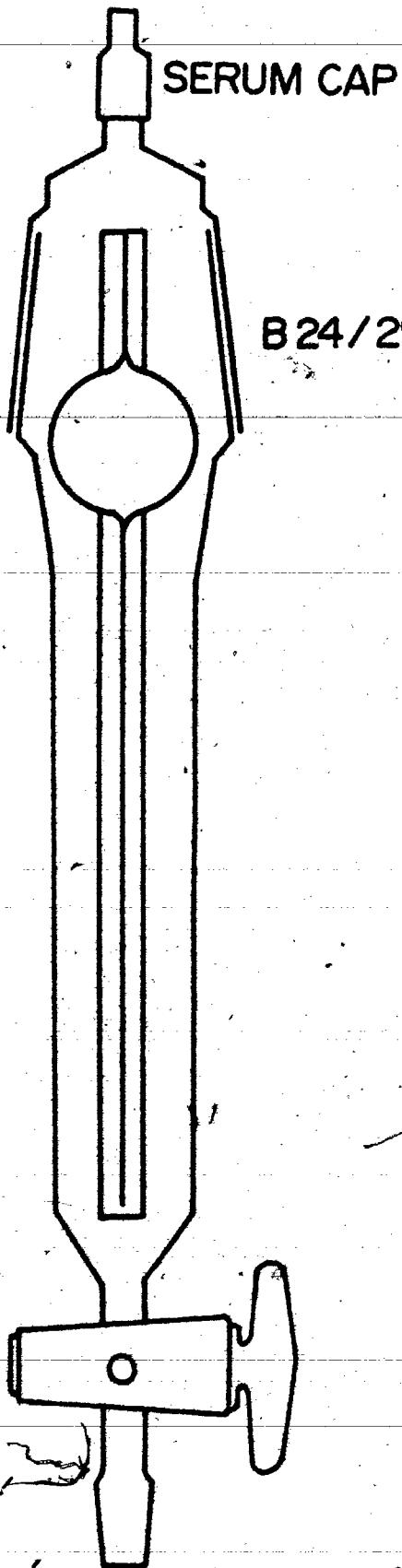
Experimental Procedure

The diffusion cell is made from precision bore tubing (1 mm diameter) and about 15 cm long. (Fig. 12) A small bulb of about 1 ml capacity is blown 2 cm from one end and the other end is sealed. To load the cell, it is first placed in the dessicator vessel and evacuated thoroughly. The whole apparatus is then flushed with the gas under investigation and re-evacuated several times. It is finally filled with gas at 1 atmosphere pressure and a few drops of the degassed solvent are transferred into the bulb of the diffusion cell through a serum cap, using a hypodermic syringe. The diffusion cell is then placed in a thermostat and after 30 minutes, more degassed solvent at the same temperature as the thermostat is quickly introduced into the capillary, displacing the gas, until a gas slug of some 5 mm length is left at the end of the capillary. The change in the position of the solvent meniscus accompanying the dissolution of the gas is followed with a microscope fitted with a calibrated filar eye piece (Gaertner Scientific Corporation). The magnification of the microscope is x 100 and the position of the meniscus can be measured as a function of time to within 0.005 mm. The whole apparatus is mounted on a concrete block to avoid mechanical

vibration. A typical run lasts about 5000 seconds and during this time the meniscus moves some 1.5 mm. For preliminary runs, capillaries of 1, 2, and 3 mm were used for the cells. The rates of absorption of carbon dioxide into water were found to be independent of the dimension of the cell within the accuracy of the experiment. The solvent, water, was purified by distillation in a Pyrex vessel and all gases used were supplied by Matheson.

Fig 12

The diffusion cell and the dessicator vessel.



SERUM CAP

B 24 / 29

Theory

A. The Solution of Fick's 2nd Law for the Methods Used in this Investigation

For the systems studied, diffusion is in a semi-infinite medium, where the boundary ($x=0$) is kept at a constant concentration, c_0 , and the initial concentration for $x>0$ is zero throughout the medium. Using the Laplace transformation we find a solution to

$$\frac{\partial c}{\partial t} = D \frac{\partial^2 c}{\partial x^2} \quad [51]$$

satisfying the boundary conditions

$$c = c_0 \quad x = 0 \quad t > 0 \quad [52]$$

$$c' = 0 \quad x > 0 \quad t = 0 \quad [53]$$

On multiplying both sides of [51] by e^{-pt} and integrating with respect to 't' from 0 to ∞

$$\int_0^{\infty} e^{-pt} \frac{\partial^2 c}{\partial x^2} dt - \frac{1}{D} \int_0^{\infty} e^{-pt} \frac{\partial c}{\partial t} dt = 0 \quad [54]$$

and assuming the orders of integration and differentiation can be interchanged we get

$$\int_0^{\infty} e^{-pt} \frac{\partial^2 c}{\partial x^2} dt = \frac{\partial^2}{\partial x^2} \int_0^{\infty} c e^{-pt} dt = \frac{\partial^2 c}{\partial x^2} \quad [55]$$

Integrating by parts, we have

$$\int_0^{\infty} e^{-pt} \frac{\partial c}{\partial t} dt = [c e^{-pt}]_0^{\infty} + p \int_0^{\infty} c e^{-pt} dt = pc \quad [56]$$

Since $[ce^{-pt}]_0^\infty$ vanishes at $t = 0$ by the virtue of the initial condition and at $t = \infty$ through the exponential factor, eq'n [51] reduces to

$$D \frac{\partial^2 \bar{c}}{\partial x^2} = p \bar{c} \quad [57]$$

By treating the boundary condition [53] in the same way we obtain

$$\int_0^\infty c_0 e^{-pt} dt = \frac{c_0}{p}, \quad x = 0 \quad [58]$$

Thus the partial differentiation eq'n [51] reduces to the ordinary differential eq'n [57]

The solution of eq'n [57] satisfying eq'n [56] and for which \bar{c} remains finite as $x \rightarrow \infty$ is

$$\bar{c} = \frac{c_0}{p} e^{-qx} \quad \text{where } q = \frac{p}{D} \quad [59]$$

The function whose transform is given by eq'n [59] is

$$c = c_0 \operatorname{erfc} \frac{x}{2\sqrt{Dt}} \quad [60]$$

c_0 is the saturation solubility of the gas in the liquid and $\operatorname{erfc}(x)$ is the compliment of the error function.

The equation for mass transfer is

$$F_{x=0} = -D \left(\frac{\partial c}{\partial x} \right)_{x=0} = \frac{1}{A} \frac{\partial m}{\partial t}$$

where $\frac{\partial m}{\partial t} = \frac{P}{RT} \frac{\partial V}{\partial T}$ assuming ideal behaviour.

Differentiating (10),

$$\frac{\partial c}{\partial x} = \frac{-c_0}{\sqrt{\pi Dt}} e^{-\frac{x^2}{4Dt}}$$

At $x = 0$, $\frac{\partial c}{\partial x} = \frac{c_0}{\sqrt{\pi Dt}}$

then $-D \frac{\partial c}{\partial x} = \frac{DC_0}{\sqrt{\pi Dt}} = c_0 \sqrt{\frac{D}{\pi t}} = \frac{P}{ART} \frac{dV}{dt}$

Separating the variables and integrating we get

$$c_0 \sqrt{\frac{D}{\pi}} \frac{ART}{P} \int t^{-\frac{1}{2}} dt = \int dV \quad [61]$$

$$V = \frac{2ART}{P} c_0 \sqrt{\frac{Dt}{\pi}} \quad [62]$$

The theory incorporating the interfacial resistance term and the convection mechanism is derived in the Appendix. A discussion of the magnitude of these terms is also given in the Appendix.

RESULTS

In figure 13 typical data for the diffusion of nitrogen into benzene solvent are given. It is seen that both the open-tube method (O.T.M.) and inverted tube method (I.T.M.) data give linear V vs \sqrt{t} plots but of greatly differing slope. If the presence of the natural convection term is ignored and the O.T.M. data interpreted according to eq'n [62] an "apparent" diffusion coefficient value of $D = 7.23 \times 10^{-5} \text{ cm}^2 \text{ sec}^{-1}$ would be found. The plot from the I.T.M. data gives a value $D = 3.90 \times 10^{-5} \text{ cm}^2 \text{ sec}^{-1}$. A similar pattern of behaviour is observed for the dissolution of argon into water, here the O.T.M. $D(\text{apparent}) = 10.3 \times 10^{-5} \text{ cm}^2 \text{ sec}^{-1}$ whilst the I.T.M. value is $D = 1.44 \times 10^{-5} \text{ cm}^2 \text{ sec}^{-1}$. All these data were measured at $25 \pm 0.01^\circ\text{C}$.

For the dissolution of argon in benzene solvent the data from the O.T.M. experiment, for a cell of cross-sectional area of 24 cm^2 , failed to give an acceptable V vs \sqrt{t} plot so that not even an apparent D value could be calculated. In contrast to this the I.T.M. data gave linear V vs \sqrt{t} plots from which a limiting slope value of $D = 3.99 \times 10^{-5} \text{ cm}^2 \text{ sec}^{-1}$ was found.

As may be seen from figure (14), however, the O.T.M. data follows a pseudo-steady state V vs \sqrt{t} relationship.

The slope of this line is quite reproducible. The considerable increase in the amount of gas absorbed as a function

of time in the O.T.M. experiment in comparison to the I.T.M. experiment is easily seen from the plot since the 'reduced' gas volume plotted is made independent of the tube cross-section area.

Measurements were made for the rate of absorption of carbon dioxide in water over the temperature range 0-35°C. The limiting slope, equation [62] was used to calculate D. In all cases a good linear V vs \sqrt{t} plot was observed. In table VII we present the slopes of the V vs \sqrt{t} plot, estimated to be accurate to 2% at room temperature. D values are also given in Table VII and are calculated using the smoothed solubility data tabulated by Lange⁽⁷¹⁾. This data was found to differ by 5% from the high temperature data of Morrison⁽⁷²⁾ but agreed to better than 1% at lower temperatures. Fig 15 shows a plot of $\log D$ vs $\frac{1}{T}$; a linear relationship is observed and the data are represented by the empirical equation

$$\log_{10}D = 1.303 - \frac{9.23}{T}$$

The measured data agreed quite well with the results of Unver and Himmelblau⁽⁷³⁾ obtained using the laminar flow method. They fitted their data to the following equation:

$$D \times 10^5 = 0.95893 + 2.4101 \times 10^{-2} \theta + 3.9813 \times 10^{-4} \theta^2$$

(temperature, $\theta^\circ\text{C}$) which is represented in figure 15 by a dotted line.

Data for the rate of absorption of Ar in water are given in Table VI, again over the temperature range 0 - 35°C. The diffusion coefficient values were calculated using the solubility data of Ben-Naim et al. (74) for the temperature range 0 - 30°C and Smith et al. (75) @ 35°C. The plot of log D vs $\frac{1}{T}$ is given in figure 16 and as seen, a slight divergence from a strictly linear relationship is observed. These data are represented by the empirical equation, $D \times 10^5 = 7.18 \times 10^{-1} + 3.60 \times 10^{-2} \theta - 2.11 \times 10^{-3} \theta^2 + 1.14 \times 10^{-4} \theta^3$ which fits the experimental data to 1% accuracy.

For the argon data we compare our value at 25°C ($D = 1.44 \times 10^{-5} \text{ cm}^2 \text{ sec}^{-1}$) with that measured by R.G. Smith et al. (76) using the "Ringbom" technique. Their value of $1.46 \times 10^{-5} \text{ cm}^2 \text{ sec}^{-1}$ is in excellent agreement with our own value even though the experimental techniques are radically different. The recent measurements of Boerboom and Kleggh (77) gave a value at 0°C of $0.663 \times 10^{-5} \text{ cm}^2 \text{ sec}^{-1}$ and at 25°C a value of $0.78 \times 10^{-5} \text{ cm}^2 \text{ sec}^{-1}$. Houghton and Wise (78) using the collapsing bubble method found D values considerably higher than our own.

For the gases studied, the 'inverted tube method' gave results in good agreement with those values obtained by other workers. It would seem that with the gas diffusing upwards into the solution, the dissolution has no appreciable density convection term.

Over the temperature range studied, all gases exhibited good, linear $\log D$ vs. $\frac{1}{T}$ plots, suggesting there is no change in the immediate environment of the gas over (Fig. 17) this temperature range. If activation energies (ΔE) are meaningful, the values obtained from the $\log D$ vs. $\frac{1}{T}$ plots, given in Table V, show reasonable constancy. The value for methane (3.06 kcal) (80) is in good agreement with the 2.90 kcal value for the diffusion of a wide range of hydro carbons in water as reported by Wither- spoon. The solubility data for methane, chloromethane, bromomethane and dichlorofluoromethane were those of Glew and Woelwyn-Hughes. (79). They claim their data is precise to $\pm 2\%$ (using a volumetric technique). When more accurate solubility data are obtained for these fluorocarbon gases, the diffusion coefficient can be recalculated, as the rates of diffusion are quoted.

Various empirical relationships have been suggested for the diffusion coefficients of gases in liquids. The diffusion of a gas through a dense solvent is controlled mainly by the size of the diffusing solute molecule and by the viscosity of the solvent. Hildebrand has suggested that the product $DV_b^{\frac{2}{3}}$, where V_v is the solute molar volume at the boiling point, should be approximately constant (81). As seen in Table V, a rough constancy is observed, though the value of this product for argon is considerably less and the value $DV_b^{\frac{2}{3}} = 29.72$ for CHCl_2F is far higher than the other gases. A rough linearity exists between $10^5 DV_b^{\frac{2}{3}}$

and the activation energy ΔE for CH_4 , CH_3Cl , and CH_3Br as might be expected from Hildebrand's arguments for the use of the $V_b^{\frac{2}{3}}$ term.

Othmer and Thakar (52) have suggested that as both diffusion and viscosity are rate processes, both varying linearly with the exponentiation of temperature, a plot of $\log D$ vs $\log \eta$ (the solvent viscosity) should give a straight line. Such a plot is given in Figure 18 and it is seen that all six gases give a good linear relationship over the temperature range measured. Wilke and Chang (50) have proposed an equation relating the diffusion coefficient of a solute to the physical properties of both solute and solvent, viz.

$$D = \frac{7.4 \times 10^{-3} \times (2.6M)^{\frac{1}{2}} T}{\eta V_b^{0.6}}$$

As may be seen from the tabulated data for each gas, and for typical systems as plotted in Figure 19, this equation is totally unable to represent the observed data. Neither does it give a good estimation of the temperature dependence of D .

If the simple Stokes-Einstein relation is examined

$$D_2 \eta_1 = kT / 3\pi \sigma_{22}$$

a reasonable consistency for the $D_2 \eta_1 / T$ term for all systems over the temperature range studied was found. Values of this term are tabulated for each system in Table V to IX. If the average value of $D_2 \eta_1 / T$ is plotted against $(1/\sigma_{22})$ it was found that though a linear relationship

exists for the CO_2 , CH_4 , Ar and CH_3Cl , the slope of the line is of the wrong sign.

The extension by Thorne (54) of the Chapman-Eskog theory of dense gases has been combined with the contact radial distribution function, obtained by Lebowitz (61) on the basis of the Percus-Yevick theory to provide expressions for the variation of the mutual diffusion D_{12} with concentration for a dense, mixed, hard-sphere fluid (53).

The McLaughlin (53) formulation of the diffusion equation, based upon the theory of Eskog (82) offers an alternative to the Stokes-Einstein equation and the many empirical relationships based on it, some of which were discussed before. To obtain mutual diffusion coefficients from equation [46] values of the self-diffusion coefficient D_1° of water are needed over the temperature range of the experiment. These values are obtained from the data of Wang, Robinson and Edelman (83). Hard-sphere diameter values (σ_{11}) of the solvent and of the various solutes are also needed. For water we use a value of 2.75\AA (84). For the solutes we use the generally accepted 12-6 Lennard-Jones potential σ values (84). D_1° data obtained with D_2O as the tracer molecule, (83) and H_2O tracer data (83) gives no better overall agreement.

As may be seen in Tables VI to XI, except for the CO_2 - H_2O system, the D_2 values obtained from equation [46] agree with experiment better than do the Wilke-Chang

equation [12] values. The values from equations [46] and [12] are compared with the experimental D_2 values for argon and methane in Fig 19. In general, the temperature dependence of D_2 is not well predicted by equation [46]. The assumption is made that the hard-sphere diameter values do not vary with temperature. The validity of this is tested by plotting in Figure 20 the diffusion coefficient of the solute (D_2) against the self-diffusion coefficient of water (D_1) at the same temperature. For all systems examined a good linear relationship exists. This suggests that the right hand side of equation [46] can indeed be considered independent of temperature.

It is seen from Table VII that for the $\text{CO}_2\text{-H}_2\text{O}$ system the agreement between the theoretical equation [12] values and experiment is not only worse than the Wilke-Chang values but far worse than those values predicted from his theory, for this system, by McLaughlin (53). McLaughlin made two approximations when using equation [46]. He obtained the σ_{22}/σ_{11} ratio from data on the low density gas viscosities of water and of CO_2 over the temperature range of the D values.

The ratio is obtained from the relationship (ref. 53)

$$(\eta_1)_{\text{gas}} = 1.016 \left(\frac{5}{16} \sigma_{11}^2 \right) (m_1 kT/\pi)^{\frac{1}{2}}$$

In this range 0-55°C he found the σ_{22}/σ_{11} ratio to vary from 0.98 to 1.01. Having found this ratio close

to unity he set the last term in equation (46) equal to unity. The very small variations in σ_{22}/σ_{11} (from gas viscosity data) over the temperature range studied support our interpretation of the linearity of the D vs D_1° plot. The σ_{22}/σ_{11} ratios from the slope of the D vs D_1° plot is obtained making the assumption that the final term in equation [46] is unity. These are given in Table V and it is seen that for the $\text{CO}_2/\text{H}_2\text{O}$ system the value of $\sigma_{22}/\sigma_{11} = 1.10$ is, in fact, self-consistent with the assumption that the final term in equation [46] is approximately unity. It agrees with the σ_{22}/σ_{11} ratio obtained from the gas viscosity data for $\text{CO}_2/\text{H}_2\text{O}$ but does not agree with the ratio obtained from accepted σ values (49). Using the σ_{22}/σ_{11} ratio obtained from the D_2 vs D_1° plot, the D_2 values obtained from equation [46] are in better agreement with the experimental values (Table V). For the $\text{CH}_3\text{Cl}/\text{H}_2\text{O}$ and the $\text{CH}_3\text{Br}/\text{H}_2\text{O}$ systems the D_2 vs D_1° plot gives σ_{22}/σ_{11} ratios close to unity. As can be seen from Tables VI and XI, using these σ ratios and making the assumption that the final term in equation [46] is unity does not improve the agreement with experiment. For the $\text{CHCl}_2\text{F}/\text{H}_2\text{O}$ system using a σ_{22} value of 2.66 Å² (85), the diffusion values obtained are in rather poor agreement with the experimental values. From the D_2 vs

D_1^0 plot the α ratio is found to be 0.60 but this ratio is not self-consistent with the assumption that the final term in equation [46] is unity. Dilute gas viscosity data for CHCl_2F are not available but it would appear that equation [46] cannot predict the D value for CHCl_2F in water with any real success.

TABLE V
DIFFUSION COEFFICIENT VALUES FOR GASES IN WATER AT 25.00 ± 0.01°C

Gas	$10^5 D_z$ cm ² sec ⁻¹	Coefficients of $\ln D_z = B/T + C$ - Bx10 ⁻³ - C		ΔE kcal. mole ⁻¹	$10^5 DV_b^2$	Average $\frac{D_{eff}}{D} \times 10^3$	$(\sigma_{22}/\sigma_{11})^a$	$(\sigma_{22}/\sigma_{11})^b$	$(\sigma_{22}/\sigma_{11})^c$	$\sigma_{22}R^c$
Ar	1.44	2.236	3.6443	4.43	13.98	4.31	1.24	0.86	1.32	3.42(1)
CO ₂	1.89	2.264	3.2164	4.48	20.91	5.97	1.454	1.05	1.10	4.06(1)
CH ₄	1.64	1.545	5.8556	3.06	18.47	5.15	1.34	1.38	1.81	3.76(1)
CH ₃ Cl	1.40	3.109	0.7415	4.15	19.00	4.28	1.22	1.26	0.96	3.37(1)
CH ₃ Br	1.35	2.337	3.4027	4.63	19.53	4.10	1.61	1.65	1.05	4.43(1)
CHCl ₂ F	1.80	3.419	-0.5389	6.77	29.72	5.19	1.62	-	0.60	2.66(2)

$(\sigma_{22}/\sigma_{11})^a$ - using σ_{22} as listed and $\sigma_{11} = 2.75$ (3)

$(\sigma_{22}/\sigma_{11})^b$ - from gas viscosity data

$(\sigma_{22}/\sigma_{11})^c$ - from slope of D vs D_1 plot

- (1) Reference 35
- (2) J.O. Hirschfelder, F.T. McClure and I.F. Weeks, J. Chem. Phys., 10, 201 (1942)
- (3) Reference 49

TABLE VI

SYSTEM Ar-H₂O

T°K (±0.01°K)	Slope of $V v_1 \sqrt{t}$ (ccsec ²)x10 ²	10 ⁵ D cm ² sec ⁻¹ EXPT	10 ⁵ D cm ² sec ⁻¹ (Wilke & Chang) Eq (13)	10 ⁵ D cm ² sec ⁻¹		$\frac{D_2 n_1}{T} \times 10^3$
				Equation (12) Approx(I)	Exact (II)	
273	1.63 ± 0.01	0.72	1.25	-	0.65	4.73
278	1.59 ± 0.02	0.85	1.51	-	0.76	4.65
283	1.54 ± 0.02	0.97	1.78	-	0.90	4.78
288	1.48 ± 0.01	1.09	2.09	-	1.03	4.31
293	1.45 ± 0.01	1.23	2.41	-	1.19	4.21
298	1.44 ± 0.02	1.44	2.76	-	1.36	4.30
303	1.60 ± 0.03	1.65	3.14	-	1.54	4.34
308	1.50 ± 0.02	1.82	3.53	-	1.77	4.25

TABLE VII
SYSTEM CO₂-H₂O

T°K (+0.01°K)	Slope of $V v_1 \sqrt{t}$ (ccsec ^{1/2})x10 ²	10 ⁵ D cm ² sec ⁻¹ EXPT	10 ⁵ D cm ² sec ⁻¹ (Wilke & Chang) Eq (13)	10 ⁵ D cm ² sec ⁻¹		$\frac{D_{21}}{T} \times 10^3$
				Approx(1)	Equation (12)† Exact(11)	
273	6.11 ± 0.03	1.00	0.88	0.84	0.51	6.52
278	5.39 ± 0.04	1.16	1.06	0.99	0.61	6.34
283	5.04 ± 0.03	1.32	1.25	1.17	0.72	6.09
288	4.67 ± 0.03	1.52	1.43	1.34	0.82	6.01
293	4.43 ± 0.01	1.74	1.67	1.55	0.95	5.92
298	4.07 ± 0.01	1.85	1.90	1.78	1.08	5.53
303	3.66 ± 0.02	2.19	2.18	2.01	1.23	5.76
308	3.62 ± 0.01	2.41	2.46	2.30	1.41	5.63

† Approx(1) - using $\left\{ \frac{\sigma_{22}}{\sigma_{11}} \right\}^c$ values, Table V
 Exact(11) - using $\left\{ \frac{\sigma_{22}}{\sigma_{11}} \right\}^a$ values, Table V

TABLE VIII
SYSTEM CH₄-H₂O

T°K (±0.01°K)	Slope of $V v_1 \sqrt{t}$ (ccsec) x 10 ²	10 ⁵ D cm ² sec ⁻¹ EXPT	10 ⁵ D cm ² sec ⁻¹ (Wilke & Chang) Eq. (13)	10 ⁵ D cm ² sec ⁻¹		$\frac{D_2 \eta_1}{T}$ x 10 ³
				Approx(i)	Exact(ii)	
273	2.00 ± 0.03	1.05	0.82	-	0.68	6.89
278	1.86 ± 0.04	1.10	0.98	-	0.80	6.07
283	1.71 ± 0.01	1.22	1.17	-	0.95	5.63
288	1.61 ± 0.05	1.33	1.37	-	1.09	5.25
293	1.53 ± 0.01	1.47	1.58	-	1.26	5.02
298	1.51 ± 0.02	1.64	1.81	-	1.44	4.89
303	1.44 ± 0.03	1.74	2.05	-	1.64	4.58
308	1.43 ± 0.02	1.96	2.31	-	1.87	4.59

TABLE IX

SYSTEM CH₃Cl-H₂O

T°K (±0.01°K)	Slope of $V \sqrt{t}$ (ccsec ^{1/2})x10 ²	10 ⁵ D ⁻¹ cm ² sec ⁻¹ EXPT	10 ⁵ D cm ² sec ⁻¹ (Wilke & Chang) Eq (13)	10 ⁵ D cm ² sec ⁻¹		$\frac{D_{21}}{T} \times 10^3$
				Approx(1)	Equation (12)† Exact(11)	
283	1.35 ± 0.04	0.83	1.76	1.25	0.89	3.83
288	1.24 ± 0.03	0.98	2.05	1.44	1.01	4.45
293	1.16 ± 0.03	1.18	2.37	1.63	1.17	4.03
298	1.09 ± 0.04	1.40	2.71	1.90	1.35	4.18
303	1.03 ± 0.02	1.65	3.08	2.16	1.52	4.34
308	0.98 ± 0.03	2.07	3.47	2.47	1.75	4.84

† Approx(1) - using (σ₂₂/σ₁₁)^c values, Table V

Exact(11) - using (σ₂₂/σ₁₁)^a values, Table V

TABLE X

SYSTEM CH₃Br-H₂O

T°K (±0.01°K)	Slope of $V v_1 \sqrt{t}$ (csec ^{1/2})x10 ²	10 ⁵ D cm ² sec ⁻¹ EXPT	10 ⁵ D cm ² sec ⁻¹ (Wilke & Chang) Eq (13)	10 ⁵ D cm ² sec ⁻¹		$\frac{D_{eff}}{D_1} \times 10^3$
				Approx(1)	Equation (12)† Exact(11)	
283	2.25 ± 0.08	0.85	2.27	1.04	0.57	3.93
288	2.01 ± 0.02	1.03	2.66	1.18	0.65	4.07
293	1.78 ± 0.03	1.16	3.07	1.37	0.75	3.97
298	1.60 ± 0.03	1.35	3.51	1.57	0.86	4.03
303	1.48 ± 0.02	1.64	3.99	1.77	0.97	4.31
308	1.35 ± 0.01	2.00	4.49	2.03	1.12	4.32

† Approx(1) - using (σ₂₂/σ₁₁)^c values, Table V

Exact(11) - using (σ₂₂/σ₁₁)^a values, Table V

TABLE XI
SYSTEM CHCl₂F-H₂O

T°K (±0.01°K)	Slope of $V v_1 / t$ (ccsec ^{1/2})x10 ²	10 ⁵ D cm ² sec ⁻¹ EXPT	10 ⁵ D cm ² sec ⁻¹ (Wilke & Chang) Eq (13)	10 ⁵ D cm ² sec ⁻¹		$\frac{D_2 \eta_1}{T}$ x 10 ³
				Equation (12)†	Exact(11)	
283	1.36 ± 0.10	0.98	1.99	1.07	0.56	4.78
288	1.19 ± 0.11	1.20	2.33	1.22	0.64	4.74
293	1.03 ± 0.08	1.50	2.69	1.42	0.74	5.13
298	0.912 ± 0.06	1.80	3.08	1.62	0.96	5.23
303	0.758 ± 0.04	2.20	3.50	1.83	1.03	5.79
308	0.677 ± 0.04	2.60	3.94	2.10	1.11	6.07

† Approx(1) - using $(\sigma_{22}/\sigma_{11}) = 1$
Exact(11) - using $(\sigma_{22}/\sigma_{11})^2$ values, Table V

Fig 13

Diffusion of nitrogen in benzene solvent.

Curve 1. Open tube method.

Curve 2. Inverted tube method.

Data at 25°C.

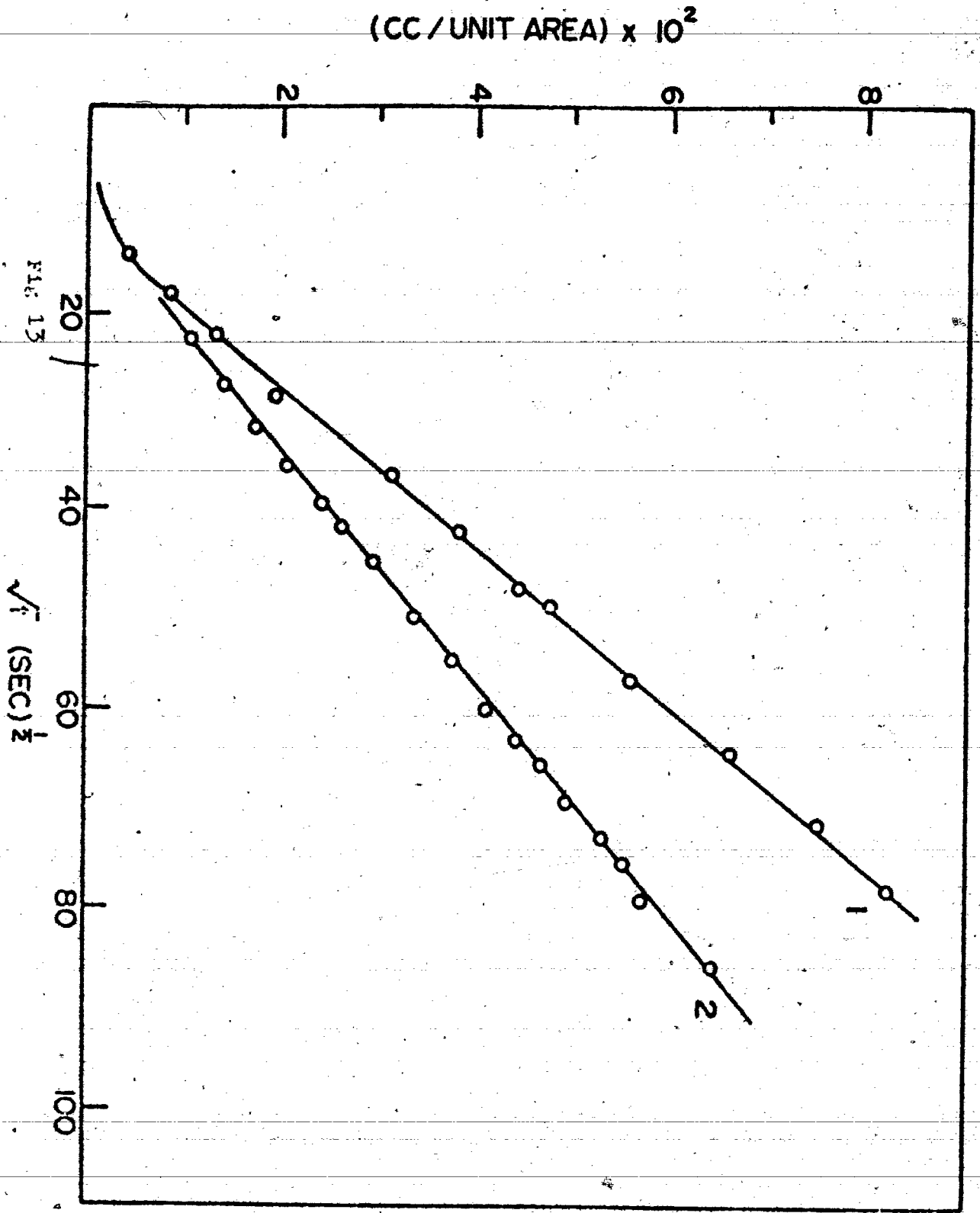


FIG. 13

Fig 14

Rate of Dissolution of Argon into Benzene

Curve 1. Open tube method.

Curve 2. Inverted tube method.

Data at 25°C.

(CC / UNIT AREA) $\times 10^2$

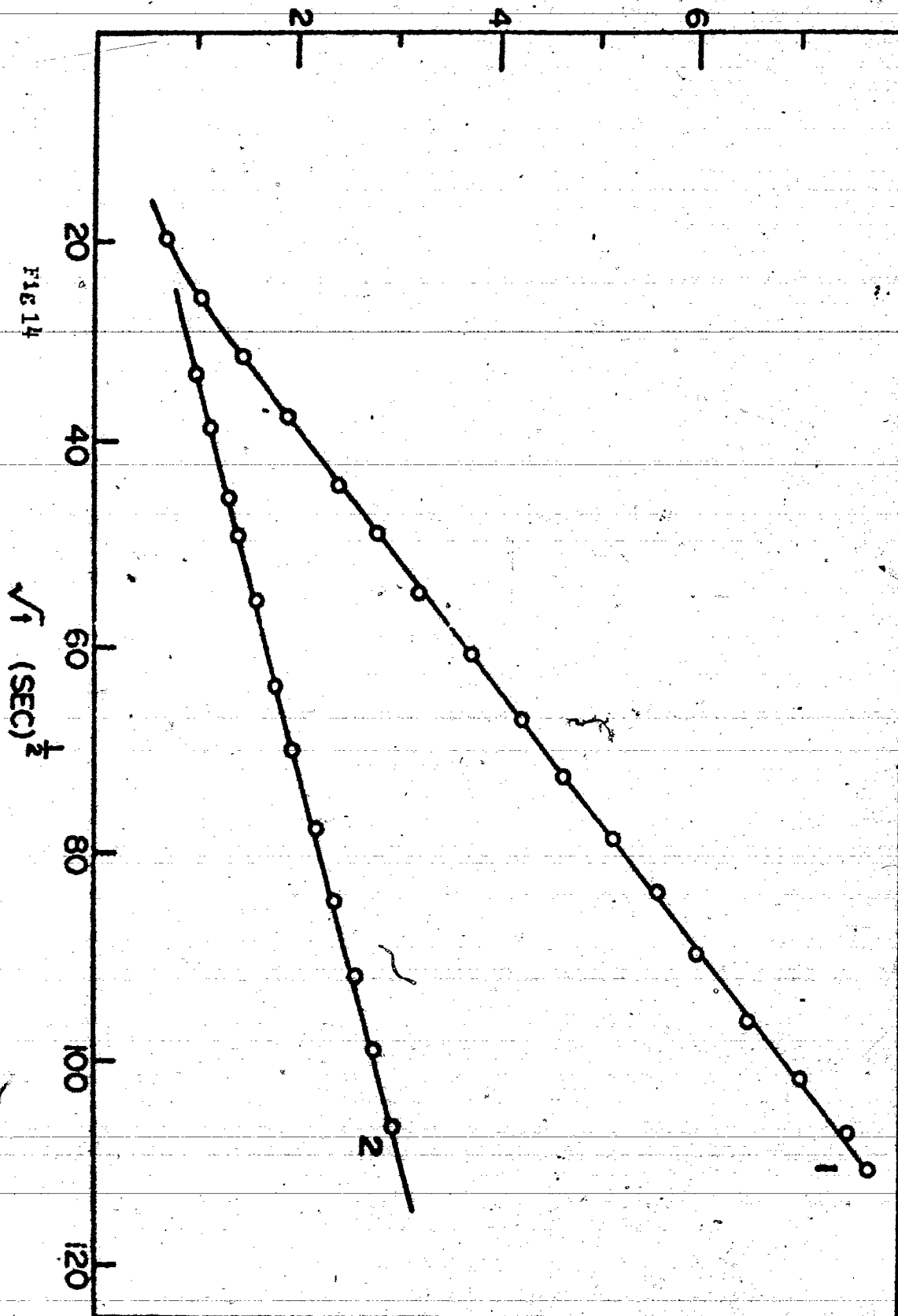


Fig 15

Temperature Dependence of diffusion of carbon dioxide
in water. —

———— Experimental data.

----- Himmelblau data.

===== Solubility data of Morrison and Lange.

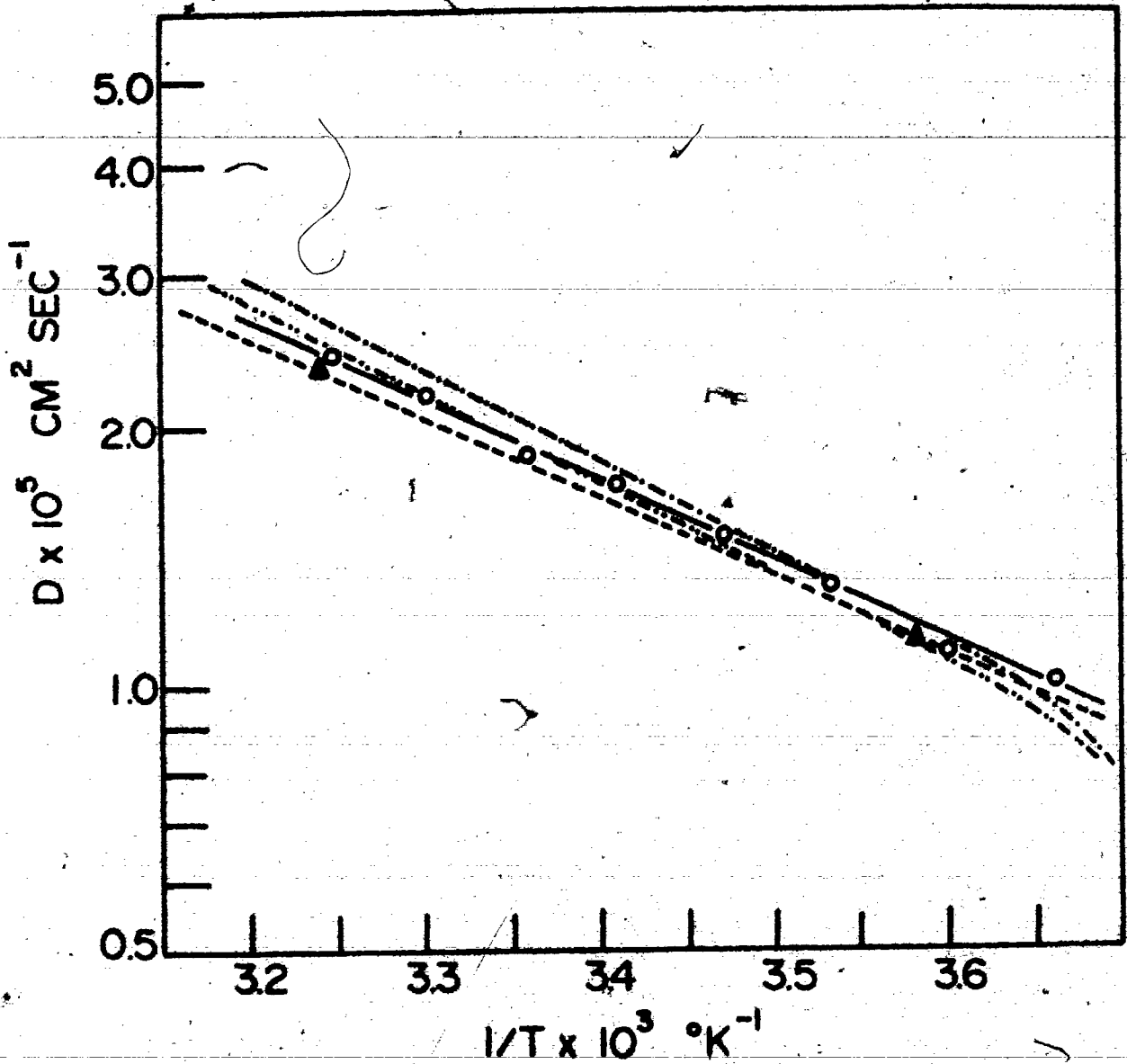


Fig 15

Fig 16

Temperature Dependence of diffusion of argon in
water.

———— Experimental data.

===== Himmelblau data using solubility data
of Lange and Morrison.

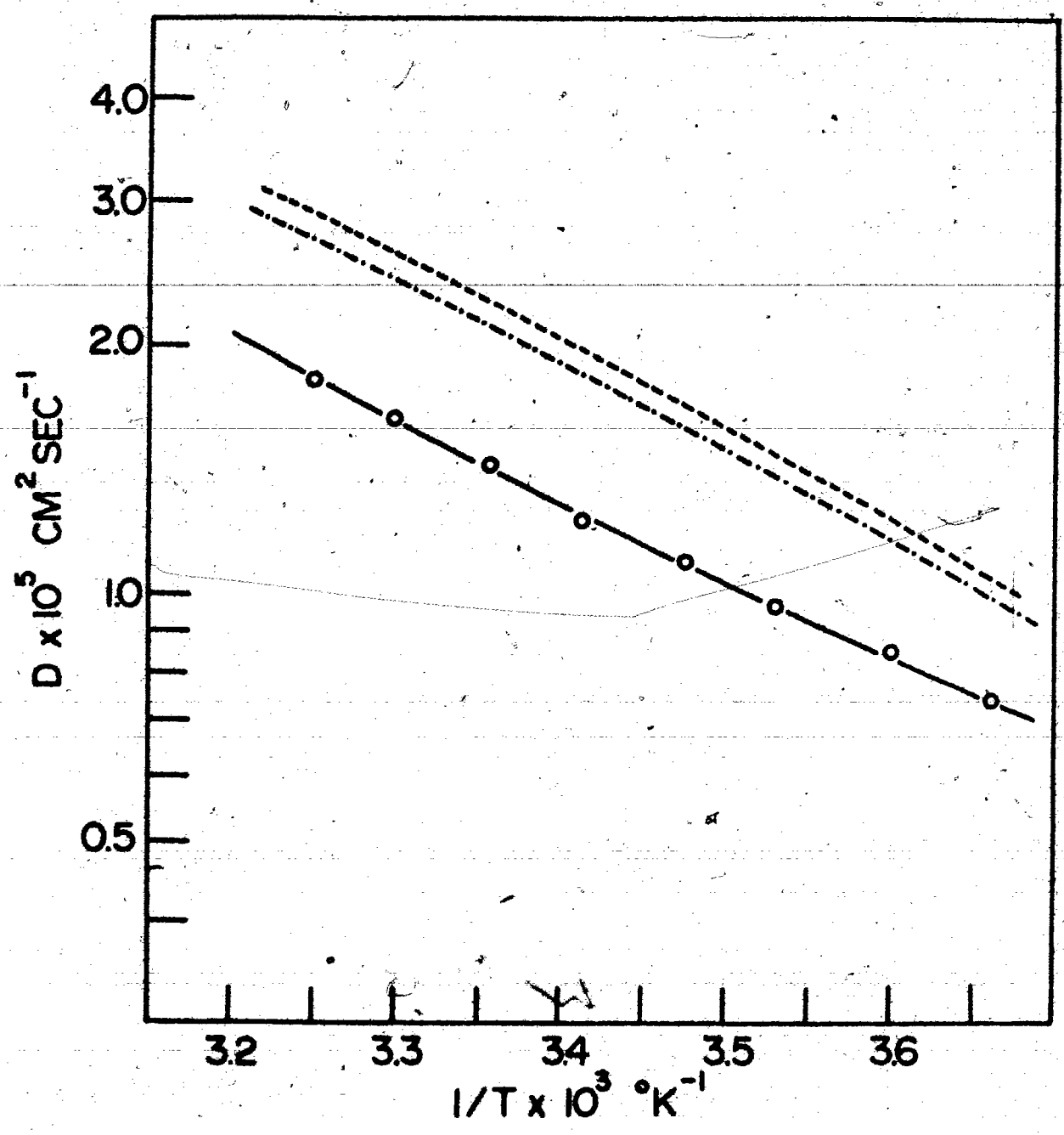


Fig 16

Fig. 17

Dependence of $\log D_2$ on the reciprocal absolute temperature ($1/T^{\circ}\text{K}^{-1}$)

Legend: CO_2 1(x)

CHCl_2F 2(∇)

CH_4 (o)

Ar (\square)

CH_3Cl (Δ)

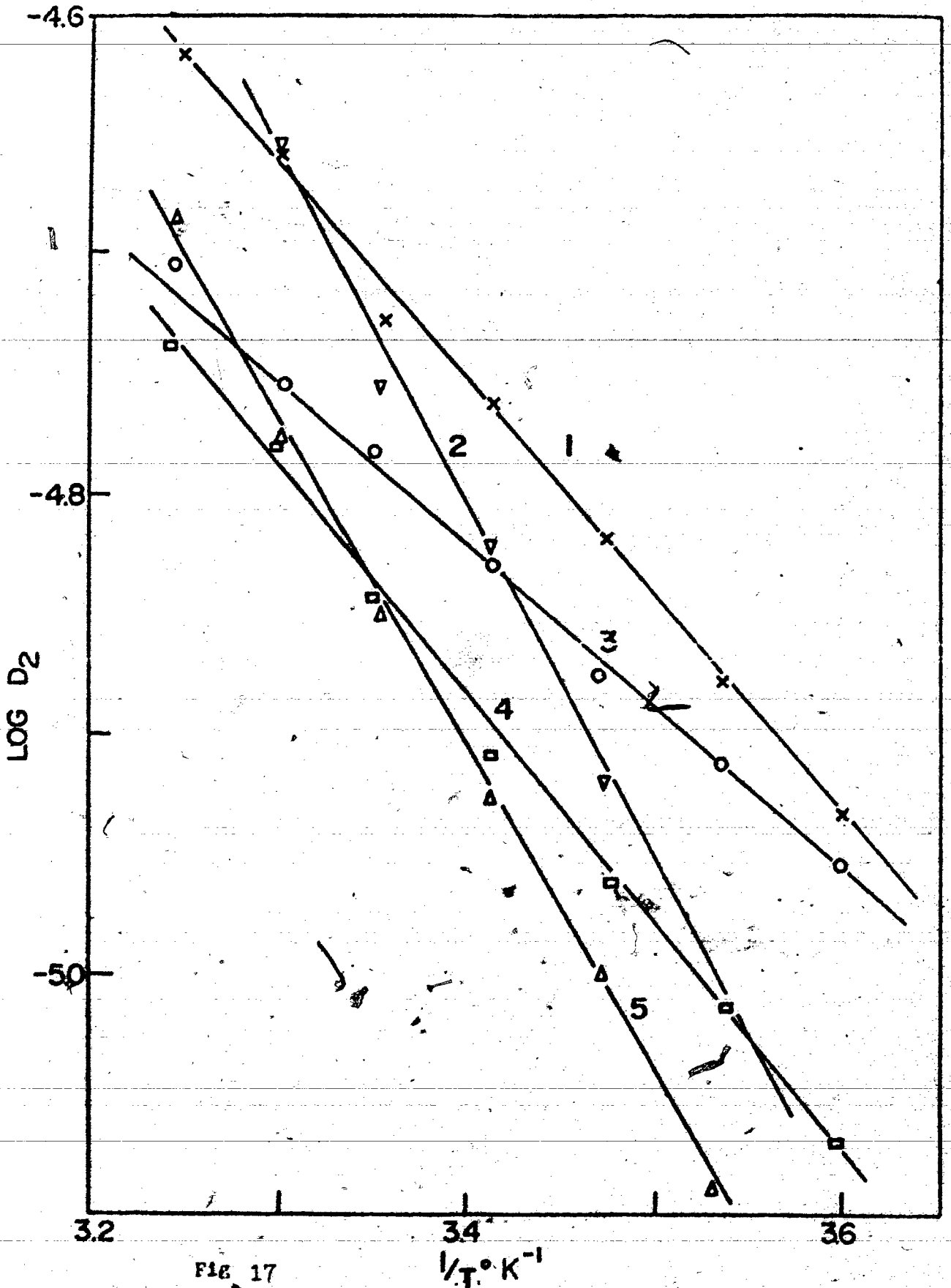


FIG 17

Fig 18

Dependence of gas diffusion coefficient ($\log D_2$)
on the viscosity of water ($\log \eta_1$).

Legend: CO_2 \circ ; CH_4 \square ; CHCl_2F ∇ ; CHCl_3 Δ

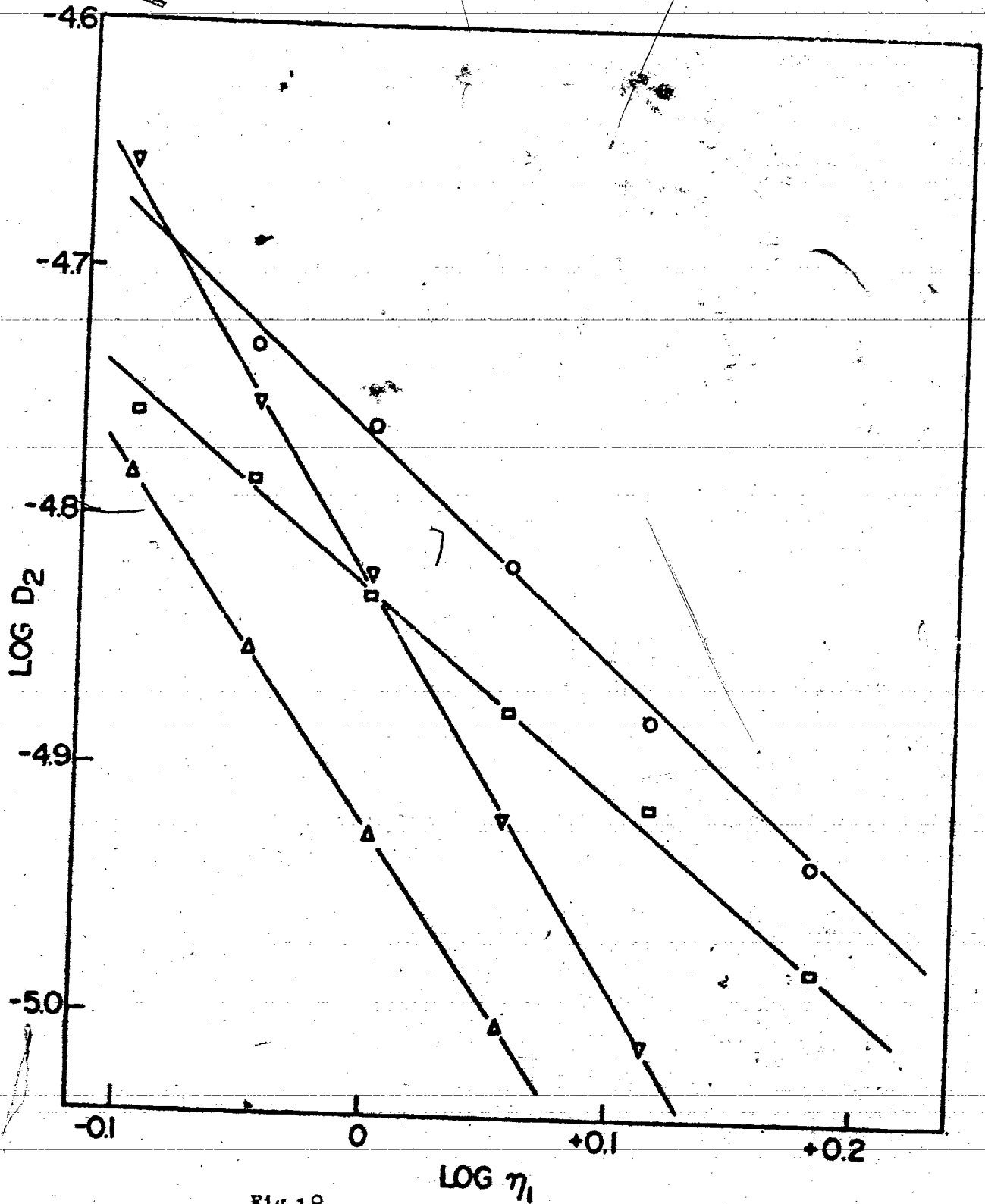


Fig 18

Fig 19

Temperature dependence of Diffusion Coefficient of argon and of methane, with Wilke-Chang and McLaughlin approximations.

Legend: Argon data - full line;
Methane data - dashed line.

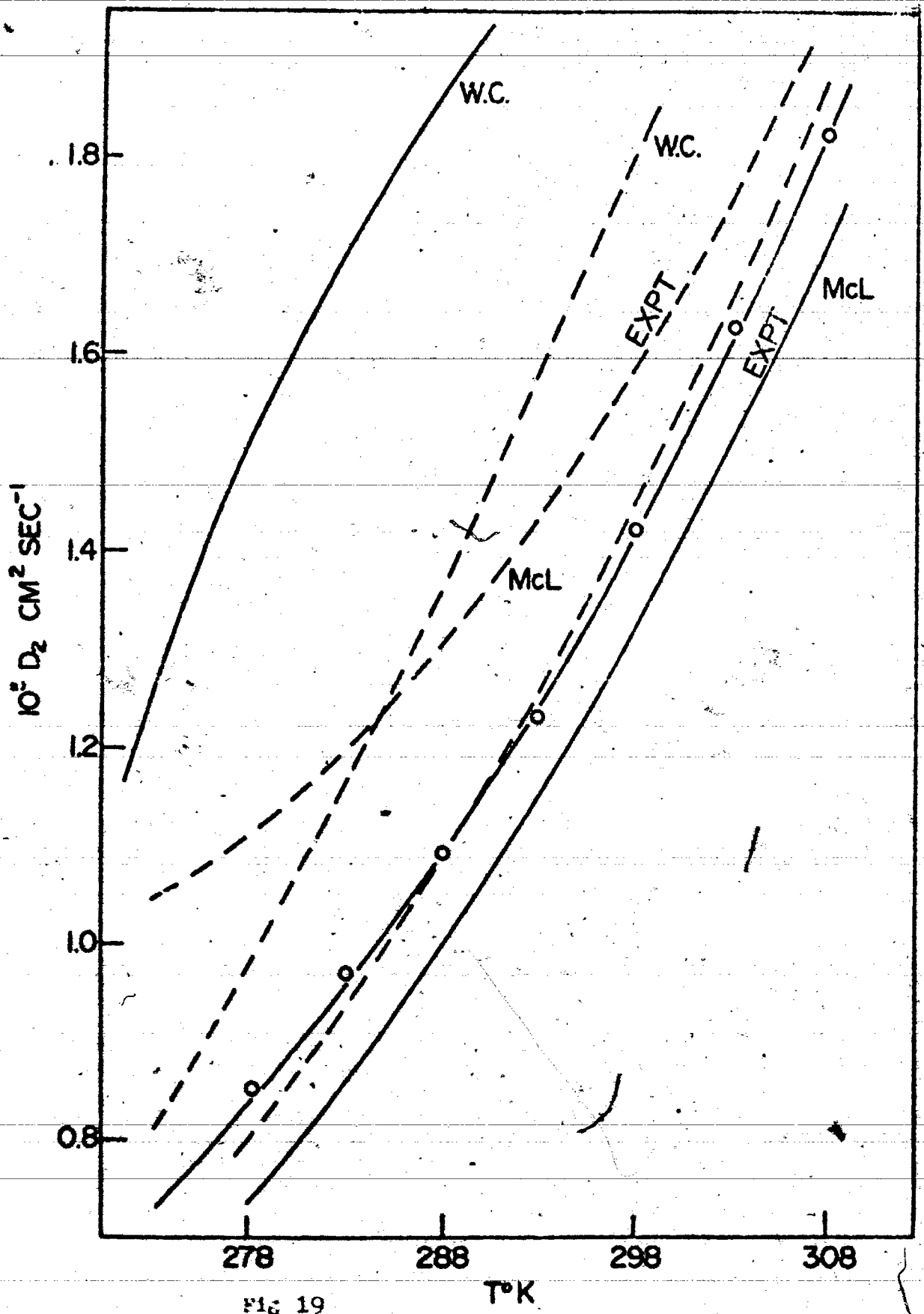


FIG 19

$T^{\circ} \text{K}$

Fig 20

Diffusion Coefficient of gas (D_2) plotted against the self-diffusion coefficient of water (D_1^0) at the same temperature.

Legend: CO_2 ∇ ; Ar Δ ; CH_4 \square ; CHCl_2F \circ

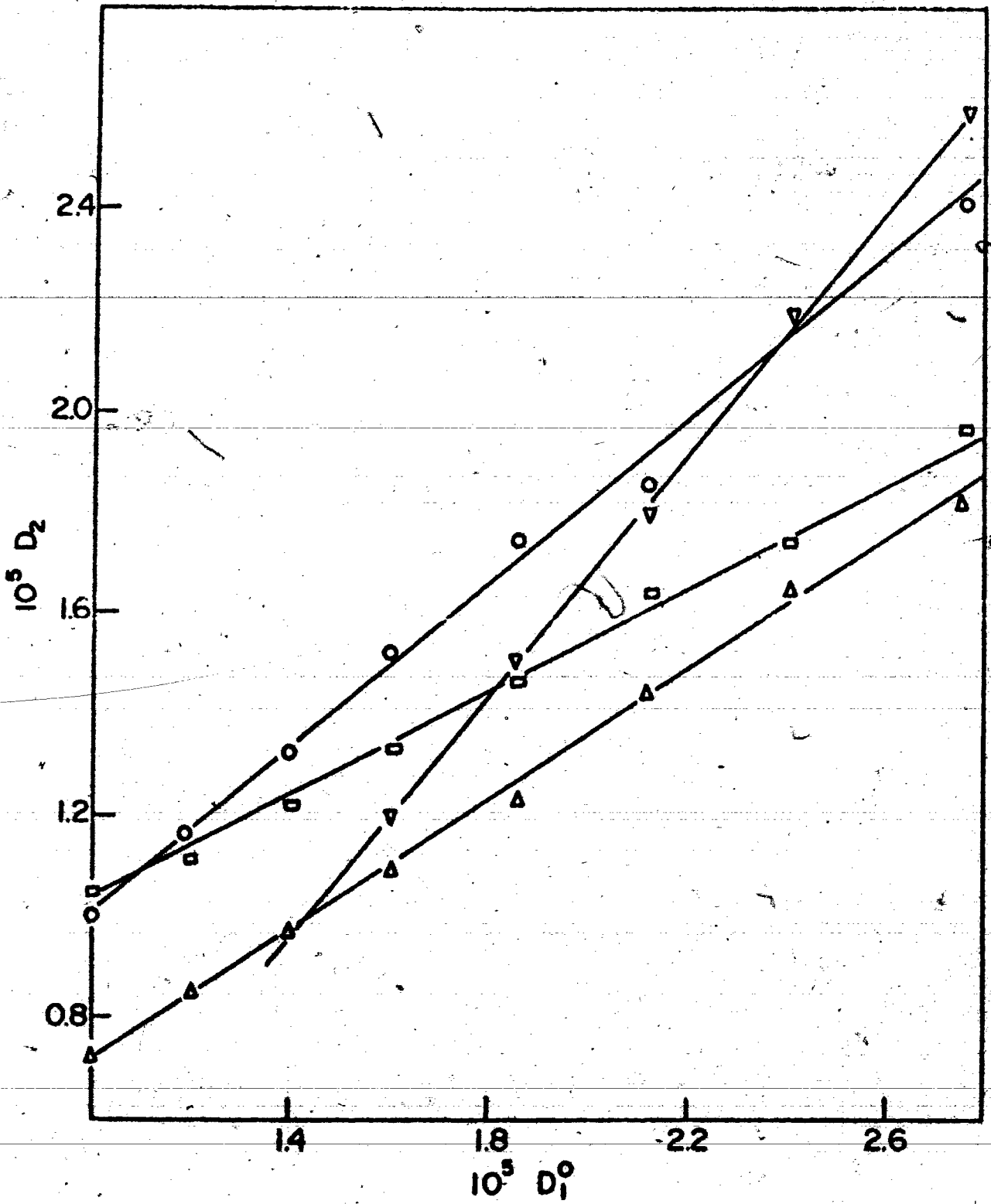


Fig. 20

CONCLUSION

The six gases studied extend over a wide range of gas-hydrate stability. No outstanding differences in actual diffusion coefficient values nor in the temperature dependence of the D values are observed. The agreement of measured values and of various empirical theories is, in general, poor but this is obviously a matter of the poverty of the empirical relationships. Huq and Wood (86) have examined a wide range of empirical and semi-empirical equations relating D values to the properties of the solute and solvent and found a similar disparity between the experimental data and the expected correlation.

The McLaughlin diffusion equation, considering its simplicity (i.e. it comes from hard-sphere theory), its sensitivity to the σ_{11} values used and even more so to the self-diffusion value of water gives remarkable agreement with experiment. It is seen, however, from the D vs D_1° plots that the temperature dependence of the diffusion coefficient of the gas solute cannot be expressed as $D = AD_1^{\circ}$ (where A is a constant for a given system). It is likely that higher terms in the Eskog theory (reflecting multiple collision) must be incorporated before it can adequately portray the temperature dependence of the diffusion of a solute in a

dense solvent medium.

The thermodynamic properties of gases dissolved in non-polar solvents and in water show considerable differences. This is generally regarded as arising through the "water structure" problem. Many studies suggest that for certain gases dissolve in water, a clathrate-type structure immediately around the gas molecule is formed (18). Thus it is expected that for these gases the diffusion process in water solvent does not depend on the solute size alone but upon the enveloping water-structure 'cage'. It might be argued that nothing in the present study mitigates against the concept that gas solutes dissolved in water are surrounded by some water-structure 'iceberg' cage. Equally so, neither the experimental data nor its interpretation in terms of possible relationships between D_1 , D_1^0 , σ_{22} etc support such a concept.

The theoretical and semi-theoretical equations do not clearly indicate the temperature dependence of the diffusivity because either they involve temperature-dependent parameters or they involve temperature-dependent variables such as the viscosity. It is also difficult to draw conclusions concerning the temperature dependence of diffusion coefficients from empirical evidence.

In extrapolating and interpolating diffusivities analytically instead of graphically a simple linear

relation should be effective over moderate temperature ranges, viz

$$\log D_{12} = \frac{A}{T} + B$$

Chapter III

"If we begin in certainties, we shall end
in doubts, but if we begin in doubts, and are
patient in them, we shall end in certainties.

Francis Bacon (1561-1626)

CONCLUSIONS

It is seen from the discussion of both diffusion and solubility studies that no detailed theoretical interpretation of the results can be found. Equally so, no really satisfactory theory of simple gas solubility in water or gas solubility in water plus other solute systems, exists. I consider it necessary at this time to obtain a wider picture of gas solubility in water and water mixtures. The experimental techniques described should be suitable for the study of the wide range of phenomena necessary before the parameters of an adequate theory of solubility can be discerned.

The experimental technique described for measuring the saturation solubility permits accurate data to be obtained for gases dissolved in water. The method appears to be precise. An accuracy of ± 0.05 cc/mole is claimed better than most other methods whose general accuracy is ± 1 cc/mole. The main advantage lies, however, in the rapidity of the determination. Because of the general importance of oxygen solubility in water, oxygen was used as one of the gas components in the gas mixture. It is to be noted that in most of our gas mixture work, analysis was only made for the dissolved oxygen, as we were only interested in the solubility behaviour of oxygen.

In the triangle binary gas mixtures that was done with

an analysis of both components (i.e. N_2/O_2 , O_2/CH_4 and CH_4/N_2) - a lowering of the saturation solubility of each component was observed in all cases. I would suggest that other experiments be done for another triangle of mixtures. The one I would suggest is Ar, Xe and Ne, as there is very little interaction of these inert gases in the gas phase.

Our data obtained from our pressure apparatus was obtained mainly to support our data obtained by other techniques. I would think that rather than study a one atmosphere pressure saturation solubility at $25^\circ C$, as is normally done, using the pressure bomb technique described, a pressure dependence of the saturation solubility (say 0-10 atmospheres) can be simply done. From this the slope K_H , (Henry's law constant) of the solubility-pressure graphs give a self consistent value for the saturation solubility.

Our pressure dependence of the O_2/N_2 mixture is of practical interest as there is a lowering of the oxygen saturation solubility. But it is found that a better experiment would be to keep gas (2) at a high pressure (say 20 atmos.) and find the change in gas (1) over 0 \rightarrow 5 atmos. range i.e. the pressure of gas (1) is a constant. This can be done by a simple modification of the bomb and the pressure gauge.

In a recent paper, Lucas (35) claims that methane behaves as a structure breaker above 28.7° and a structure maker below this. A temperature dependence study of the

the solubility of the pure gases and their mixtures is worthwhile; from this one could obtain ΔH and ΔS values for such transitions if they do occur. We can do solubility at any temperature without any modification of our present apparatus.

Our present methods of measuring solubility can be used for any solvent. The only modification is choosing a column which will separate the solvent from the gas mixture. It would be interesting to do the solubility of mixture of gases in benzene, as one would then have data for a solvent "without a structure."

The solubility of air in water obtained by chemical analysis contradicts our results (87) obtained both from mixtures made by proportioning and from pre-mixed gases obtained from Matheson and Co. A percent error of ± 0.10 mls. in the titration using the Winkler method results in $\pm 5\%$ in their value for the oxygen saturation solubility. Since the value of oxygen saturation solubility in air is very small, a small error in the titration can lead to a high degree of inaccuracy, this may have been overlooked.

The technique devised for measuring diffusion is obviously suitable for doing temperature dependence studies. It is not easily adapted for pressure dependence studies. It is found that for a wide range of gases D_2 is linear in $\frac{1}{T}$ between $5 \rightarrow 35^\circ\text{C}$. This suggests that there is no particularly strange behaviour, as convection, occurring (81). In view of

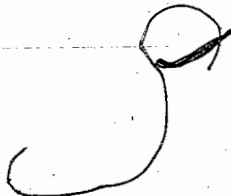
other work in this area, diffusion in D_2O should be measured, as well as diffusion in water (and D_2O) - alcohol, and dioxane mixtures. As there is a large discrepancy in results obtained using different techniques for measuring diffusion coefficient, probably due to "convection", the ultimate experiment is study diffusion using an isotopic method so as to eliminate this convection problem. In a method wherein an isotopically labelled dilute solute, in a saturated solution, diffuses into a saturated solution containing the non-labelled species the counter diffusion of the solute species takes place without change in solute concentration and hence without change in local solvent density.

As solubility data for mixtures of gases in water are now available, diffusion of mixture of gases should be done. I would predict that the rate of diffusion is less than that for the pure components, because the rate of diffusion is directly proportional to the saturation solubility.

Gubbins (14) recently used an improved hard-sphere model to calculate partial molal volumes and diffusion coefficients of gases in aqueous electrolytes. He found good qualitative agreement between experiment and theory. It is to be noted that his theory is only good for water plus a solute which is fairly highly soluble. It would not work as well for our very dilute systems. Also, perhaps such studies are of

little use in the interpretation of the binary gas solubility effect since salts appear to have very large effects upon the water structure.

Our observed mutual lowering of the solubility of binary gases in water should encourage other workers to pursue this field by other techniques as mass-spectrometry, as there are wide practical applications for such data. Until other methods have been tried, one is not in a position to make any concrete statements about our observed phenomena.



REFERENCES

1. J.D. Bernal and R.H. Fowler, J. Chem. Phys., 1, 515 (1933).
2. H.S. Frank, Proc. Roy. Soc., A247, 481 (1958).
3. H.S. Frank and W.Y. Wen, Disc. Farad. Soc., 24, 133 (1957).
4. G. Nemethy and H.A. Scheraga, J. Chem. Phys., 36, 3883 (1962).
5. O.Y. Samoilov, Zh. Fiz. Khim., 20, 12 (1946).
6. E. Forslind, Acta Polytech., 155, 9 (1952).
7. J.A. Pople, Proc. Roy. Soc., A205, 163 (1951).
8. H.S. Frank and A.S. Quist, J. Chem. Phys., 34, 604 (1961).
9. C.M. Davis and T.A. Litovitz, J. Chem. Phys., 42, 2563 (1965).
10. G. Wada, Bull. Chem. Soc. Japan, 34, 955 (1961).
11. H.H. Uhlig, J. Phys. Chem., 41, 1215 (1937).
12. D.D. Eley, Trans. Farad. Soc. 35, 1281 (1939).
13. F.A. Long and W.F. McDevit, Chem. Rev., 57, 119 (1952).
14. K.E. Gubbins, J. Phys. Chem. 76, 3044 (1972).
15. W.L. Masterton and T.P. Lee, J. Phys. Chem., 74, 1776 (1970).
16. R.A. Pierotti, J. Phys. Chem., 69, 281 (1965).
17. L. Pauling and R. Marsch, Proc. Nat. Acad. Sci. Wash., 38, 112 (1952).
18. W.F. Claussen and M.F. Polglas, J. Amer. Chem. Soc., 74, 4817 (1952).

19. K. Grjotheim, J. Frogh-Moe, Acta Chem. Scand., 8, 7, 1193 (1954).
20. H.S. Frank and M.W. Evans, J. Chem. Phys., 13, 507 (1945).
21. A. Ben-Naim and S. Baer, Trans. Farad. Soc., 60, 173 (1964).
22. A. Ben-Naim and G. Moran, Trans. Farad. Soc., 61, 821 (1965).
23. Yu V. Gurikov, Zh. Strukt. Khim, 10, 583 (1969).
24. S.K. Lachowics, Imp. Coll. Chem. Eng. Soc., 8, 51 (1954).
25. I.R. Krichevsky and I.S. Kasarnovsky, J. Am. Chem. Soc., 57, 2168 (1935).
26. K.W. Miller and J.H. Hildebrand, J. Amer. Chem. Soc., 90, 3001 (1968).
27. R. Battino and H.L. Clever, Chem. Rev. 66, 395 (1966).
28. K. Benbigh, "The Principles of Chemical Equilibrium", Cambridge Press (1966) p. 237.
29. R. Wiebe and V.L. Gaddy, J. Am. Chem. Soc., 62, 815 (1940).
30. K.E. Gubbins, S.N. Carden and R.D. Walker, J. Gas Chromatog., 3, 330 (1965).
31. J.W. Swinnerton, V.J. Linnebom and C.H. Cheek, Anal. Chem., 34, 483 (1962).
32. A. Ben-Naim, J. Chem. Phys., 42, 1512 (1965).
33. A. Ben-Naim, J. Wilf and M. Yaacobi, J. Phys. Chem., 77, 95 (1973).
34. A.L. Meyers and J.A. Quinn, Nature, Vol. 239, 31 (1972).
35. M. Lucas, J. Phys. Chem., 76, 4030 (1972).
36. A. Ben-Naim, J. Wilf and M. Yaccobi, J. Phys. Chem., 77, 95 (1973).

37. A. Ben-Naim, J. Chem. Phys., 54, 1387 (1971).
38. Wen-Yang Wen and J.H. Hung, J. Phys. Chem., 74, 170 (1970).
39. A. Yu Namiot, Zh. Strukt. Khim, 2, 408 (1961).
40. S.K. Shoor and K.E. Gubbins, J. Phys. Chem., 73, 498 (1969).
41. S.A. Shchukarev and T.A. Tolmacheva, Zh. Strukt. Khim, 9, 21 (1968).
42. A. Ben-Naim, J. Chem. Phys., 45, 2706 (1966).
43. W. Nernst, Z. Physik. Chem., 2, 613 (1888).
44. A. Einstein, Ann. Phys., 17, 549 (1905).
45. S.R. Degroot and P. Mazur, "Non-equilibrium Thermodynamics" - North-Holland Pub. Co., Amsterdam, (1962).
46. J.H. Arnold, J. Am. Chem. Soc., 52, 3937 (1930).
47. E.R. Gilliland, in T.K. Sherwood, "Absorption and Extraction", 1st Ed., McGraw Hill, N.Y. (1937).
48. H. Eyring and T. Ree, Proc. Natl. Acad. Sci., 47, 526 (1961).
49. D.R. Olander, J. Phys. Chem., 67, 1011 (1963).
50. C.R. Wilke and P. Chang, A.I. Ch. E.J. 1, 264 (1955).
51. E.G. Scheibel, Ind. Eng. Chem., 46, 2007 (1954).
52. D.F. Othmer and M.S. Thakar, Ind. Eng. Chem., 45, 589 (1953).
53. E. McLaughlin, J. Chem. Phys., 50, 1254 (1969).
54. S. Chapman and T.G. Cowling, "The Mathematical Theory of Non-Uniform Gases" (Cambridge University Press, England, 1939) p. 140.
55. J.S. Rowlinson, Rept. Prog. Phys., 28, 169 (1965).
56. M.S. Wertheim, J. Math. Phys., 5, 643 (1964).

57. E. Thiele, J. Chem. Phys., 39, 474 (1963).
58. J.L. Lebowitz, Phys. Rev., 133A, 895 (1964).
59. H.C. Longuet-Higgins, J.A. Pople and J.P. Valleau, "Transport Processes in Statistical Mechanics" (Interscience Pub. Inc. London, 1958).
60. H.C. Longuet-Higgins and J.A. Pople, J. Chem. Phys., 25, 884
61. J.L. Lebowitz and J.S. Rowlinson, J. Chem. Phys., 41, B 133 (1964).
62. A. Fick, Ann. Phys. (Leipzig), 170, 59 (1855).
63. R.M. Barrer, "Diffusion in and through Solids", Cambridge (1941) p. 129.
64. H.S. Carslaw and J.C. Jaeger, "Conduction of Heat in Solids", 2nd Edition, Oxford, (1959) p. 562.
65. J. Crank, "The Mathematics of Diffusion", Oxford (1956) p. 184.
66. W. Jost, "Diffusion", Acad. Press, (1952) p. 98.
67. D.M. Himmelblau, Chem. Rev., 66, 527 (1964).
68. L.E. Scriven, Ph.D. Dissertation, University of Delaware (1965).
69. G. Houghton, A.S. Kesten, J.E. Funk and J. Coull, J.P. Chem., 65, 649 (1961).
70. P.V. Danckwerts, Trans. Farad. Soc., 46, 701 (1950).
71. N.A. Lange, "Handbook of Chemistry", 10th Ed., McGraw-Hill Co., Inc., N.Y. (1961).
72. T.J. Morrison, J. Chem. Soc., 3814 (1952).
73. A.A. Unver and D.M. Himmelblau, J. Chem. Eng. Data, 9, 428 (1964).
74. A. Ben-Naim, Trans. Farad. Soc., 59, 2735 (1963).
75. J.T. Ashton, R.A. Dawe, K.W. Miller, E.B. Smith and B.J. Stickins, J. Chem. Soc. (C) 1793 (1969).

76. R.G. Smith, G.T. Kriess and M.F. Moraler, J. Phys. Chem., 59, 382 (1955).
77. A.J.H. Boerboom and G. Klegh, J. Chem. Phys., 50, 1086 (1969).
78. D.L. Houghton and D.L. Wise, Chem.-Exp. Sci., 21, 999 (1966).
79. D.N. Glew and E.A. Noelwyn-Hughes, Disc. Farad. Soc, 15, 150 (1953).
80. P.A. Witherspoon and D.N. Saraf, J. Phys. Chem., 69, 3752 (1965).
81. J.H. Hildebrand, Proc. Nat. Acad. Sci., 64, 1329 (1969).
82. J.V. Sengers, Phys. Fluids, 9, 1685 (1966).
83. J.H. Wang, C.U. Robinson and I.S. Edelman, J.A.C.S., 75, 466 (1953).
84. H.L. Johnston and K.E. McCloskey, J. Phys. Chem., 44, 1038 (1940).
85. J.O. Hirschfelder, C.F. Curtiss, R.B. Bird, "Molecular Theory of Gases and Liquids", Wiley, N.Y. (1966).
86. D. Huq and H. Wood, J. Chem. Phys., 51, 105 (1969).
87. C.N. Murray and J.P. Riley, Deep-sea Research, 16, 311 (1969).

Theory Incorporating the Interfacial Tension 'h' and the Convection 'u'.

1) Open tube Method (No convection term but an interfacial tension).

Experimentally the gas is placed above the pure degassed solvent and the volume of gas (V) moving across the solvent interface (of interfacial tension h) is measured as a function of the time 't'.

The solution for Fick's laws of linear diffusion, viz.

$$J_x = -D \frac{\partial c}{\partial x}$$

$$\frac{\partial c}{\partial t} = D \frac{\partial^2 c}{\partial x^2}$$

[1]

satisfying the experimental conditions:

$$c = 0, x > 0, t = 0$$

$$c = c_0, x = 0, t > 0$$

was derived earlier. It is

$$c = c_0 \operatorname{erfc}(x/2\sqrt{Dt})$$

For mass transfer across an interface

$$J_x = -D \frac{\partial c}{\partial x} = -\alpha(c_s - c_0), X = 0 \quad [2]$$

where α is the reciprocal of the interfacial resistance and c_s is the solute concentration at the interface at time t.

Eq'n [1] can be written using the Laplace transformation

$$L \left\{ \frac{\partial c}{\partial t} \right\} = pL \{c\} - c_0(x) \quad [3]$$

$$L \left\{ D \frac{\partial^2 c}{\partial x^2} \right\} = D \frac{\partial^2 \bar{c}}{\partial x^2} \quad [4]$$

Using the condition that

$$c = 0 \quad x > 0 \quad t = 0$$

we have

$$\frac{d^2 \bar{c}}{dx^2} = q^2 \bar{c} \quad [5]$$

where

$$q^2 = \frac{c}{D} \quad \text{and} \quad \bar{c} = \int_0^{\infty} e^{-pt} c dt$$

Therefore the solution for the ordinary differential eq'n [5] are Be^{qx} and Ae^{-qx} . Since \bar{c} is finite as $x \rightarrow \infty$ the solution for eq'n (5) is

$$\bar{c} = Ae^{-qx} \quad [6]$$

Using the condition that the mass transfer across the interface is a function of c_0 , the Laplace transformation of $\frac{dc}{dx} = h(c - c_0)$ is

$$\frac{d\bar{c}}{dx} = h\bar{c} - hc_0 \quad [7]$$

where

$$h = \frac{q}{D}$$

Using eq'n [6], we have

$$\frac{d\bar{c}}{dx} = -q Ae^{-qx} \quad [8]$$

$$h\bar{c} = h Ae^{-qx}$$

Thus, eq'n [7] becomes

$$-q A e^{-qx} = h A e^{-qx} - h \frac{c_0}{p} \quad [9]$$

Solving for A, we get

$$A = \frac{h c_0}{P(c+q)} e^{+qx} \quad [10]$$

At $x = 0$

$$A = \frac{h c_0}{P(h+q)}$$

Substituting into [5] we have a solution

$$\bar{c} = \frac{h c_0 e^{-qx}}{P(q+h)}$$

A solution for which

$$c = c_d \operatorname{erfc}\left(\frac{x}{2/Dt}\right) - e^{hx + h^2Dt} \operatorname{erfc}\left(\frac{x}{2/Dt} + h/Dt\right) \quad [11]$$

The flux across $x = 0$

$$J_{x=0} = \frac{D}{A} \frac{dc}{dx} = -D \left(\frac{\partial c}{\partial x}\right)_{x=0}$$

Using eq'n [11]

$$\left(\frac{\partial c}{\partial x}\right) = c_0 \cdot \left(\frac{2}{2/Dt}\right)^2 \cdot \frac{1}{2/Dt} - h e^{hx+h^2Dt}$$

$$+ e^{hx+h^2Dt} \cdot \frac{2}{2/\pi} e^{-\left(\frac{x}{2/Dt} + h/Dt\right)^2} \cdot \frac{1}{2/Dt} \quad [12]$$

So, at interface, $x=0$, then

$$\begin{aligned} \left(\frac{\partial c}{\partial x}\right)_{x=0} &= c_0 \frac{-2}{2/Dt} - h e^{h^2 Dt} \operatorname{erfc}(h\sqrt{Dt}) + e^{h^2 Dt} \frac{2}{\sqrt{\pi}} e^{-(h\sqrt{Dt})^2} \frac{1}{2/Dt} \\ &= c_0 \frac{-1}{\sqrt{\pi Dt}} - h e^{h^2 Dt} \operatorname{erfc}(h\sqrt{Dt}) + e^{h^2 Dt} e^{-h^2 Dt} \frac{1}{\sqrt{\pi Dt}} \\ &= c_0 \left[-h e^{h^2 Dt} \operatorname{erfc}(h\sqrt{Dt}) - \frac{1}{\sqrt{\pi Dt}} + \frac{1}{\sqrt{\pi Dt}} \right] \\ &= -c_0 h e^{h^2 Dt} \operatorname{erfc}(h\sqrt{Dt}) \end{aligned}$$

Thus, $-D \left(\frac{\partial c}{\partial x}\right)_{x=0} = D c_0 h e^{h^2 Dt} \operatorname{erfc}(h\sqrt{Dt})$

But $-D \left(\frac{\partial c}{\partial x}\right)_{x=0} = \frac{1}{A} \frac{dm}{dt}$

Assuming ideal gas behaviour for the gas above the solvent, we have

$$\frac{1}{A} \frac{dm}{dt} = \frac{P dV}{RTAdt}$$

Thus,

$$dV = \frac{RTAD}{P} [c_0 h e^{h^2 Dt} \operatorname{erfc}(h\sqrt{Dt})] dt \quad [13]$$

On integration,

$$V = \frac{RTA}{Ph} c_0 \left[e^{h^2 Dt} \operatorname{erfc}(h\sqrt{Dt}) - 1 + 2h \frac{Dt}{\pi} \right]$$

On substituting, $c_0 = \frac{P_{x_2}}{V_2}$ (Henry's Law)

$$V = \frac{RTAx_2}{hV_2} e^{h^2Dt} \operatorname{erfc}(h\sqrt{Dt}) - 1 + 2h \frac{Dt}{\pi} \quad [14]$$

Typical data are shown in Fig. 24. Eq'n [14] represents the non-steady state diffusion in terms of the total volume of gas absorbed as a function of the time t . The equation has been found to fit experimental data well. It is found that there is a rapid approach to asymptotic limiting behaviour of the slope $(2 RTAx_2/V_2)\sqrt{Dt}/\pi$, allowing D to be fairly accurately estimated from the linear portion of the curve. Data over the whole range of experimental measurement can be fitted to equation [14] by a least squares method, allowing an accurate value of D , as well as h , to be obtained.

The interfacial resistance term is not the only problem associated with the diffusion of gases in liquids. When the dissolution of a gas through a liquid interface into a pure solvent brings about a density increase, with respect to the pure solvent, a convection term must be included in the diffusion equation. Such an equation is derived below for the 'open-tube' method, where the gas is held above the solvent into which it dissolves.

11) Open Tube Method (with convection term)

Fick's laws for linear diffusion including convection are written using a velocity term 'u', viz,

$$J_{x=0} = -D \frac{\partial c}{\partial x} - uc_{x=0}$$

and

$$\frac{\partial c}{\partial t} = D \frac{\partial^2 c}{\partial x^2} - u \frac{\partial c}{\partial x}$$

Boundary conditions are those used earlier.

Using the Laplace transformation

$$\frac{d^2 \bar{c}}{dx^2} - \frac{u}{D} \frac{d\bar{c}}{dx} - \frac{P}{D} \bar{c} = 0 \quad [15]$$

Solutions for eq'n (15)

$$m^2 - \frac{u}{D} m - \frac{P}{D} = 0$$

$$m = \frac{u}{D} \pm \frac{\frac{u^2}{D^2} + \frac{4P}{D}}{2}$$

Thus,

$$\bar{c} = A e^{\left(\frac{u}{D} \pm \frac{\frac{u^2}{D^2} + \frac{4P}{D}}{2} \right) x}$$

At $x=0$,

$$\bar{c} = A.$$

Using tables we find a solution

$$c = \frac{c_0}{2} \operatorname{erfc} \left(\frac{x-ut}{2\sqrt{Dt}} \right) + e^{-\frac{ux}{D}} \operatorname{erfc} \left(\frac{x+ut}{2\sqrt{Dt}} \right)$$

$$\frac{\partial c}{\partial x} = \frac{c_0}{2} \frac{-2}{\sqrt{\pi}} e^{-\frac{(x-ut)^2}{2/Dt}} \frac{1}{2/Dt} + e^{\frac{ux}{D}} \frac{u}{D} \operatorname{erfc} \left(\frac{x+ut}{2/Dt} \right) + e^{\frac{ux}{D}} \frac{-2}{\sqrt{\pi}} e^{-\frac{(x+ut)^2}{2/Dt}} \frac{1}{2/Dt}$$

$$\left(\frac{\partial c}{\partial x} \right)_{x=0} = \frac{c_0}{2} \frac{-1}{\sqrt{\pi Dt}} e^{-\frac{4^2 t}{4D}} + \frac{u}{D} \operatorname{erfc} \left(\frac{u}{2} \frac{t}{D} \right) - \frac{1}{\sqrt{\pi Dt}} e^{-\frac{u^2 t}{4D}}$$

The flux at the interface without the velocity term is

$$J_{x=0} = -D \left(\frac{\partial c}{\partial x} \right)_{x=0} = \frac{D c_0}{\sqrt{\pi Dt}} e^{-\frac{u^2 t}{4D}} + \frac{u}{2} \operatorname{erfc} \left(\frac{u}{2} \frac{t}{D} \right) \quad [16]$$

The flux at the interface with the velocity term is

$$J_{x=0} - u c_{x=0}$$

$$u c_{x=0} = \frac{u c_0}{2} \operatorname{erfc} \left(\frac{-ut}{2/Dt} \right) + \operatorname{erfc} \left(\frac{ut}{2/Dt} \right) \quad [17]$$

Thus $J_{x=0} - u c_{x=0}$

is eq'n [16] - eq'n [17].

Noting that $\operatorname{erfc}(-x) = 2 - \operatorname{erfc}(x)$ we get

$$c_0 \sqrt{\frac{D}{\pi}} t^{-\frac{1}{2}} e^{-\frac{u^2 t}{4D}} - \frac{c_0 u}{2} \operatorname{erfc}\left(\frac{u}{2} \sqrt{\frac{t}{D}}\right) - u c_0$$

or

$$c_0 \left\{ \sqrt{\frac{D}{\pi}} t^{-\frac{1}{2}} e^{-\frac{u^2 t}{4D}} - \frac{u}{2} \operatorname{erfc}\left(\frac{u}{2} \sqrt{\frac{t}{D}}\right) - u \right\}$$

But the flux is equal to

$$\frac{1}{A} \frac{dm}{dt} = \frac{1}{A} \frac{PdV}{RTdt}$$

Thus,

$$dV = \frac{ART c_0}{P} \left[\sqrt{\frac{D}{\pi}} t^{-\frac{1}{2}} e^{-\frac{u^2 t}{4D}} dt - \frac{u}{2} \operatorname{erfc}\left(\frac{u}{2} \sqrt{\frac{t}{D}}\right) dt - u dt \right]$$

Integrating,

$$V = \frac{ART c_0}{P} \left[\sqrt{\frac{D}{\pi}} \int_0^t t^{-\frac{1}{2}} e^{-\frac{u^2 t}{4D}} dt - \frac{u}{2} \int_0^t \operatorname{erfc} \frac{u}{2\sqrt{D}} \sqrt{t} dt - ut \right]$$

[18]

iii) Solution to the Diffusion Equation with 'u' and 'h' included.

In deriving eq'n [18] we included only the velocity term, leaving out the interfacial tension. To be realistic, we have to include both terms, as they both play an essential part in the process of diffusion.

We are interested in finding a solution to

$$\frac{\partial^2 c}{\partial x^2} - \frac{u}{D} \frac{\partial c}{\partial x} - \frac{1}{D} \frac{\partial c}{\partial t} = 0$$

[19]

with the inclusion of the condition

$$D \frac{\partial c}{\partial x} = h(c - c_0) - \frac{u}{D} c, \quad x=0 \quad [20]$$

in addition to

$$c=0 \quad x > 0 \quad t=0$$

In the previous section, we found solutions to eq'n (19) to be

$$\bar{c} = A_1 e^{\frac{u}{2D} x - \frac{u^2}{4D^2} t + \frac{P}{D} x} \quad [21]$$

$$\text{and } \bar{c} = A_1 \text{ when } x = 0 \quad [22]$$

From eq'n (20), using the Laplace transformation

$$\frac{d\bar{c}}{dx} = h\bar{c} - \frac{h c_0}{P} - \frac{u}{D} \bar{c} \quad x=0 \quad [23]$$

then from (21)

$$\frac{d\bar{c}}{dx} = A_1 \left[\frac{u}{2D} - \frac{u^2}{4D^2} + \frac{P}{D} \right] e^{\frac{u}{2D} x - \frac{u^2}{4D^2} t + \frac{P}{D} x} \quad [24]$$

At $x=0$,

$$\frac{d\bar{c}}{dx} = A_1 \left[\frac{u}{2D} - \frac{u^2}{4D^2} + \frac{P}{D} \right] \quad [25]$$

Thus,

$$A_1 \left[\frac{u}{2D} - \frac{u^2}{4D^2} + \frac{P}{D} \right] = A_1 \left[h - \frac{u}{D} - \frac{h c_0}{P} \right] (x=0) \quad [26]$$

or

$$A_1 = \frac{h c_0}{P} \frac{1}{\frac{u^2}{4D^2} + \frac{P}{D} - \frac{u}{2D} + h - \frac{u}{D}}$$

Substituting into eq'n (21)

$$\bar{c} = \frac{h c_0}{P} \left(\frac{1}{\frac{u^2}{4D^2} + \frac{P}{D} + h - \frac{3}{2} \frac{u}{D}} \exp \frac{u x}{2D} - \frac{u^2}{4D^2} + \frac{P}{D} x \right) \quad [27]$$

To simplify, let

$$\alpha = \frac{u^2}{4D} \quad \text{and} \quad k = h - \frac{3}{2} \frac{u}{D}$$

Since we can only solve this equation by an Inverse Laplacian transformation we look for a solution whose Laplace is eq'n [27]. Thus, we have

$$c = \int \frac{h c_0}{(p-x)(q-k)} e^{\frac{ux}{2D} - qx} e^{-at} \quad [28]$$

or

$$c = h c_0 e^{\frac{ux}{2D}} \int \frac{e^{-qx}}{(p-\alpha)(q-k)} e^{-at} \quad [29]$$

Looking at Tables (Carslaw and Jaeger) (64)

$$\int \frac{e^{-qx}}{(p-\alpha)(q-k)} = \frac{1}{2} e^{at} \frac{D^{\frac{1}{2}}}{hD^{\frac{1}{2}} + \alpha^{\frac{1}{2}}} e^{-\frac{\alpha}{D} x} \operatorname{erfc} \frac{x}{2/Dt} \sqrt{at}$$

$$+ \frac{D^{\frac{1}{2}}}{hD^{\frac{1}{2}} - \alpha^{\frac{1}{2}}} e^{\frac{\alpha}{D} x} \operatorname{erfc} \frac{x}{2/Dt} + \sqrt{at}$$

$$-\frac{hD}{h^2d-a} e^{hx+h^2Dt} \operatorname{erfc} \frac{x}{2/Dt} + h\sqrt{Dt} \quad [30]$$

Thus,

$$c = h c_0 e^{\frac{ux}{2D}} \left(\frac{1}{(h-\frac{3}{2}\frac{u}{D})D^{\frac{1}{2}} + \frac{u}{2D^{\frac{1}{2}}}} \right) e^{-\frac{u}{2D}x} \operatorname{erfc} \frac{x-ut}{2/Dt}$$

$$+ \frac{D^{\frac{1}{2}}}{(h-\frac{3}{2}\frac{u}{D})D^{\frac{1}{2}} - \frac{u}{2D^{\frac{1}{2}}}} e^{\frac{u}{2D}x} \operatorname{erfc} \frac{x+ut}{2/Dt}$$

$$- \frac{(h-\frac{3}{2}\frac{u}{D})D}{(h-\frac{3}{2}\frac{u}{D})^2 D - \frac{u^2}{4D}} e^{(h-\frac{3}{2}\frac{u}{D})x} + (h-\frac{3}{2}\frac{u}{D})^2 Dt$$

$$- \frac{u^2 t}{4D} \operatorname{erfc} \frac{x + (h-\frac{3}{2}\frac{u}{D}) 2Dt}{2/Dt} \quad [31]$$

or

$$c = c_0 \frac{Dh}{2Dh-2u} \operatorname{erfc} \frac{x-ut}{2/Dt} + \frac{Dh}{2Dh-4u} e^{\frac{ux}{D}}$$

$$\operatorname{erfc} \frac{x+ut}{2/Dt} - \frac{2h^2D^2 - 3uhD}{2h^2D^2 - 6uhD + 4u^2} \exp \frac{(h-u)x}{D}$$

$$+ (h^2D - 3uh + 2\frac{u^2}{D})t \operatorname{erfc} \frac{x + (2hD - 3u)t}{2/Dt} \quad [32]$$

Now,

$$\frac{\partial c}{\partial x} = c_0 \frac{Dh}{2Dh - 2u} - \frac{2}{\sqrt{\pi}} e^{-\frac{(x - ut)^2}{(2/Dt)^2}} \frac{1}{2/Dt}$$

$$+ \frac{Dh}{2Dh - 4u} \operatorname{erfc} \frac{x + ut}{2/Dt} e^{\frac{u}{D} x} \frac{u}{D} +$$

$$\frac{Dh}{2Dh - 4u} e^{\frac{u}{D} x} - \frac{2}{\sqrt{\pi}} e^{-\frac{(x + ut)^2}{(2/Dt)^2}} \frac{1}{2/Dt}$$

$$- \frac{2h^2D^2 - 3uhD}{2h^2D^2 - 6uhD - 4u^2} \operatorname{erfc} \frac{x + (2hd - 3u)t}{2/Dt}$$

$$\frac{(h - \frac{u}{D})x + (h^2D - 3uh + 2\frac{u^2}{D})t}{(h - \frac{u}{D})}$$

$$- \frac{2h^2D^2 - 3uhD}{2h^2D^2 - 6uhD - 4u^2} e^{\frac{(h - \frac{u}{D})x + (h^2D - 3uh + 2\frac{u^2}{D})t}{D}}$$

$$- \frac{2}{\sqrt{\pi}} e^{-\frac{[x + (2hD - 3u)t]^2}{(2/Dt)^2}} \frac{1}{2/Dt}$$

[33]

Now,

$$-D \left(\frac{\partial c}{\partial x} \right)_{x=0} = Dc_0 \frac{Dh}{(2Dh - 2u)\sqrt{\pi Dt}} e^{-\frac{u^2 t}{4D}}$$

$$- \frac{Dh}{2Dh - 4u} \frac{u}{D} \operatorname{erfc} \left(\frac{ut}{2/Dt} \right) - \frac{1}{\sqrt{\pi Dt}} e^{-\frac{u^2 t}{4D}}$$

$$\begin{aligned}
 & + \frac{2h^2D^2 - 3uhD}{2h^2D^2 - 6uhD - 4u^2} \left(h - \frac{u}{D}\right) e^{\frac{(h^2D - 3uh + 2u^2)t}{D}} \\
 \text{erfc} & \frac{(2hD - 3u)t}{2/Dt} - e^{\frac{(h^2D - 3uh + 2u^2)t}{D}} \\
 e^{-\left(\frac{2hD - 3u}{2/Dt}\right)^2 t^2} & \frac{1}{\sqrt{\pi Dt}} \quad [34]
 \end{aligned}$$

Also,

$$c_{x=0} = c_0 \frac{Dh}{2Dh - 2u} \text{erfc} \frac{-ut}{2/Dt} + \frac{Dh}{2Dh - 4u}$$

$$\text{erfc} \frac{ut}{2/Dt} - \frac{2h^2D^2 - 3uhD}{2h^2D^2 - 6uhD - 4u^2}$$

$$e^{\frac{(h^2D - 3uh + 2u^2)t}{D}} \text{erfc} \frac{(2hD - 3u)t}{2/Dt} \quad [35]$$

The equation for mass transfer is

$$J_{x=0} = -D \left(\frac{\partial c}{\partial x}\right)_{x=0} - u c_{x=0}$$

$$= \frac{1}{A} \frac{dm}{dt} = \frac{P}{ART} \frac{dV}{dt}$$

If we let $\frac{P}{cART} \frac{dV}{dt} = \frac{dV^*}{dt}$

we get

$$\frac{dV^*}{dt} = D \frac{Dh}{(2Dh - 2u)\sqrt{\pi Dt}} e^{-\frac{u^2 t}{4D}}$$

$$\frac{Dh}{2Dh - 4u} \frac{u}{D} \operatorname{erfc} \left(\frac{u}{2} \sqrt{\frac{t}{D}} \right) - \frac{1}{\sqrt{\pi Dt}} e^{-\frac{u^2 t}{4D}}$$

$$- \frac{1}{\sqrt{\pi Dt}} e^{-\frac{u^2 t}{4D}} - u \frac{Dh}{2Dh - 2u} \left\{ 1 + \operatorname{erf} \left(\frac{u}{2} \sqrt{\frac{t}{D}} \right) \right\}$$

$$+ \frac{Dh}{2Dh - 4u} \operatorname{erfc} \left(\frac{u}{2} \sqrt{\frac{t}{D}} \right)$$

$$- \frac{2h^2 D^2 - 3uhD}{2h^2 D^2 - 6uhD - 4u^2} e^{(h^2 D - 3uh + 2 \frac{u^2}{D})t}$$

$$\operatorname{erfc} \left(hD - \frac{3}{2}u \right) \sqrt{\frac{t}{D}}$$

or

$$\frac{V_2}{RTAX_2} \frac{dV}{dt} = \frac{-Dhu}{2(Dh-u)} \operatorname{erfc} \left(\frac{u}{2} \sqrt{\frac{t}{D}} \right)$$

$$- \frac{Dhu}{(Dh-2u)} \operatorname{erfc} \left(\frac{u}{2} \sqrt{\frac{t}{D}} \right)$$

$$+ \frac{2h^2 D^2 - 3uhD}{2(h^2 D^2 - 3uhD)} e^{(h^2 D - 3uh + 2 \frac{u^2}{D})t}$$

$$\text{erfc} \frac{(2hD - 3u)}{2} \frac{t}{D} \quad Dh \quad [36]$$

For large 't' and 'h'

$$\frac{V_2}{RTAX_2} \frac{dV}{dt} = \sqrt{\frac{D}{\pi t}} e^{-\frac{u^2 t}{4D}} - \frac{u}{2} \text{erfc} \frac{u}{2} \frac{t}{D} \quad [37]$$

-u

It will be shown later, by putting numerical values into these equations how the interfacial resistance 'h' and the velocity 'u' affect the rate of diffusion.

Discussion

It is seen from figure 13 and 14 that the O.T.M. (down) data can give either a pseudo-steady state uptake of gas (i.e. V vs \sqrt{t}) or a pseudo-steady state uptake (V vs \sqrt{t}). If it is not recognized that the latter relationship can still contain a natural convection mechanism in the gas dissolution process, the interpretation of the data can obviously lead to erroneously high values. In figures 22 and 23 we show the volume of gas absorbed as a function of time according to equation [37]. We have chosen a value of $D = 4 \times 10^{-5} \text{ cm sec}^{-1}$ and plot the expected relationship for a range of convection, u , values. The change from the pseudo un-steady state relationship to a pseudo steady state relationship is clearly seen.

Within the constraints discussed above we may assume that for Ar/C₆H₆ system the I.T.M. value, $D = 3.99 \times 10^{-5} \text{ cm}^2\text{sec}^{-1}$, is the "correct" value of the diffusion coefficient. Using this value of D we now calculate the expected V vs t relationship from the (asymptotic) equation [37] for various values of u . A comparison of the experimental curve to the calculated set of theoretical curves is given in figure (24). It is recognized that it is impossible to 'fit' D , h , and u to the experimental data uniquely, but as discussed above, the interfacial resistance term merely shifts

the limiting slope portion of the relationship along the time axis. The asymptotic slope is not a function of h . For $D = 3.9 \times 10^{-5} \text{ cm}^2 \text{ sec}^{-1}$, it is noticed that the theoretical expression, equation [37] only gives an asymptotic slope in agreement with that experimentally observed for a value of $u = 13 \times 10^{-5} \text{ cm}^2 \text{ sec}^{-1}$. It is found that for such a high value of u the asymptotic slope value is not very sensitive to D . As may be seen from figure 24, it is, however, sensitive to u , particularly at low u values. A similar comparison of the theoretical expression, equation (37), to the experimental data for $\text{N}_2/\text{C}_6\text{H}_6$ system using the I.T.M. value for D ($= 3.9 \times 10^{-5} \text{ cm}^2 \text{ sec}^{-1}$) gives a value $u = 1.5 \times 10^{-5} \text{ cm}^2 \text{ sec}^{-1}$ as the matching asymptotic slope value.

Within the limitations of the reported data little can be said of the actual values found for u , the natural convection term. Simple Stokes law argument would lead to an expected value of the order of $10^{-9} \text{ cm sec}^{-1}$. The likelihood of Stokes law applying to a gas molecule in solution is hardly to be expected as the natural convection term is simply a matter of the gas molecule descending through the liquid under the pull of gravity. It is a complex convection process and the u term merely represents the added rate of gas dissolution because of its presence. At this time no simple argument can be put forward to

account for the actual u values. It is obvious, however, that the presence of this convection term greatly increases the rate of gas dissolution. In figure (25) we plot the volume of the gas absorbed as a function of time for the CO_2 - water system at 25°C for both I.T.M. and O.T.M. data. For the open-tube method the gas uptake follows a pseudo steady-state relationship. The convection term increases the volume uptake of gas by a factor of 3 in the first 1000 seconds. A similar enhancement in uptake occurs in the $\text{Ar}/\text{H}_2\text{O}$ system but in this case a pseudo non-steady state law is followed, as shown in figure (11). This latter system has been used for a very preliminary study of O.T.M. cross-sectional tube area dependence of u . It is seen that the 'effective' D value (obtained from the slope of the v vs \sqrt{t} linear plots) approaches that value found from I.T.M. experiments (of $1.44 \times 10^{-5} \text{ cm}^2 \text{ sec}^{-1}$). Using this latter value for the true D value the fitting procedure described above was used to find u values for each cross-sectional tube area considered. Figure(26) shows that a roughly linear u vs cross-sectional area relationship exists.

This work is pertinent in that several workers have interpreted the pseudo non-steady state behavior

ignoring the 'u' term and so report only the "apparent" D value. The same comment may be made for all studies involving the dissolution of a gas from a bubble into a solvent. Even ignoring other errors to which these techniques are prone (e.g. simple hydrodynamic problems of a shrinking bubble) the error in ignoring the u-term must lead to high "apparent" D values.

The role played by the gravity induced convection term in the dissipation of a gas into a liquid has not been previously demonstrated in a simple manner. Other workers have commented that such a term may exist, such as for the dissolution of carbon dioxide in water. The comparative rates of absorption of the gas for the O.T.M. and I.T.M. experiments demonstrate the importance of this term. It is pertinent to question the role of this term in many pharmacological processes, or perhaps the lack of this term in extended non-gravitational situations.

Fig 21

Diffusion of nitrogen gas in benzene at 25°C,

$$D = 7.23 \text{ cm}^2\text{sec}^{-1}.$$

○ Experimental results.

--- Equation 16 (no interfacial resistance)

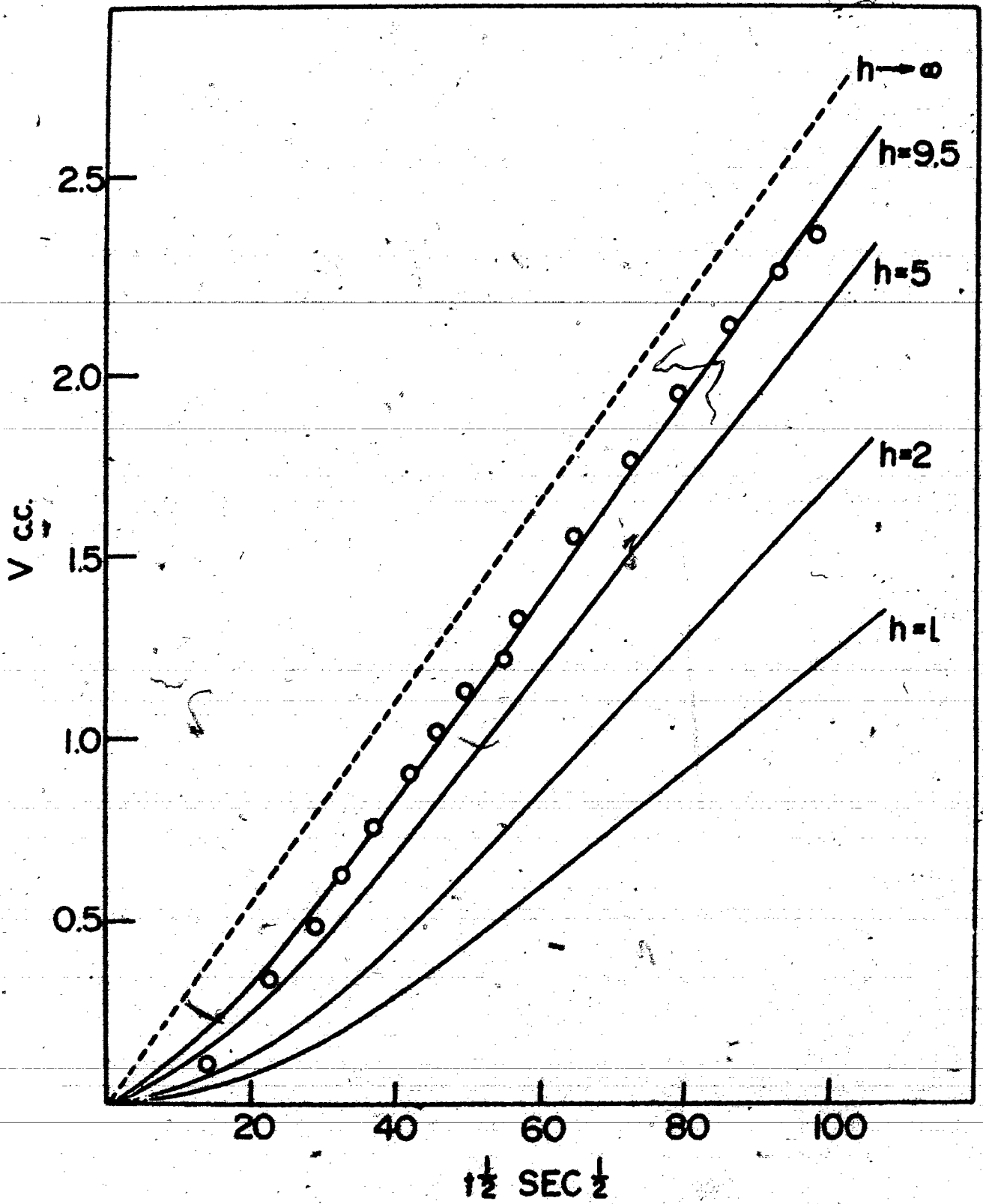


Fig 21

Fig 22

Pseudo non-steady state diffusion in presence of natural convection. $V^* = (PV/ARTC_0)$.

$$D = 4 \times 10^{-5} \text{ cm}^2\text{sec}^{-1}; h = 3.$$

Curve 1. $u = 1 \times 10^{-4} \text{ cm sec}^{-1}$

Curve 2. $u = 6 \times 10^{-6} \text{ cm sec}^{-1}$

Curve 3. $u = 2 \times 10^{-6} \text{ cm sec}^{-1}$

Curve 4. $u = 1 \times 10^{-6} \text{ cm sec}^{-1}$

Fig 22

Pseudo non-steady state diffusion in presence
of natural convection. $V^* = (PV/ARTC_0)$.

$$D = 4 \times 10^{-5} \text{ cm}^2 \text{ sec}^{-1}; h = 3.$$

$$\text{Curve 1. } u = 1 \times 10^{-4} \text{ cm sec}^{-1}$$

$$\text{Curve 2. } u = 6 \times 10^{-6} \text{ cm sec}^{-1}$$

$$\text{Curve 3. } u = 2 \times 10^{-6} \text{ cm sec}^{-1}$$

$$\text{Curve 4. } u = 1 \times 10^{-6} \text{ cm sec}^{-1}$$

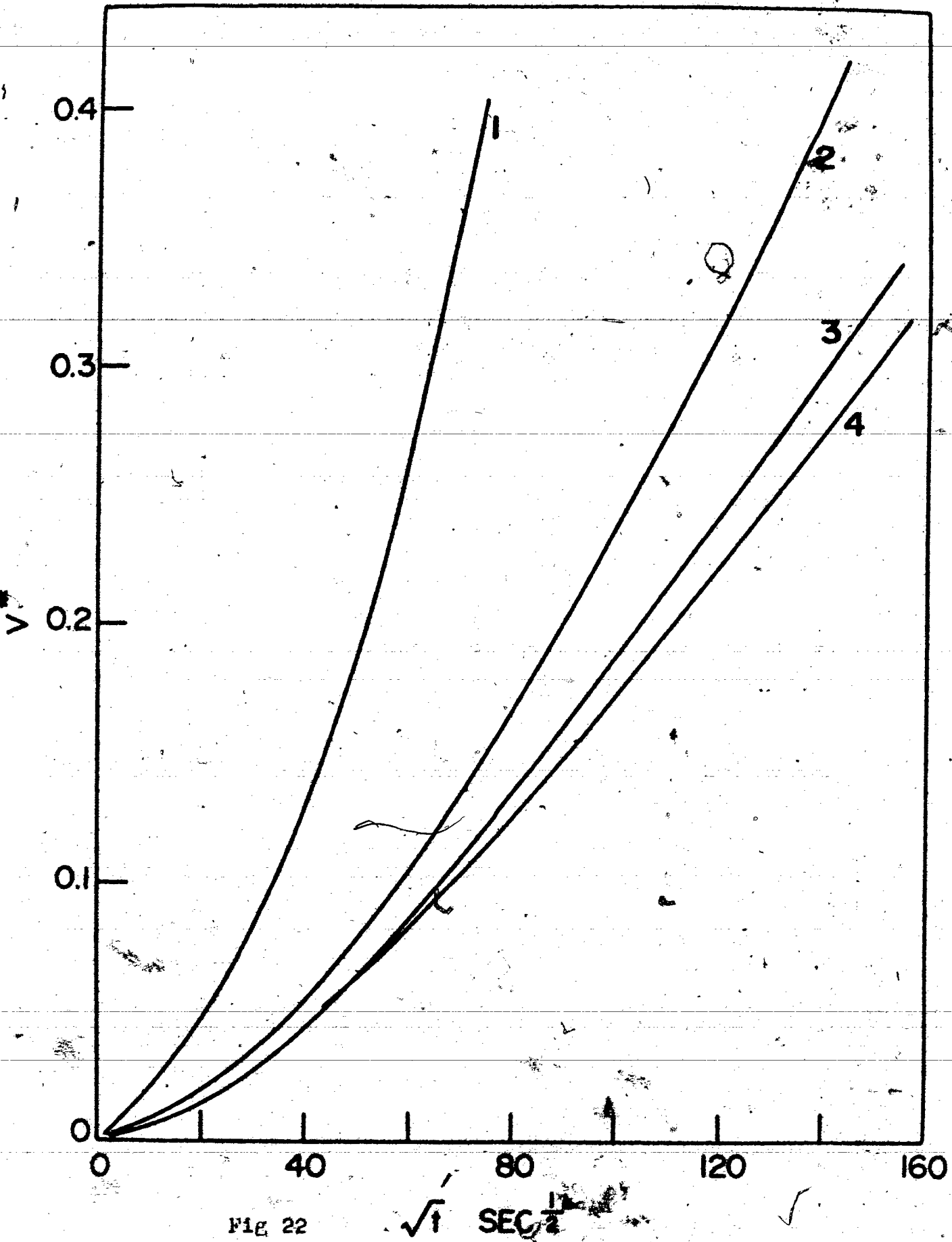


FIG 22

\sqrt{t} SEC^{1/2}

Fig 23

Pseudo steady-state diffusion in presence of natural convection.

$$D = 4 \times 10^{-5} \text{ cm}^2 \text{ sec}^{-1} \quad V^* = (PV/ARTC_0)$$

$$\text{Curve 1. } u = 6 \times 10^{-4} \text{ cm sec}^{-1}$$

$$\text{Curve 2. } u = 1 \times 10^{-4} \text{ cm sec}^{-1}$$

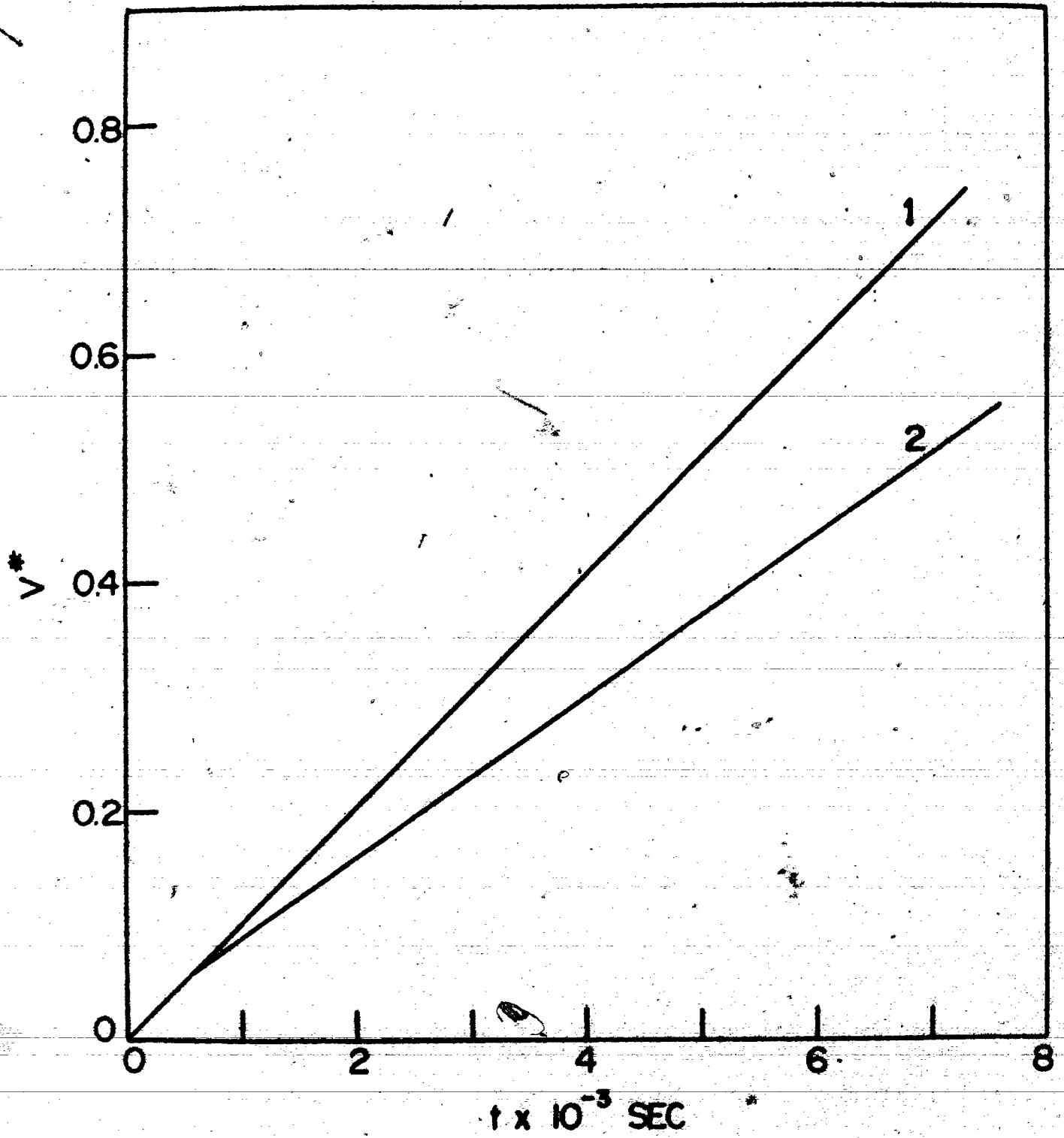


Fig 23

Fig 24

Dissolution of Ar into benzene solvent (25°C).
Comparison of experimental curve to the asymptotic theoretical expression, equation (38).

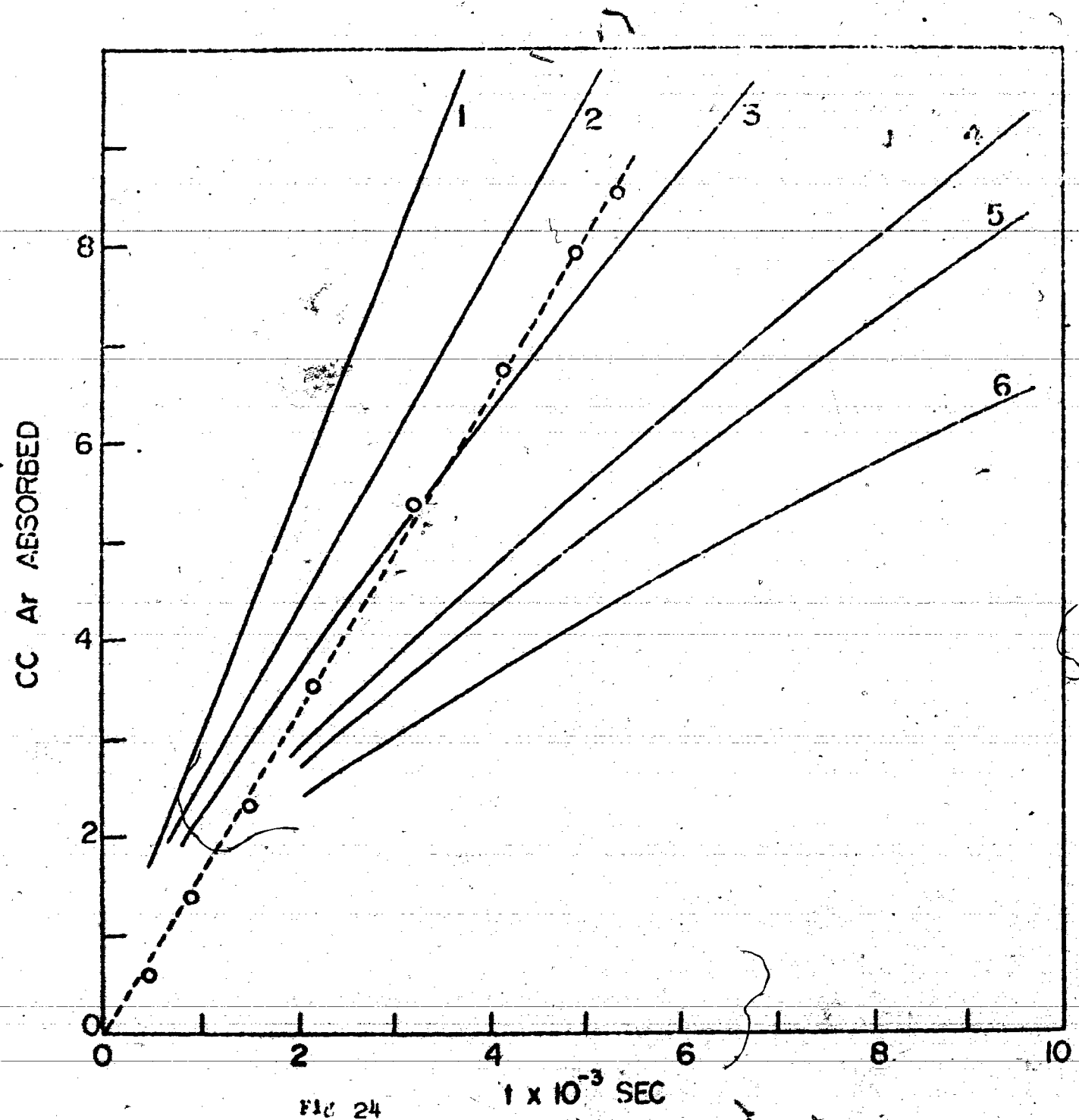


FIG 24

Fig 25

Absorption of CO₂ in water at 25°C.

1. Open tube method

Area of cell = 0.33 cm²

2. Inverted tube method.

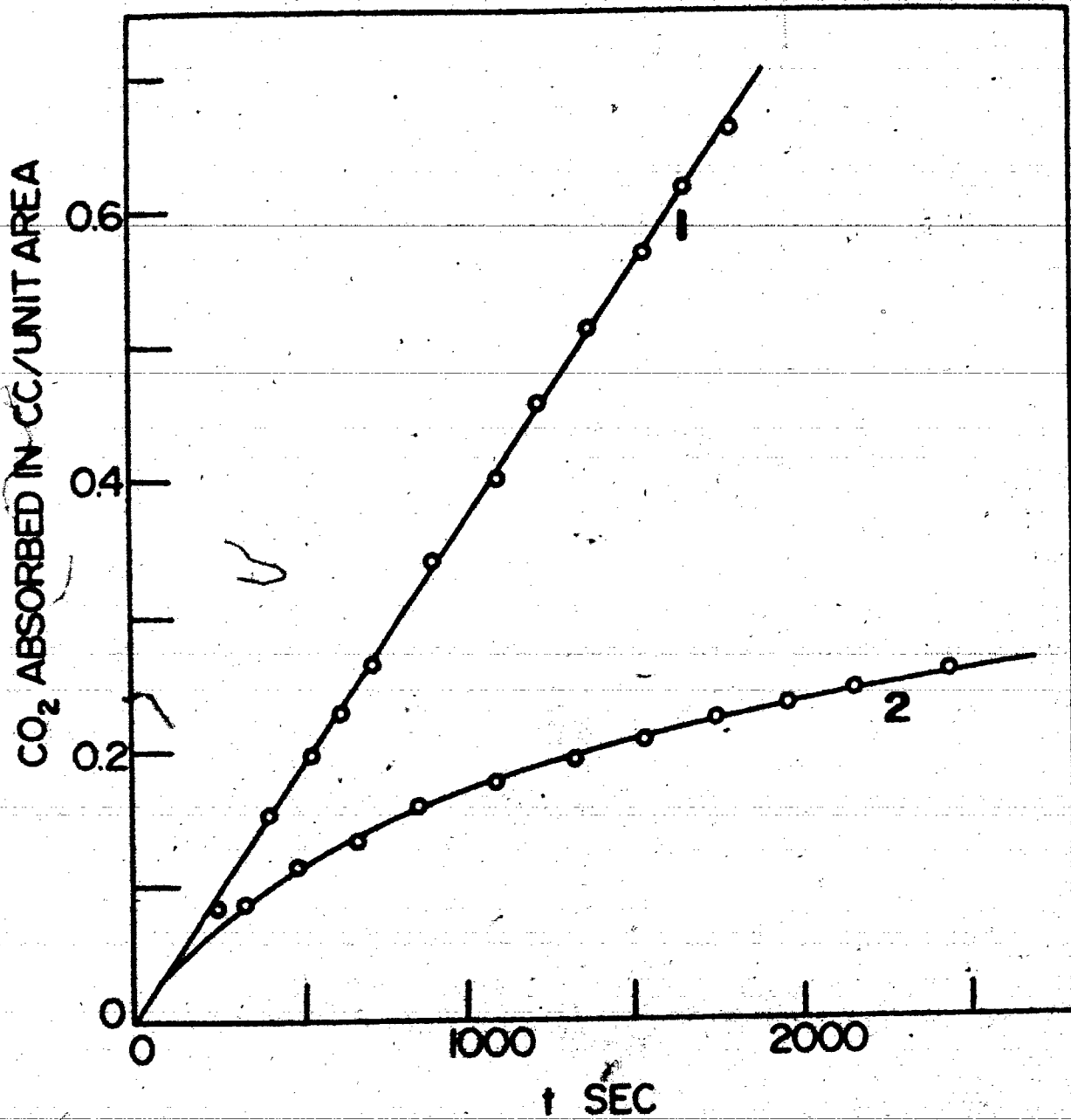


Fig 25

Fig. 26

Area dependence of the velocity 'u'

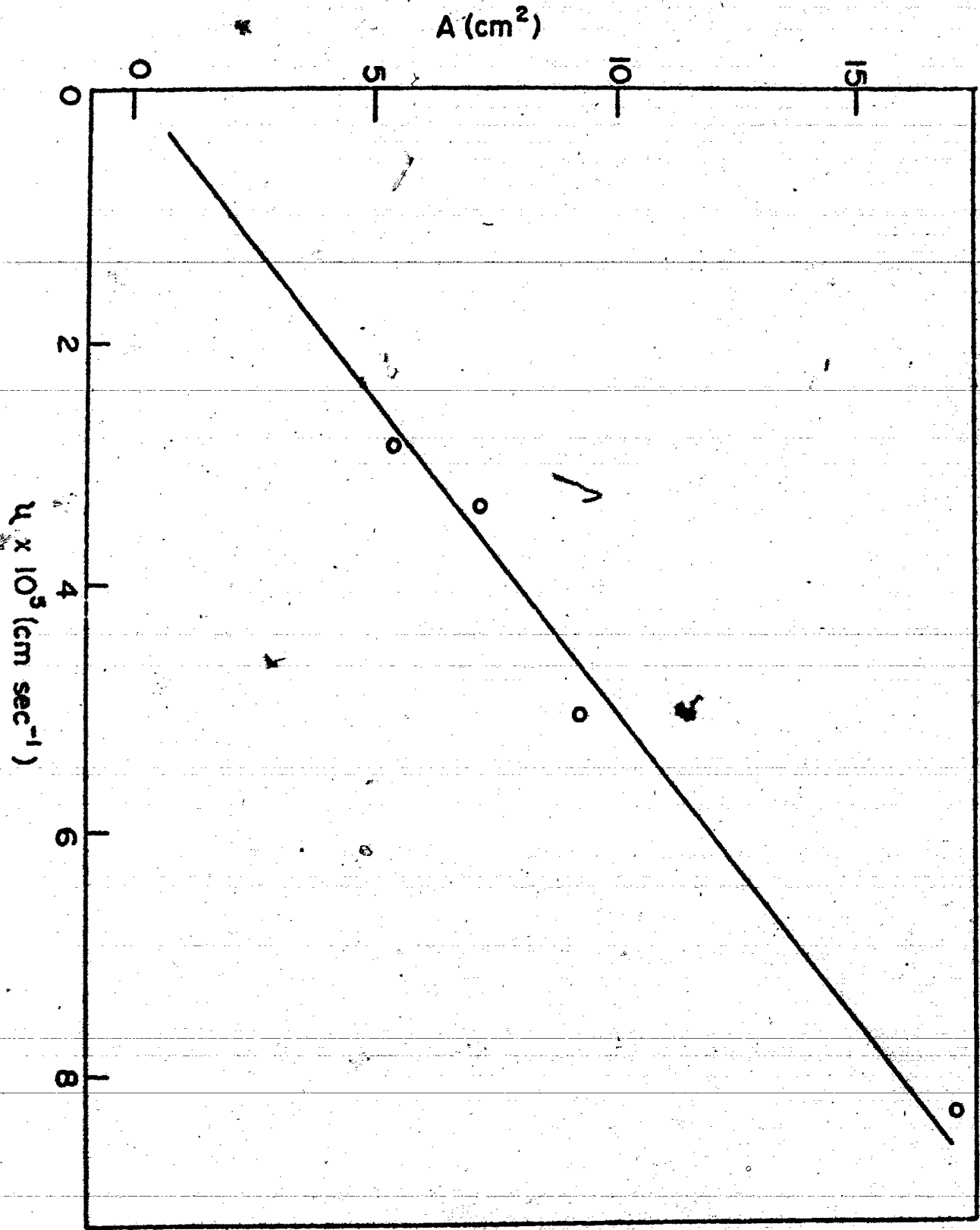


Fig. 26